ON THE DETERMINATION OF EFFECTIVE MODULI OF COMPOSITE MATERIALS BY A THREE-DIMENSIONAL FINITE ELEMENT METHOD

A THESIS

Presented to

The Faculty of the Division of Graduate Studies and Research

By

Sei In Kang

In Partial Fulfillment

of the Requirements for the Degree

Doctor of Philosophy in the School

of Engineering Science and Mechanics

Georgia Institute of Technology

December, 1973

ON THE DETERMINATION OF EFFECTIVE MODULI

OF COMPOSITE MATERIALS BY A

THREE-DIMENSIONAL FINITE ELEMENT METHOD

Approved:

George M. Rentzepis, Chairman

Leroy Z. Emkin

C. Virgil Smith, Jr.

Charles E. Ueng

James T. S. Wang

Date approved by Chairman: 23 X 73

ACKNOWLEDGMENTS

I would like to express my appreciation to my thesis advisor, Dr. George M. Rentzepis, for his helpful assistance and guidance while this research was being conducted. I would also like to express my appreciation to Dr. C. Virgil Smith, Jr. and Dr. James T. S. Wang for their constructive criticism and suggestions of the manuscript.

I wish to thank Dr. Milton E. Raville, Director of the School of Engineering Science and Mechanics, who arranged financial assistance during the period of my study at the Georgia Institute of Technology. I would also like to acknowledge the financial support of the NDEA fellowship which I received in 1970.

My deepest appreciation goes to my wife and daughter for their love, patience, and unending source of strength.

Finally, I would like to thank my parents who for many years have offered their guidance and encouragement to make my life more meaningful.

TABLE OF CONTENTS

Page

ACKNOWLEDGMENTS iii

LIST OF TABLES vi

LIST OF ILLUSTRATIONS viii

LIST OF SYMBOLS xii

SUMMARY xv

Chapter

I. INTRODUCTION 1

II. ABOUT THE FINITE ELEMENT METHOD 6

General Comments
Equilibrium Equation
Assemblage of the Individual Element to the Whole Structure
Boundary Condition

III. THREE-DIMENSIONAL FINITE ELEMENT WITH A SPECIFIC SHAPE FUNCTION 15

The Shape Function
The Strain Matrix
Element Stiffness Matrix
Element Loading Vector
Static Condensation of the Element Equilibrium Equation
Integration Algorithm

IV. COMPUTATION OF EFFECTIVE MODULI. 30

V. UNIDIRECTIONAL FIBER COMPOSITES. 35

Scope of the Investigation
Unidirectional Fiber Composites with Square Cross-Section Fibers
Unidirectional Fiber Composites Whose Cross-Section are not Square
Results on the Unidirectional Fiber Composites

TABLE OF CONTENTS (Concluded)

Page

Chapter

VI. LAMELLAR COMPOSITES 51

Description of the Problem
Results

VII. SHORT FIBER COMPOSITES 54

Description of the problem
Results

VIII. THE LAMINATED COMPOSITES 57

Description of the Problem
Results

TABLES. 68

FIGURES 89

APPENDICES

A. REDUCTION OF ELASTIC MODULI DUE TO SYMMETRIES. . . . 141

Unidirectional Fiber, Lamellar, and Short Fiber Composites
Laminated Composite

B. BEHRENS' RESULTS 147

Lamellar Composites
Unidirectional Fiber Composites with Rectangular Cross-Section

REFERENCES. 150

VITA 152

LIST OF TABLES

Table		Page
1.	Values of the Argument and the Weighting Factors for Gauss-Legendre Formula	69
2.	Displacements of the Nodal Points for the Discretized Model Shown in Figure 12 Which is Loaded with T_{xx}= -10,000 psi	70
3.	Displacements of the Nodal Points for the Discretized Model Shown in Figure 12 Which is Loaded with T_{zz}= -10,000 psi	71
4.	Average Displacements and Strain	72
5.	Displacements of the Nodal Points for the Discretized Model Shown in Figure 16 Loaded by Pure Shear T_{xy}= -10,000 psi	73
6.	Displacements of the Nodal Points for the Discretized Model Shown in Figure 16 Loaded by Pure Shear T_{yz}= -10,000 psi	74
7.	Effective Moduli of Unidirectional Fiber Composites at Various Volumetric Ratios	75
8.	Effective Modulus C^*_{44} of Unidirectional Fiber Composites at Various Volumetric Ratios	76
9.	Effective Modulus C^*_{66} of Unidirectional Fiber Composites at Various Volumetric Ratios	77
10.	Effective Moduli of Unidirectional Fiber Composites from Behrens' Results	78
11.	Effective Moduli of Lamellar Composites at Various Volumetric Ratios	79
12.	Effective Modulus C^*_{66} of Lamellar Composites at Various Volumetric Ratios	79
13.	Effective Modulus C^*_{44} of Lamellar Composites at Various Volumetric Ratios	79

TABLE OF CONTENTS (Concluded)

Table		Page
14.	Effective Moduli of Lamellar Composites from Behrens' Results	80
15.	Effective Moduli of Short Fiber Composites at Various Volumetric Ratios	81
16.	Displacements of the Nodal Points for the Discretized Model Shown in Figure 49 Loaded by T_{zz}=-10,000 psi . . .	82
17.	Displacements of the Nodal Points for the Discretized Model Shown in Figure 49 Loaded by T_{yy}=-10,000 psi . . .	83
18.	Displacement of the Nodal Points for the Discretized Model Shown in Figure 49 Loaded by T_{xz}=10,000 psi . . .	85
19.	Displacements of the Nodal Points for the Discretized Model Shown in Figure 49 Loaded by T_{yz}=10,000 psi . . .	87

LIST OF ILLUSTRATIONS

Figure		Page
1.	Composite Material	90
2.	Equivalent Material	90
3.	Discretization of a Continuum	91
4.	An Element	91
5.	An Example of a Total Structure	92
6.	Coordinate Systems	93
7.	Coordinates of the Nodal Points in Local Coordinate System.	93
8.	Actual Composite	94
9.	Equivalent Material	94
10.	Unidirectional Square-Fiber Composite	95
11.	A Representative Basic Cell for the Composite Shown in Figure 10	95
12.	Discretization of One Octant of the Basic Cell Shown in Figure 11	96
13.	The v-Component of the Displacement of the Nodal Points on the Plane y = 5	97
14.	Schematic Deformation of the Unidirectional Fiber Composite	98
15.	Schematic Deformation of the Equivalent Material	98
16.	Discretization of the Basic Cell for the Shear Test	99
17.	The Deformed Shape Due to the Shear Test	100
18.	Discretization of One Half of the Basic Cell for the Shear Test	101

LIST OF ILLUSTRATION (Continued)

Figure		Page
19.	Schematic Drawing of the Displacement Due to the Shear Test Loaded by T_{yz}	102
20.	The Basic Cell of the Unidirectional Fiber Composite Whose Fiber Shape is Fixed-Height Cross	103
21.	The Basic Cell of the Unidirectional Fiber Composite Whose Fiber Shape is Varying-Height Cross	103
22.	The Effective Modulus C^*_{11} of the Unidirectional Fiber Composites	104
23.	The Effective Modulus C^*_{33} of the Unidirectional Fiber Composites	105
24.	The Effective Modulus C^*_{12} of the Unidirectional Fiber Composites	106
25.	The Effective Modulus C^*_{13} of the Unidirectional Fiber Composites	107
26.	The Effective Modulus C^*_{44} of the Unidirectional Fiber Composites	108
27.	The Effective Modulus C^*_{66} of the Unidirectional Fiber Composites	109
28.	Lamellar Composite	110
29.	Basic Cell	110
30.	Discretization of One Octant of the Basic Cell of the Lamellar Composite	111
31.	Discretization of a Basic Cell of a Lamellar Composite for the Shear Test Loaded by T_{yz}	112
32.	The Discretization of One Half of the Basic Cell of a Lamellar Composite for the Shear Test Loaded by T_{yz}	113
33.	The Effective Modulus C^*_{11} of the Lamellar Composites	114
34.	The Effective Modulus C^*_{33} of the Lamellar Composites	115
35.	The Effective Modulus C^*_{12} of the Lamellar Composites	116

LIST OF ILLUSTRATION (Continued)

Figures		Page
36.	The Effective Modulus C^*_{13} of the Lamellar Composites . .	117
37.	The Effective Modulus C^*_{44} of the Lamallar Composites . .	118
38.	The Effective Modulus C^*_{66} of the Lamellar Composites . .	119
39.	A Short Fiber Composite	120
40.	Basic Cell of the Short Fiber Composite	121
41.	Equivalent Material	121
42.	Discretization of One Octant of a Short Fiber Composite	122
43.	The Effective Modulus C^*_{11} of the Short Fiber Composites .	123
44.	The Effective Modulus C^*_{12} of the Short Fiber Composites .	124
45.	Discretization of One Half of a Basic Cell of a Short Fiber Composite for the Shear Test Loaded by T_{xy}	125
46.	Laminated Composte	126
47.	Possible Basic Cells for the Laminated Composite	127
48.	The Basic Cell of the Laminated Composite	128
49.	Discretization of the Basic Cell for the Laminated Composite	129
50.	Shear Test Loaded by T_{zx}	130
51.	Deformed and Undeformed Shapes	130
52.	Shear Test Loaded by T_{yz}	131
53.	Average Shearing Strain	131
54.	Compression Test Loaded along z-Direction	132
55.	Compression Test Loaded along y-Direction	132
56.	The Effective Modulus C^*_{11} of the Laminated Composites . .	133

LIST OF ILLUSTRATION (Concluded)

Figure		Page
57.	The Effective Modulus C^*_{22} of the Laminated Composites . .	134
58.	The Effective Modulus C^*_{12} of the Laminated Composites . .	135
59.	The Effective Modulus C^*_{13} of the Laminated Composites . .	136
60.	The Effective Modulus C^*_{66} of the Laminated Composites . .	137
61.	The Effective Modulus C^*_{44} of the Laminated Composites . .	138
62.	Two Illustration of Changing the Volumetric Ratio of Laminated Composites	139
63.	Lamellar Composite	140
64.	Unidirectional Fiber Composite	140

LIST OF SYMBOLS

Symbol	Definition
a_i	Coefficient of the shape function
A_i	Weighting factors in Gaussian quadrature or area of an element face
[B]	B-matrix
[C]	Elastic moduli matrix
C_{ijkl} or C_{ij}	Elastic moduli
C^*_{ijkl} or C^*_{ij}	Effective elastic moduli
D_{ij}	Partial differential operator
E or E_i	Young's modulus or moduli
$\{f\}^e$	Load vector of a finite element
{F}	Load vector of a entire structure
[J]	Jacobian matrix
J'_{ij}	Matrix element of $[J]^{-1}$
k_{ij}	Matrix element of element stiffness matrix
$[k]^e$	Element stiffness matrix
[K]	Stiffness matrix of entire structure
m	Mass of a composite
m^*	mass of a equivalent material
[N]	Shape function in matrix form
{P}	Body force matrix
S_{ijkl}, S_{ij}	Compliances
T_{ij}	Traction
{T}	Surface traction matrix

LIST OF SYMBOLS (Continued)

Symbol	Definition
u, v, w	Displacements
u_x, u_y, u_z	Displacements of a point
$u_{x_i}, u_{y_i}, u_{z_i}$	Displacement of a nodal point
$\bar{u}_i$	Average displacement
$\{u\}^e$	Displacement matrix of element nodal points
$\{u\}$	Displacement matrix of a point
$\{U\}$	Displacement matrix of the nodal points of the entire structure
U	Strain energy of a composite
U^*	Strain energy of a equivalent material
V_0	Undeformed volume of a composite
V_1	Deformed volume of a composite
V_0^*	Undeformed volume of an equivalent material
V_1^*	Deformed volume of an equivalent material
W	Actual strain or complementary energy
W^ε	Admissible strain energy
W^c	Admissible complementary energy
x, y, z	Coordinates of a point in global coordinate system
x_i, y_i, z_i	Coordinates of the nodal points in global coordinate system
ξ, η, ζ	Coordinates in local coordinate system
$\mu, \mu_i, \lambda, \lambda_i$	Lame constants
$\bar{\theta}_i$	Average angle of rotation

LIST OF SYMBOLS (Concluded)

Symbol	Definition
σ_{ij}	Stresses
ε_{ij}	Strains

SUMMARY

In this dissertation the analytic study of computing the effective moduli of various composites - unidirectional fiber composites of different shapes of fiber cross-section, lamellar composites, short fiber composites, and laminated composites - is presented using a three-dimensional finite element method. Six highlights are emphasized:

(1) The three-dimensional finite element method is formulated employing the modified isoparametric formulation of displacement method. The element equilibrium equation and the assembling procedure are explicitly shown in Chapters II and III.

(2) The procedure of computing the effective moduli is described for a general composite material by employing the finite element method. For the composites which exhibit specific symmetries, an effort was devoted to compute the effective moduli more economically by taking advantage of their geometric shapes. The essential procedure is described in Chapters IV and V.

(3) The results obtained by the finite element method are compared with available information to test their validity and the reliability of the proposed procedure. This is done in Chapter V for the unidirectional fiber composites and in Chapter VI for the lamellar composites.

(4) A special case of short fiber composites which reveal homogeneous and isotropic property in the large are analyzed in Chapter VII.

(5) The two-layered laminated composite ($+45^{\circ}$, -45°) is analyzed and all of the six effective moduli of the composite are computed in Chapter VIII.

(6) Accomplishments of this investigation and discussions are summarized in Chapter IX.

CHAPTER I

INTRODUCTION

Prediction of the effective moduli for a multi-phased or composite material has been an interest of many analysts as well as experimentalists for decades. The interest is increasing rapidly in the recent years as the modern technology requires materials having specified properties which often do not exist in a natural form of material. Some of the specified properties can be generated by manufacturing a composite material with appropriate distribution and selection of the constituents which exist in natural form. Undoubtedly, then the problem of prediction of mechanical properties in the large or bulk properties of a composite prior to its manufacture becomes important.

A very general form of a composite material may be considered to be a body composed of a number of different homogeneous materials including some multiply-connected regions as shown schematically in Figure 1. The general problem is to construct an equivalent material which responds in the same manner as the actual composite in an average sense. The equivalent material should be homogeneous by construction and the rest of its properties are to be defined as necessary to achieve the desired response. The average values of the physical constants of the composite material which will guarantee the appropriate response, in the large, of the equivalent material are defined as the effective moduli of the composite. The equivalent material for the composite shown in Figure 1 is shown schematically in Figure 2.

To reduce the general problem to a manageable and workable complexity, only the problem of predicting the equivalent elastic constants using linear theory of elasticity is considered in this investigation. One can immediately realize that the closed form solution satisfying given boundary conditions and the elasticity equations for a heterogeneous system such as shown in Figure 1 is extremely difficult to obtain even if it may be possible.

Historically the attempt to investigate the heterogeneous material started with Einstein [1] in 1906 in his investigation of the viscosity of a dilute suspension of rigid spheres in a Newtonian viscous fluid. Jeffery [2] in 1923 and by Taylor [3] in 1932 extended the theory of dilute suspensions to analyze Einstein's problem for rigid ellipsoidal particles and for viscous spheres with surface tension. Further investigations were performed by other investigators for many different types of inclusions in a viscous fluid with factors such as slippage and friction.

The problem of elastic inclusions dispersed in a matrix having different elastic moduli in which both matrix and inclusions are elastic was first treated by Bruggemen [4]. He found the correct expression for the bulk modulus. The expression for the shear modulus was derived by Dewey [5]. Without the knowledge of Dewey's results, the more special elastic-spherical voids case was solved by Mackenzie [6]. Eshelby gave a method of solution for ellipsoidal inclusions [7].

In contrast with the investigators who dealt with small inclusions, Kerner [8] is known as the first investigator who treated the finite inclusion. Hashin [9] derived upper and lower bounds for the

effective elastic moduli of elastic-elastic suspensions which are composed of homogeneous isotropic materials by use of the principles of minimum potential energy and minimum complementary energy. Krivoglaz and Cherevko [10] treated the elastic spherical two-phase suspension with moderate difference between the two sets of moduli by perturbation method.

The problem of the elastic behavior of fiber reinforced materials was first investigated by Hill and Crossley [11]. Hashin and Rosen [12] have obtained the bounds of effective elastic moduli of materials reinforced by parallel hollow or solid circular fibers by using extremum principles of elasticity [9]. This particular composite is characterized by five independent elastic constants. The bounding method that is described in the references [9] and [12] is briefly summarized as follows: Assume that either the displacements or the tractions acting on the boundary of the specimen are specified. The strain or complementary energy, W, of the actual strain or stress field is always less than the strain energy, W^{ε}, or the complementary energy, W^{C}, of some admissible strain or stress field, or

$$W^{\varepsilon} \geq W \tag{1-1}$$

$$W^{C} \geq W \tag{1-2}$$

The effective Hooke's law yields

$$\sigma_{ij} = C^{*}_{ijkl}\, \varepsilon_{kl} \tag{1-3}$$

$$\varepsilon_{ij} = S^{*}_{ijkl}\, \sigma_{kl} \tag{1-4}$$

where σ_{ij}, ε_{ij}, C^*_{ijkl}, and S^*_{ijkl} are the average stress and strain and the effective moduli and the compliances respectively. With the use of Equations (1-1) and (1-3), the upper bound and the use of Equations (1-2) and (1-4) the lower bound of the effective moduli are obtained respectively. Since the material under consideration requires five effective moduli, five relationships or equations are required. Hence a number of boundary value problems must be formulated and solved. Hashin and Rosen have found such boundary value problems for the composite that can be solved. Although the same approach may be tempting to apply to other geometric shapes of constituents, there is no assurance as to whether the boundary value problems can be solved.

The general multiphase medium of random geometry was first discussed by Hill [11]. Paul [13] derived the bound of effective moduli. Hashin and Shtrikman [14, 15] constructed improved bounds for arbitrary constituent geometry.

Dong, Pister, and Taylor [16] analyzed laminated plates and shells. A vast material on the subject may be found in the references [17, 18].

In contrast with approaches stated above, all of which are based on static analysis in the theory of elasticity, Behrens computed the effective moduli of lamellar composite [19] and of filamentary composites with rectangular symmetry [20] based on the analysis of long-waves propagation through the media.

A third method is proposed here to predict the effective moduli of composite materials. The method proposed is to simulate numerically the laboratory tests involved in obtaining the effective moduli for a

given composite specimen. The test specimen and the load(s) are simulated with a three-dimensional finite element method and the results are analyzed using energy theorems and some invariant quantities of the two systems to predict the effective moduli.

The principal advantage of this method is that it can handle very large classes of the posed problems many of which could not be treated with the first two approaches due to mathematical complexity.

CHAPTER II

ABOUT THE FINITE ELEMENT METHOD

General Comments

The finite element method is a method of approximate simulation of a continuum. It is possible to consider very general problems such as the dynamic response of systems with nonlinear material characteristics and geometric nonlinearities, including the effects of arbitrary temperature distributions, etc. In this dissertation, however, the employment of the finite element method is limited to the simulation of isothermal, static, linear elastic problems.

With this limited scope, the simulation procedure is summarized as follows: The region occupied by the continuum under consideration is divided into a finite number of subregions. The geometric shape of the subregions is chosen so as to facilitate the subsequent study of the subregions. This step of the procedure is usually referred to as discretization, the subregions as elements, and it is demonstrated in Figures 3 and 4. Subsequently the displacement functions are constructed. In this work, the displacement functions are chosen to be of polynomial form and in terms of the displacement of some reference points of the element which are usually referred to as nodal points and some additional parameters to permit additional freedom. The number of degrees of freedom depends upon the number of reference points and the desired order of variation of the strain field. The displacement functions are structured in such a way as to include the rigid

body motion, constant strain, and continuity of displacement at the common boundary elements.

These displacement functions are often called the shape functions. It is apparent that the degree of approximation depends upon the number of the nodal points in such element, the degree of polynomials, and the other parameters included in the shape functions.

Equilibrium Equation

The equilibrium equations for a single element are derived first and subsequently they are extended to cover the entire body under consideration. Under the assumption that the forces acting on the body are conservative the principle of minimum potential may be invoked,

$$\delta\pi = \delta(U + V) = 0 \tag{2-1}$$

where V is the potential of the forces acting on the body,

$$V = - W \tag{2-2}$$

with W being the work done by the forces. Assuming that the region is occupied by a linear elastic medium, one has

$$U = \tfrac{1}{2} \int \{\varepsilon\}^T \{\sigma\} \, dv \tag{2-3}$$

where

$$\{\sigma\} = [C] \{\varepsilon\} \tag{2-4}$$

and

$$[C] = \begin{bmatrix} C_{11} & C_{12} & C_{13} & C_{14} & C_{15} & C_{16} \\ C_{12} & C_{22} & C_{23} & C_{24} & C_{25} & C_{26} \\ C_{13} & C_{23} & C_{33} & C_{34} & C_{35} & C_{36} \\ C_{14} & C_{24} & C_{34} & C_{44} & C_{45} & C_{46} \\ C_{15} & C_{25} & C_{35} & C_{45} & C_{55} & C_{56} \\ C_{16} & C_{26} & C_{36} & C_{46} & C_{56} & C_{66} \end{bmatrix} \tag{2-5}$$

Hence, Equation (2-3) may be written as

$$U = (1/2) \int \{\varepsilon\}^T [C] \{\varepsilon\} \, dv \tag{2-6}$$

The strain field is given by

$$\varepsilon_{ij} = (1/2) \left[\frac{\partial u_i}{\partial x_j} + \frac{\partial u_j}{\partial x_i} \right] \tag{2-7}$$

where u is the displacement vector at some arbitrary point in the element. In the development which follows, the displacement field is assumed to be expressed only in terms of displacement vectors, $\{u\}^e$, of the nodal points. The procedure can easily be extended to include additional degrees of freedom as will be shown in Chapter III. With this assumption, it follows that

$$\{u\} = [N] \{u\}^e \tag{2-8}$$

The shape functions are chosen so that

$$N_i (r_j) = \delta_{ij} \tag{2-9}$$

where r_j is the position vector of the j-nodal point and δ_{ij} is Kronecker delta. Substituting Equations (2-8) and (2-9) into

Equation (2-7), one has the strain field in terms of the nodal displacement function. Denoting the result of the above mentioned operations by the matrix [B], the strain field at an arbitrary point in the element takes the form

$$\{\varepsilon\} = [B]\ \{u\}^e \tag{2-10}$$

and the strain energy becomes

$$U = (1/2) \int \{u\}^{e^T}\ [B]^T\ [C]\ [B]\ \{u\}^e\ dv \tag{2-11}$$

If {P} and {T} are the body force and tractions acting on the element, then the work done by them is

$$W = \int_v \{u\}^T\ \{P\}\ dv + \int_s \{u\}^T\ \{T\}\ ds \tag{2-12}$$

or in terms of the displacement vectors of the nodal points, by means of Equation (2-8)

$$W = \int_v \{u\}^{e^T}\ [N]^T\ \{P\}\ dv + \int_s \{u\}^{e^T} [N]^T \{T\} ds \tag{2-13}$$

Substituting Equations (2-11) and (2-13) into Equation (2-1) one obtains

$$\delta \left\{ (1/2) \int_v \left[\{u\}^{e^T}\ [B]^T\ [C]\ [B] \{u\}^e - 2\{u\}^{e^T}\ [N]^T\ \{P\} \right] dv \right.$$
$$\left. - \int_s \{u\}^{e^T}\ [N]^T\ \{T\}\ ds \right\} = 0 \tag{2-14}$$

which yields

$$\delta\{u\}^{e^T}\left\{\int_v [B]^T[C][B]\,dv\,\{u\}^e - \int_v [N]^T\{P\}\,dv - \int_s [N]^T\{T\}\,ds\right\} = 0 \quad (2\text{-}15)$$

But the arbitrariness of $\delta\{u\}^e$ demands that the expression within the bracket vanish. Adopting the notation

$$[k]^e = \int_v [B]^T\,[C]\,[B]\,dv \quad (2\text{-}16)$$

$$\{f\}^e = \int_v [N]^T\,\{P\}\,dv + \int_s [N]^T\,\{T\}\,ds \quad (2\text{-}17)$$

one obtains

$$[k]^e\,\{u\}^e = \{f\}^e \quad (2\text{-}18)$$

The equations in Equation (2-18) are the element equilibrium equations. $[k]^e$ is the element stiffness matrix, while $\{f\}^e$ is the load vector corresponding to the nodal points.

Assemblage of the Individual Element to the Whole Structure

To extend the equation of equilibrium to the whole structure, it is sufficient to recognize that continuity of displacement requires that adjacent elements have the same displacement at common nodes.

Consequently the corresponding stiffness matrix components are the sum of the corresponding components of the stiffness matrices of the elements containing the points under consideration. A similar statement is true for the force matrix.

As an example, consider the body consisting of two elements as shown in Figure 5. Each element has eight nodal points, four of which are common to both. The resulting equilibrium equations are given by Equation (2-19) where $[k^m_{ij}]$ is nodal force at i^{th} node of element m due

$$
\begin{bmatrix}
[k^1_{11}] & [k^1_{12}] & [k^1_{13}] & [k^1_{14}] & [k^1_{15}] & [k^1_{16}] & [k^1_{17}] & [k^1_{18}] & [0] & [0] & [0] & [0] \\
[k^1_{21}] & [k^1_{22}] & [k^1_{23}] & [k^1_{24}] & [k^1_{25}] & [k^1_{26}] & [k^1_{27}] & [k^1_{28}] & [0] & [0] & [0] & [0] \\
[k^1_{31}] & [k^1_{32}] & [k^1_{33}] & [k^1_{34}] & [k^1_{35}] & [k^1_{36}] & [k^1_{37}] & [k^1_{38}] & [0] & [0] & [0] & [0] \\
[k^1_{41}] & [k^1_{42}] & [k^1_{43}] & [k^1_{44}] & [k^1_{45}] & [k^1_{46}] & [k^1_{47}] & [k^1_{48}] & [0] & [0] & [0] & [0] \\
[k^1_{51}] & [k^1_{52}] & [k^1_{53}] & [k^1_{54}] & \begin{bmatrix} k^1_{55} \\ +k^2_{11} \end{bmatrix} & \begin{bmatrix} k^1_{56} \\ +k^2_{12} \end{bmatrix} & \begin{bmatrix} k^1_{57} \\ +k^2_{13} \end{bmatrix} & \begin{bmatrix} k^1_{58} \\ +k^2_{14} \end{bmatrix} & [k^2_{15}] & [k^2_{16}] & [k^2_{17}] & [k^2_{18}] \\
[k^1_{61}] & [k^1_{62}] & [k^1_{63}] & [k^1_{64}] & \begin{bmatrix} k^1_{65} \\ +k^2_{21} \end{bmatrix} & \begin{bmatrix} k^1_{66} \\ +k^2_{22} \end{bmatrix} & \begin{bmatrix} k^1_{67} \\ +k^2_{23} \end{bmatrix} & \begin{bmatrix} k^1_{68} \\ +k^2_{24} \end{bmatrix} & [k^2_{25}] & [k^2_{26}] & [k^2_{27}] & [k^2_{28}] \\
[k^1_{71}] & [k^1_{72}] & [k^1_{73}] & [k^1_{74}] & \begin{bmatrix} k^1_{75} \\ +k^2_{31} \end{bmatrix} & \begin{bmatrix} k^1_{76} \\ +k^2_{32} \end{bmatrix} & \begin{bmatrix} k^1_{77} \\ +k^2_{33} \end{bmatrix} & \begin{bmatrix} k^1_{78} \\ +k^2_{34} \end{bmatrix} & [k^2_{35}] & [k^2_{36}] & [k^2_{37}] & [k^2_{38}] \\
[k^1_{81}] & [k^1_{82}] & [k^1_{83}] & [k^1_{84}] & \begin{bmatrix} k^1_{85} \\ +k^2_{41} \end{bmatrix} & \begin{bmatrix} k^1_{86} \\ +k^2_{42} \end{bmatrix} & \begin{bmatrix} k^1_{87} \\ +k^2_{43} \end{bmatrix} & \begin{bmatrix} k^1_{88} \\ +k^2_{44} \end{bmatrix} & [k^2_{45}] & [k^2_{46}] & [k^2_{47}] & [k^2_{48}] \\
[0] & [0] & [0] & [0] & [k^2_{51}] & [k^2_{52}] & [k^2_{53}] & [k^2_{54}] & [k^2_{55}] & [k^2_{56}] & [k^2_{57}] & [k^2_{58}] \\
[0] & [0] & [0] & [0] & [k^2_{61}] & [k^2_{62}] & [k^2_{63}] & [k^2_{64}] & [k^2_{65}] & [k^2_{66}] & [k^2_{67}] & [k^2_{68}] \\
[0] & [0] & [0] & [0] & [k^2_{71}] & [k^2_{72}] & [k^2_{73}] & [k^2_{74}] & [k^2_{75}] & [k^2_{76}] & [k^2_{77}] & [k^2_{78}] \\
[0] & [0] & [0] & [0] & [k^2_{81}] & [k^2_{82}] & [k^2_{83}] & [k^2_{84}] & [k^2_{85}] & [k^2_{86}] & [k^2_{87}] & [k^2_{88}]
\end{bmatrix}
\begin{Bmatrix} \{\vec{u}_1\} \\ \{\vec{u}_2\} \\ \{\vec{u}_3\} \\ \{\vec{u}_4\} \\ \{\vec{u}_5\} \\ \{\vec{u}_6\} \\ \{\vec{u}_7\} \\ \{\vec{u}_8\} \\ \{\vec{u}_9\} \\ \{\vec{u}_{10}\} \\ \{\vec{u}_{11}\} \\ \{\vec{u}_{12}\} \end{Bmatrix}
=
\begin{Bmatrix} \{\vec{f}^1_1\} \\ \{\vec{f}^1_2\} \\ \{\vec{f}^1_3\} \\ \{\vec{f}^1_4\} \\ \{\vec{f}^1_5\}+\{\vec{f}^2_1\} \\ \{\vec{f}^1_6\}+\{\vec{f}^2_2\} \\ \{\vec{f}^1_7\}+\{\vec{f}^2_3\} \\ \{\vec{f}^1_8\}+\{\vec{f}^2_4\} \\ \{\vec{f}^2_5\} \\ \{\vec{f}^2_6\} \\ \{\vec{f}^2_7\} \\ \{\vec{f}^2_8\} \end{Bmatrix}
$$

(2-19)

to unit displacement of j^{th} node of element m. In general the equilibrium equations for the whole body have the form

$$[K]\ \{U\} = \{F\} \tag{2-20}$$

where [K] is the stiffness matrix of the whole body compiled from the stiffness matrix of the individual elements comprising the body, {F} is the force column containing all the forces associated with all the nodal points.

Boundary Condition

The force boundary conditions are easily applied on the overall equilibrium equation by inserting the amount of the prescribed forces for the nodal points into the corresponding row of the load vector. To apply the displacement boundary conditions, the stiffness matrix as well as the load vector need be modified. Consider the overall equilibrium equation as shown in Equation (2-21). Suppose one wants to specify the i^{th} displacement to be equal to δ. This can be done by setting all of the elements in the i^{th} row of the stiffness matrix equal to zero except k_{ii} and by setting $F_i = k_{ii}\delta$ as shown in Equation (2-22). However, by doing so, we have destroyed the symmetric form of the stiffness matrix. To maintain the symmetric form, the load vector as well as the stiffness matrix need be modified as shown in Equation (2-23) [18].

After the boundary conditions are applied, the overall equilibrium equations are solved for the nodal displacement. Formally, one may write

$$\begin{bmatrix} K_{11} & \cdots & K_{1i} & \cdots & K_{1N} \\ \vdots & & \vdots & & \vdots \\ K_{i1} & \cdots & K_{ii} & \cdots & K_{iN} \\ \vdots & & \vdots & & \vdots \\ K_{N1} & \cdots & K_{Ni} & & K_{NN} \end{bmatrix} \begin{Bmatrix} U_1 \\ \vdots \\ U_i \\ \vdots \\ U_N \end{Bmatrix} = \begin{Bmatrix} F_1 \\ \vdots \\ F_i \\ \vdots \\ F_N \end{Bmatrix} \tag{2-21}$$

$$\begin{bmatrix} K_{11} & \cdots & K_{1i} & \cdots & K_{1N} \\ \vdots & & \vdots & & \vdots \\ 0 & \cdots & K_{ii} & \cdots & 0 \\ \vdots & & \vdots & & \vdots \\ K_{N1} & \cdots & K_{Ni} & \cdots & K_{NN} \end{bmatrix} \begin{Bmatrix} U_1 \\ \vdots \\ U_i \\ \vdots \\ U_N \end{Bmatrix} = \begin{Bmatrix} F_1 \\ \vdots \\ K_{ii}\delta \\ \vdots \\ F_N \end{Bmatrix} \tag{2-22}$$

$$\begin{bmatrix} K_{11} & \cdots & 0 & \cdots & K_{1N} \\ \vdots & & \vdots & & \vdots \\ 0 & \cdots & K_{ii} & \cdots & 0 \\ \vdots & & \vdots & & \vdots \\ K_{N1} & \cdots & 0 & \cdots & K_{NN} \end{bmatrix} \begin{Bmatrix} U_1 \\ \vdots \\ U_i \\ \vdots \\ U_N \end{Bmatrix} = \begin{Bmatrix} F_1 - K_{1i}\delta \\ \vdots \\ K_{ii}\delta \\ \vdots \\ F_N - K_{Ni}\delta \end{Bmatrix} \tag{2-23}$$

$$\{U\} = [K]^{-1} \{F\} \tag{2-24}$$

where $\{U\}$ contains all of the nodal displacement components of the entire structure.

CHAPTER III

THREE-DIMENSIONAL FINITE ELEMENT WITH A SPECIFIC SHAPE FUNCTION

The Shape Function

As it was pointed out in the previous chapter that the body under consideration is divided into a number of elements. In each element the nodal points are chosen and in terms of the displacements of these points the equilibrium equations are formed. Let such an element be a curvilinear hexadedron as shown in Figure 6. Introduce now two frames of reference, one global which refers to the whole body, and a local one whose origin is at the centroid of the hexahedron. The transformation of the global coordinates into the local coordinates is constructed in such a way as to map the hexahedron into a cube as shown in Figure 7. This construction is used to permit the division of the body into convenient subregions and yet the individual subregions, the elements, be eventually mapped into regions of simple geometry. Such a procedure simplifies significantly the subsequent numerical operations. The following is such a transformation:

$$x = \sum_{i=1}^{8} a_i \, x_i$$

$$y = \sum_{i=1}^{8} a_i \, y_i \qquad (3\text{-}1)$$

$$z = \sum_{i=1}^{8} a_i \, z_i$$

where

$$\begin{aligned}
a_1 &= 1/8 \ (1+\xi)(1-\eta)(1-\zeta) \\
a_2 &= 1/8 \ (1+\xi)(1+\eta)(1-\zeta) \\
a_3 &= 1/8 \ (1-\xi)(1+\eta)(1-\zeta) \\
a_4 &= 1/8 \ (1-\xi)(1-\eta)(1-\zeta) \\
a_5 &= 1/8 \ (1+\xi)(1-\eta)(1+\zeta) \\
a_6 &= 1/8 \ (1+\xi)(1+\eta)(1+\zeta) \\
a_7 &= 1/8 \ (1-\xi)(1+\eta)(1+\zeta) \\
a_8 &= 1/8 \ (1-\xi)(1-\eta)(1+\zeta)
\end{aligned} \qquad (3\text{-}2)$$

and x, y, z are the global coordinates of an arbitrary point in the element, x_i, y_i, z_i are the global coordinates of the nodal points, ξ, η, ζ are the local coordinates of an arbitrary point in the element.

As it was pointed out previously, the displacement functions structured in polynomial form in terms of the displacements of the nodal points. A suitable set of such polynomial is

$$\begin{aligned}
u_x &= \sum_{i=1}^{8} a_i \, u_{x_i} \\
u_y &= \sum_{i=1}^{8} a_i \, u_{y_i} \\
u_z &= \sum_{i=1}^{8} a_i \, u_{z_i}
\end{aligned} \qquad (3\text{-}3)$$

and is referred to as "isoparametric representation," [21]. In this work, however, a modified isoparametric representation is adopted, [22].

$$
\begin{aligned}
u_x &= \sum_{i=1}^{8} a_i u_{x_i} + a_9 \alpha_{x_1} + a_{10} \alpha_{x_2} + a_{11} \alpha_{x_3} \\
u_y &= \sum_{i=1}^{8} a_i u_{y_i} + a_9 \alpha_{y_1} + a_{10} \alpha_{y_2} + a_{11} \alpha_{y_3} \\
u_z &= \sum_{i=1}^{8} a_i u_{z_i} + a_9 \alpha_{z_1} + a_{10} \alpha_{z_2} + a_{11} \alpha_{z_3}
\end{aligned}
\tag{3-4}
$$

where

$$
\begin{aligned}
a_9 &= (1-\xi^2) \\
a_{10} &= (1-\eta^2) \\
a_{11} &= (1-\zeta^2)
\end{aligned}
\tag{3-5}
$$

and the constants $\alpha_{x_1}, \ldots, \alpha_{z_3}$ are introduced to allow linear variation in the strain field. Equation (3-4) is used as the shape function of the displacement field for the rest of this formulation.

With this choice of the shape functions, the constant, the linear, and some terms of the quadratic distribution of the strain field can be simulated. However, since the undeformed shape of an element is a hexahedron, it may require many elements to discretize a curved boundary surface of a structure. Due to the additional constants $\alpha_{x_1}, \ldots, \alpha_{z_3}$, continuity between the adjacent elements is assured only at the nodal points. Despite the violation of continuity with adjacent elements in general, the modified isoparametric shape function

behaves superior over the isoparametric shape function due to the introduction of the linear variation of the strain field, [22].

The Strain Matrix

The strain-displacement relationship in matrix form is given by

$$\begin{Bmatrix} \varepsilon_{xx} \\ \varepsilon_{yy} \\ \varepsilon_{zz} \\ 2\,\varepsilon_{xy} \\ 2\,\varepsilon_{yz} \\ 2\,\varepsilon_{xz} \end{Bmatrix} = \begin{Bmatrix} \frac{\partial u_x}{\partial x} \\ \frac{\partial u_y}{\partial y} \\ \frac{\partial u_z}{\partial z} \\ \frac{\partial u_x}{\partial y} + \frac{\partial u_y}{\partial x} \\ \frac{\partial u_y}{\partial z} + \frac{\partial u_z}{\partial y} \\ \frac{\partial u_x}{\partial z} + \frac{\partial u_z}{\partial x} \end{Bmatrix} \tag{3-6}$$

From Equation (3-4) it can be seen that the displacement {u} of an arbitrary point is a function of ξ, η, ζ. Since

$$\begin{aligned} \frac{\partial}{\partial \xi} &= \frac{\partial}{\partial x}\frac{\partial x}{\partial \xi} + \frac{\partial}{\partial y}\frac{\partial y}{\partial \xi} + \frac{\partial}{\partial z}\frac{\partial z}{\partial \xi} \\ \frac{\partial}{\partial \eta} &= \frac{\partial}{\partial x}\frac{\partial x}{\partial \eta} + \frac{\partial}{\partial y}\frac{\partial y}{\partial \eta} + \frac{\partial}{\partial z}\frac{\partial z}{\partial \eta} \\ \frac{\partial}{\partial \zeta} &= \frac{\partial}{\partial x}\frac{\partial x}{\partial \zeta} + \frac{\partial}{\partial y}\frac{\partial}{\partial \zeta} + \frac{\partial}{\partial z}\frac{\partial z}{\partial \zeta} \end{aligned} \tag{3-7}$$

or in matrix form

$$\begin{Bmatrix} \frac{\partial}{\partial \xi} \\ \frac{\partial}{\partial \eta} \\ \frac{\partial}{\partial \zeta} \end{Bmatrix} = \begin{bmatrix} \frac{\partial x}{\partial \xi} & \frac{\partial y}{\partial \xi} & \frac{\partial z}{\partial \xi} \\ \frac{\partial x}{\partial \eta} & \frac{\partial y}{\partial \eta} & \frac{\partial z}{\partial \eta} \\ \frac{\partial x}{\partial \zeta} & \frac{\partial y}{\partial \zeta} & \frac{\partial z}{\partial \zeta} \end{bmatrix} \begin{Bmatrix} \frac{\partial}{\partial x} \\ \frac{\partial}{\partial y} \\ \frac{\partial}{\partial z} \end{Bmatrix} = [J] \begin{Bmatrix} \frac{\partial}{\partial x} \\ \frac{\partial}{\partial y} \\ \frac{\partial}{\partial z} \end{Bmatrix} \tag{3-8}$$

the partial derivative operator becomes

$$\begin{Bmatrix} \frac{\partial}{\partial x} \\ \frac{\partial}{\partial y} \\ \frac{\partial}{\partial z} \end{Bmatrix} = [J]^{-1} \begin{Bmatrix} \frac{\partial}{\partial \xi} \\ \frac{\partial}{\partial \eta} \\ \frac{\partial}{\partial \zeta} \end{Bmatrix} \tag{3-9}$$

Substituting Equation (3-9) into Equation (3-6), one obtains the strain-displacement relationship as shown in Equation (3-10) where J'_{ij} is an element of the matrix $[J]^{-1}$. Introducing [D] matrix which is the 6 by 3 matrix whose elements are partial differential operators such as

$$D_{11} = J'_{11} \frac{\partial}{\partial \xi} + J'_{12} \frac{\partial}{\partial \eta} + J'_{13} \frac{\partial}{\partial \zeta} \tag{3-11}$$

etc., Equation (3-10) is expressed as

$$\{\varepsilon\} = [D] \{u\} \tag{3-12}$$

It is noted that

$$\begin{aligned} D_{11} &= D_{42} = D_{63} \\ D_{22} &= D_{41} = D_{53} \\ D_{33} &= D_{61} = D_{52} \end{aligned} \tag{3-13}$$

$$
\begin{Bmatrix} \varepsilon_{xx} \\ \varepsilon_{yy} \\ \varepsilon_{zz} \\ 2\varepsilon_{xy} \\ 2\varepsilon_{yz} \\ 2\varepsilon_{zx} \end{Bmatrix} =
\left[\begin{array}{c|c|c}
J'_{11}\frac{\partial}{\partial\xi} + J'_{12}\frac{\partial}{\partial\eta} + J'_{13}\frac{\partial}{\partial\zeta} & 0 & 0 \\ \hline
0 & J'_{21}\frac{\partial}{\partial\xi} + J'_{22}\frac{\partial}{\partial\eta} + J'_{23}\frac{\partial}{\partial\zeta} & 0 \\ \hline
0 & 0 & J'_{31}\frac{\partial}{\partial\xi} + J'_{32}\frac{\partial}{\partial\eta} + J'_{33}\frac{\partial}{\partial\zeta} \\ \hline
J'_{21}\frac{\partial}{\partial\xi} + J'_{22}\frac{\partial}{\partial\eta} + J'_{23}\frac{\partial}{\partial\zeta} & J'_{11}\frac{\partial}{\partial\xi} + J'_{12}\frac{\partial}{\partial\eta} + J'_{13}\frac{\partial}{\partial\zeta} & 0 \\ \hline
0 & J'_{31}\frac{\partial}{\partial\xi} + J'_{32}\frac{\partial}{\partial\eta} + J'_{33}\frac{\partial}{\partial\zeta} & J'_{21}\frac{\partial}{\partial\xi} + J'_{22}\frac{\partial}{\partial\eta} + J'_{23}\frac{\partial}{\partial\zeta} \\ \hline
J'_{31}\frac{\partial}{\partial\xi} + J'_{32}\frac{\partial}{\partial\eta} + J'_{33}\frac{\partial}{\partial\zeta} & 0 & J'_{11}\frac{\partial}{\partial\xi} + J'_{12}\frac{\partial}{\partial\eta} + J'_{13}\frac{\partial}{\partial\zeta}
\end{array}\right]
\begin{Bmatrix} u_x \\ u_y \\ u_z \end{Bmatrix}
$$

(3-10)

Substituting Eq. (3-4) into Eq. (3-10) and using the notation introduced in Eq. (3-11), it gives the following expression for the strain at any point in terms of the nodal displacements and the parameters α :

$$
\begin{Bmatrix} \varepsilon_{xx} \\ \varepsilon_{yy} \\ \varepsilon_{zz} \\ 2\varepsilon_{xy} \\ 2\varepsilon_{yz} \\ 2\varepsilon_{xz} \end{Bmatrix} =
\left[\begin{array}{c|c|c}
[a_1 D_{11}, \ldots, a_{11} D_{11}] & [\quad 0 \quad] & [\quad 0 \quad] \\
\hline
[\quad 0 \quad] & [a_1 D_{22}, \ldots, a_{11} D_{22}] & [\quad 0 \quad] \\
\hline
[\quad 0 \quad] & [\quad 0 \quad] & [a_1 D_{33}, \ldots, a_{11} D_{33}] \\
\hline
[a_1 D_{22}, \ldots, a_{11} D_{22}] & [a_1 D_{11}, \ldots, a_{11} D_{11}] & [\quad 0 \quad] \\
\hline
[\quad 0 \quad] & [a_1 D_{33}, \ldots, a_{11} D_{33}] & [a_1 D_{22}, \ldots, a_{11} D_{22}] \\
\hline
[a_1 D_{33}, \ldots, a_{11} D_{33}] & [\quad 0 \quad] & [a_1 D_{11}, \ldots, a_{11} D_{11}]
\end{array}\right]
\left\{\begin{array}{c}
\left\{\begin{array}{c} u_{x_1} \\ \vdots \\ u_{x_8} \end{array}\right\} \\
\left\{\begin{array}{c} \alpha_{x_1} \\ \alpha_{x_2} \\ \alpha_{x_3} \end{array}\right\} \\
\left\{\begin{array}{c} u_{y_1} \\ \vdots \\ u_{y_8} \end{array}\right\} \\
\left\{\begin{array}{c} \alpha_{y_1} \\ \alpha_{y_2} \\ \alpha_{y_3} \end{array}\right\} \\
\left\{\begin{array}{c} u_{z_1} \\ \vdots \\ u_{z_8} \end{array}\right\} \\
\left\{\begin{array}{c} \alpha_{z_1} \\ \alpha_{z_2} \\ \alpha_{z_3} \end{array}\right\}
\end{array}\right\}
\tag{3-14}
$$

Defining

$$[a_1 D_{11}, \ldots, a_{11} D_{11}] = [B_{11}]$$

$$[a_1 D_{22}, \ldots, a_{11} D_{22}] = [B_{22}] \qquad (3\text{-}15)$$

$$\ldots\ldots\ldots\ldots$$

etc., Equation (3-14) can be written in terms of $[B_{ij}]$ as

$$\begin{Bmatrix} \varepsilon_{xx} \\ \varepsilon_{yy} \\ \varepsilon_{zz} \\ 2\,\varepsilon_{xy} \\ 2\,\varepsilon_{yz} \\ 2\,\varepsilon_{xz} \end{Bmatrix} = \begin{bmatrix} [B_{11}] & [0] & [0] \\ [0] & [B_{22}] & [0] \\ [0] & [0] & [B_{33}] \\ [B_{41}] & [B_{42}] & [0] \\ [0] & [B_{52}] & [B_{53}] \\ [B_{61}] & [0] & [B_{63}] \end{bmatrix} \begin{Bmatrix} \begin{Bmatrix} u_{x_1} \\ \cdot \\ \cdot \\ \cdot \\ \alpha_{x_3} \end{Bmatrix} \\ \begin{Bmatrix} u_{y_1} \\ \cdot \\ \cdot \\ \cdot \\ \alpha_{y_3} \end{Bmatrix} \\ \begin{Bmatrix} u_{z_1} \\ \cdot \\ \cdot \\ \cdot \\ \alpha_{z_3} \end{Bmatrix} \end{Bmatrix} \qquad (3\text{-}16)$$

Using the simple notation introduced, Equation (3-16) is written as

$$\{\varepsilon\} = [B]\,\{u\}^e \qquad (3\text{-}17)$$

The strain-displacement relationship has now been established as shown in Equation (2-10) with the inclusion of the α parameters.

Element Stiffness Matrix

The element stiffness matrix given by Equation (2-16) now has to be written as

$$[k]^e = \int_{-1}^{+1}\int_{-1}^{+1}\int_{-1}^{+1} |J|\,[B]^T[C][B]\,d\xi\,d\eta\,d\zeta \qquad (3\text{-}18)$$

where $|J|$ is the determinant of the Jacobian that is introduced in Equation (3-8). The matrix multiplication in Equation (3-18) yields

$$[B]^T\,[C]\,[B]$$

$$= \frac{E}{(1+\nu)(1-2\nu)} \left[\begin{array}{c|c|c}
(1-\nu)\{B_{11}\}[B_{11}] & \nu\{B_{11}\}[B_{22}] & \nu\{B_{11}\}[B_{33}] \\
+\frac{(1-2\nu)}{2}\{B_{41}\}[B_{41}] & +\frac{(1-2\nu)}{2}\{B_{41}\}[B_{42}] & +\frac{(1-2\nu)}{2}\{B_{61}\}[B_{63}] \\
+\frac{(1-2\nu)}{2}\{B_{61}\}[B_{61}] & & \\
\hline
\nu\{B_{22}\}[B_{11}] & (1-\nu)\{B_{22}\}[B_{22}] & \nu\{B_{22}\}[B_{33}] \\
+\frac{(1-2\nu)}{2}\{B_{42}\}[B_{41}] & +\frac{(1-2\nu)}{2}\{B_{42}\}[B_{42}] & +\frac{(1-2\nu)}{2}\{B_{52}\}[B_{53}] \\
 & \frac{(1-2\nu)}{2}\{B_{52}\}[B_{52}] & \\
\hline
\nu\{B_{33}\}[B_{11}] & \nu\{B_{33}\}[B_{22}] & (1-\nu)\{B_{33}\}[B_{33}] \\
+\frac{(1-2\nu)}{2}\{B_{63}\}[B_{61}] & +\frac{(1-2\nu)}{2}\{B_{53}\}[B_{52}] & +\frac{(1-2\nu)}{2}\{B_{53}\}[B_{53}] \\
 & & +\frac{(1-2\nu)}{2}\{B_{63}\}[B_{63}]
\end{array}\right] \qquad (3\text{-}19)$$

where the matrix multiplication

$$\{B_{11}\}[B_{11}] = \begin{Bmatrix} a_1 D_{11} \\ \cdot \\ \cdot \\ \cdot \\ a_{11} D_{11} \end{Bmatrix} [a_1 D_{11} \cdots a_{11} D_{11}] = \begin{bmatrix} a_1 a_1 D_{11} D_{11} \cdots a_1 a_{11} D_{11} D_{11} \\ \cdot \quad\quad\quad\quad \cdot \\ \cdot \quad\quad\quad\quad \cdot \\ \cdot \quad\quad\quad\quad \cdot \\ a_{11} a_1 D_{11} D_{11} \cdots a_{11} a_{11} D_{11} D_{11} \end{bmatrix}$$

(3-20)

etc.

Element Loading Vector

Equation (2-17) provides the general expression which could be used to calculate the work-equivalent generalized forces associated with each generalized displacement. In the work which follows, the forces associated with the additional α parameters are set equal to zero. This simplifying assumption can be physically interpreted as implying that all real external forces are applied at the nodes. If the external forces are actually distributed, the associated nodal forces can be deduced from Equation (2-17) by neglecting the α parameters in the displacement assumptions.

Static Condensation of the Element Equilibrium Equation

The equilibrium equations as shown in Equation (3-21) contain the parameters α_{x_i},..., etc. To attain the desired form from these equations, the α_{x_i},..., etc. must be eliminated. This goal is achieved in the following manner. The equilibrium equations at this stage are shown in Equation (3-22) where [k] is the stiffness matrix of Equation (3-21). Rearrange the matrix elements in Equation (3-22)

$$
\begin{Bmatrix} f_{x_1} \\ \vdots \\ f_{x_8} \\ 0\,0\,0 \\ f_{y_1} \\ \vdots \\ f_{y_8} \\ 0\,0\,0 \\ f_{z_1} \\ \vdots \\ f_{z_8} \\ 0\,0\,0 \end{Bmatrix} = \int_{-1}^{+1}\int_{-1}^{+1}\int_{-1}^{+1} \frac{E\,|J|}{(1+\nu)(1-2\nu)}
$$

$$
\begin{bmatrix}
(1-\nu)\begin{bmatrix} a_1a_1D_{11}D_{11} & \cdots & a_1a_{11}D_{11}D_{11} \\ \vdots & & \vdots \\ a_{11}a_1D_{11}D_{11} & \cdots & a_{11}a_{11}D_{11}D_{11} \end{bmatrix} & \nu\begin{bmatrix} a_1a_1D_{11}D_{22} & \cdots & a_1a_{11}D_{11}D_{22} \\ \vdots & & \vdots \\ a_{11}a_1D_{11}D_{22} & \cdots & a_{11}a_{11}D_{11}D_{22} \end{bmatrix} & \nu\begin{bmatrix} a_1a_1D_{11}D_{33} & \cdots & a_1a_{11}D_{11}D_{33} \\ \vdots & & \vdots \\ a_{11}a_1D_{11}D_{33} & \cdots & a_{11}a_{11}D_{11}D_{33} \end{bmatrix} \\
+\frac{(1-2\nu)}{2}\begin{bmatrix} a_1a_1D_{22}D_{22} & \cdots & a_1a_{11}D_{22}D_{22} \\ \vdots & & \vdots \\ a_{11}a_1D_{22}D_{22} & \cdots & a_{11}a_{11}D_{22}D_{22} \end{bmatrix} & +\frac{(1-2\nu)}{2}\begin{bmatrix} a_1a_1D_{22}D_{11} & \cdots & a_1a_{11}D_{22}D_{11} \\ \vdots & & \vdots \\ a_{11}a_1D_{22}D_{11} & \cdots & a_{11}a_{11}D_{22}D_{11} \end{bmatrix} & +\frac{(1-2\nu)}{2}\begin{bmatrix} a_1a_1D_{33}D_{11} & \cdots & a_1a_{11}D_{33}D_{11} \\ \vdots & & \vdots \\ a_{11}a_1D_{33}D_{11} & \cdots & a_{11}a_{11}D_{33}D_{11} \end{bmatrix} \\
+\frac{(1-2\nu)}{2}\begin{bmatrix} a_1a_1D_{33}D_{33} & \cdots & a_1a_{11}D_{33}D_{33} \\ \vdots & & \vdots \\ a_{11}a_1D_{33}D_{33} & \cdots & a_{11}a_{11}D_{33}D_{33} \end{bmatrix} & & & \\
\nu\begin{bmatrix} a_1a_1D_{22}D_{11} & \cdots & a_1a_{11}D_{22}D_{11} \\ \vdots & & \vdots \\ a_{11}a_1D_{22}D_{11} & \cdots & a_{11}a_{11}D_{22}D_{11} \end{bmatrix} & (1-\nu)\begin{bmatrix} a_1a_1D_{22}D_{22} & \cdots & a_1a_{11}D_{22}D_{22} \\ \vdots & & \vdots \\ a_{11}a_1D_{22}D_{22} & \cdots & a_{11}a_{11}D_{22}D_{22} \end{bmatrix} & \nu\begin{bmatrix} a_1a_1D_{22}D_{33} & \cdots & a_1a_{11}D_{22}D_{33} \\ \vdots & & \vdots \\ a_{11}a_1D_{22}D_{33} & \cdots & a_{11}a_{11}D_{22}D_{33} \end{bmatrix} \\
+\frac{(1-2\nu)}{2}\begin{bmatrix} a_1a_1D_{11}D_{22} & \cdots & a_1a_{11}D_{11}D_{22} \\ \vdots & & \vdots \\ a_{11}a_1D_{11}D_{22} & \cdots & a_{11}a_{11}D_{11}D_{22} \end{bmatrix} & +\frac{(1-2\nu)}{2}\begin{bmatrix} a_1a_1D_{11}D_{11} & \cdots & a_1a_{11}D_{11}D_{11} \\ \vdots & & \vdots \\ a_{11}a_1D_{11}D_{11} & \cdots & a_{11}a_{11}D_{11}D_{11} \end{bmatrix} & +\frac{(1-2\nu)}{2}\begin{bmatrix} a_1a_1D_{33}D_{22} & \cdots & a_1a_{11}D_{33}D_{22} \\ \vdots & & \vdots \\ a_{11}a_1D_{33}D_{22} & \cdots & a_{11}a_{11}D_{33}D_{22} \end{bmatrix} \\
& +\frac{(1-2\nu)}{2}\begin{bmatrix} a_1a_1D_{33}D_{33} & \cdots & a_1a_{11}D_{33}D_{33} \\ \vdots & & \vdots \\ a_{11}a_1D_{33}D_{33} & \cdots & a_{11}a_{11}D_{33}D_{33} \end{bmatrix} & & \\
\nu\begin{bmatrix} a_1a_1D_{33}D_{11} & \cdots & a_1a_{11}D_{33}D_{11} \\ \vdots & & \vdots \\ a_{11}a_1D_{33}D_{11} & \cdots & a_{11}a_{11}D_{33}D_{11} \end{bmatrix} & \begin{bmatrix} a_1a_1D_{33}D_{22} & \cdots & a_1a_{11}D_{33}D_{22} \\ \vdots & & \vdots \\ a_{11}a_1D_{33}D_{22} & \cdots & a_{11}a_{11}D_{33}D_{22} \end{bmatrix} & (1-\nu)\begin{bmatrix} a_1a_1D_{33}D_{33} & \cdots & a_1a_{11}D_{33}D_{33} \\ \vdots & & \vdots \\ a_{11}a_1D_{33}D_{33} & \cdots & a_{11}a_{11}D_{33}D_{33} \end{bmatrix} \\
+\frac{(1-2\nu)}{2}\begin{bmatrix} a_1a_1D_{11}D_{33} & \cdots & a_1a_{11}D_{11}D_{33} \\ \vdots & & \vdots \\ a_{11}a_1D_{11}D_{33} & \cdots & a_{11}a_{11}D_{11}D_{33} \end{bmatrix} & +\frac{(1-2\nu)}{2}\begin{bmatrix} a_1a_1D_{22}D_{33} & \cdots & a_1a_{11}D_{22}D_{33} \\ \vdots & & \vdots \\ a_{11}a_1D_{22}D_{33} & \cdots & a_{11}a_{11}D_{22}D_{33} \end{bmatrix} & +\frac{(1-2\nu)}{2}\begin{bmatrix} a_1a_1D_{22}D_{22} & \cdots & a_1a_{11}D_{22}D_{22} \\ \vdots & & \vdots \\ a_{11}a_1D_{22}D_{22} & \cdots & a_{11}a_{11}D_{22}D_{22} \end{bmatrix} \\
& & +\frac{(1-2\nu)}{2}\begin{bmatrix} a_1a_1D_{11}D_{11} & \cdots & a_1a_{11}D_{11}D_{11} \\ \vdots & & \vdots \\ a_{11}a_1D_{11}D_{11} & \cdots & a_{11}a_{11}D_{11}D_{11} \end{bmatrix}
\end{bmatrix}
\begin{Bmatrix} u_{x_1} \\ \vdots \\ u_{x_8} \\ \alpha_{x_1} \\ \alpha_{x_2} \\ \alpha_{x_3} \\ u_{y_1} \\ \vdots \\ u_{y_8} \\ \alpha_{y_1} \\ \alpha_{y_2} \\ \alpha_{y_3} \\ u_{z_1} \\ \vdots \\ u_{z_8} \\ \alpha_{z_1} \\ \alpha_{z_2} \\ \alpha_{z_3} \end{Bmatrix} d\xi\, d\eta\, d\zeta \qquad (3\text{-}21)
$$

$$\left\{\begin{Bmatrix} F_{x_1} \\ \cdot \\ \cdot \\ \cdot \\ F_{x_8} \\ 0 \\ 0 \\ 0 \end{Bmatrix} \begin{Bmatrix} F_{y_1} \\ \cdot \\ \cdot \\ \cdot \\ F_{y_8} \\ 0 \\ 0 \\ 0 \end{Bmatrix} \begin{Bmatrix} F_{z_1} \\ \cdot \\ \cdot \\ \cdot \\ F_{z_8} \\ 0 \\ 0 \\ 0 \end{Bmatrix}\right\} = \left[\quad k \quad\right] \left\{\begin{Bmatrix} u_{x_1} \\ \cdot \\ \cdot \\ \cdot \\ u_{x_8} \\ \alpha_{x_1} \\ \alpha_{x_2} \\ \alpha_{x_3} \end{Bmatrix} \begin{Bmatrix} u_{y_1} \\ \cdot \\ \cdot \\ \cdot \\ u_{y_8} \\ \alpha_{y_1} \\ \alpha_{y_2} \\ \alpha_{y_3} \end{Bmatrix} \begin{Bmatrix} u_{z_1} \\ \cdot \\ \cdot \\ \cdot \\ u_{z_8} \\ \alpha_{z_1} \\ \alpha_{z_2} \\ \alpha_{z_3} \end{Bmatrix}\right\}$$

(3-22)

$$
\left\{\begin{array}{c}
\left\{\begin{array}{c} F_{x_1} \\ F_{y_1} \\ F_{z_1} \end{array}\right\} \\
\cdot \\ \cdot \\ \cdot \\
\left\{\begin{array}{c} F_{x_8} \\ F_{y_8} \\ F_{z_8} \end{array}\right\} \\
\hline
\left\{\begin{array}{c} 0 \\ 0 \\ 0 \end{array}\right\} \\
\left\{\begin{array}{c} 0 \\ 0 \\ 0 \end{array}\right\} \\
\left\{\begin{array}{c} 0 \\ 0 \\ 0 \end{array}\right\}
\end{array}\right\}
=
\left[\begin{array}{c|c}
k_{aa} & k_{ab} \\
\hline
k_{ba} & k_{bb}
\end{array}\right]
\left\{\begin{array}{c}
\left\{\begin{array}{c} u_{x_1} \\ u_{y_1} \\ u_{z_1} \end{array}\right\} \\
\cdot \\ \cdot \\ \cdot \\
\left\{\begin{array}{c} u_{x_8} \\ u_{y_8} \\ u_{z_8} \end{array}\right\} \\
\hline
\left\{\begin{array}{c} \alpha_{x_1} \\ \alpha_{y_1} \\ \alpha_{z_1} \end{array}\right\} \\
\left\{\begin{array}{c} \alpha_{x_2} \\ \alpha_{y_2} \\ \alpha_{z_2} \end{array}\right\} \\
\left\{\begin{array}{c} \alpha_{x_3} \\ \alpha_{y_3} \\ \alpha_{z_3} \end{array}\right\}
\end{array}\right\}
\tag{3-23}
$$

so that all of the elements corresponding to α's are on the bottom of the matrix as shown in Equation (3-23), where the original matrix elements in [k] are renamed according to their new position. In abbreviated notation, Equation (3-23) becomes

$$\begin{Bmatrix} \{F_a\} \\ \{F_b\} \end{Bmatrix} = \begin{bmatrix} [k_{aa}] & [k_{ab}] \\ [k_{ba}] & [k_{bb}] \end{bmatrix} \begin{Bmatrix} \{u\}^e \\ \{\alpha\} \end{Bmatrix} \tag{3-24}$$

or

$$\{F\}_a = [k_{aa}]\{u\}^e + [k_{ab}]\{\alpha\} \tag{3-25}$$

$$\{F_b\} = [k_{ba}]\{u\}^e + [k_{bb}]\{\alpha\} \tag{3-26}$$

where $\{F_b\} = 0$ since the forces are applied only at the nodal points in this investigation. Solving for $\{\alpha\}$ in Equation (3-26)

$$\{\alpha\} = -[k_{bb}]^{-1}[k_{ba}]\{u\}^e \tag{3-27}$$

Substituting Equation (3-27) into Equation (3-25), one has

$$\begin{aligned} \{F_a\} &= [k_{aa}]\{u\}^e - [k_{ab}][k_{bb}]^{-1}[k_{ba}]\{u\} \\ &= ([k_{aa}] - [k_{ab}][k_{bb}]^{-1}[k_{ba}])\{u\}^e \end{aligned} \tag{3-28}$$

Let

$$[k^*]^e = ([k_{aa}] - [k_{ab}][k_{bb}]^{-1}[k_{ba}] \tag{3-29}$$

Then

$$\{F_a\} = [k^*]^e\{u\}^e \tag{3-30}$$

The equations of equilibrium, Equation (3-30), now have the desired form of Equation (2-18).

Integration Algorithm

The integration required in Equation (3-18) is performed by using the Gaussian integration scheme, since economy of integration procedure is vital to this and any large computer simulation. An advantage of a Gaussian integration scheme is that it can approximate the integration very accurately with comparatively small number of points and values of functions associated with these points. For example, the Gauss-Legendre integration formula has following form in three-dimension [23]:

$$\int_{-1}^{+1}\int_{-1}^{+1}\int_{-1}^{+1} f(x,y,z)dx\ dy\ dz \simeq \sum_{i=1}^{l}\sum_{j=1}^{m}\sum_{k=1}^{n} A_i\ A_j\ A_k\ f(x_i,y_j,z_k) \tag{3-30}$$

The particular choice of the argument x_i, y_j, z_k and corresponding weighting factors are listed in Table 1.

The mathematical basis of this scheme is treated extensively in references [24], [25], [26], [27] and will not be repeated here.

CHAPTER IV

COMPUTATION OF EFFECTIVE MODULI

With the scope as stated in Chapter I, the major interest of this investigation is to generate a homogeneous equivalent material which responds the same manner, in the large, as the actual composite. It is expected that this homogeneous material will not exhibit the same mechanical behavior as the heterogeneous material in the small. However, it is required that the equivalent material responds in a same manner as the actual composite in the large. Once this has been accomplished, the total structure is analyzed as if the structure is made of the equivalent material.

Suppose that the composite material consists of two different isotropic materials and that an equivalent material has been generated; the two material specimens are schematically drawn in Figures 8 and 9. In the figures V_0, V_1, V_0^*, and V_1^* are the undeformed and deformed volume of the composite material and undeformed and deformed volume of the equivalent material respectively. ν_1, E_1, ν_2, and E_2 are the elastic moduli of the two constituents of the composite and C_{ij}^* are the moduli of the equivalent material. m, U, m^*, and U^* are the masses of the specimens and the strain energies due to the same loads on the composite and the equivalent material respectively.

In a very general case of the equivalent material the generalized Hooke's law becomes:

$$\begin{Bmatrix} \sigma_{xx} \\ \sigma_{yy} \\ \sigma_{zz} \\ \sigma_{xy} \\ \sigma_{yz} \\ \sigma_{zx} \end{Bmatrix} = \begin{bmatrix} C^*_{11} & C^*_{12} & C^*_{13} & C^*_{14} & C^*_{15} & C^*_{16} \\ C^*_{21} & C^*_{22} & C^*_{23} & C^*_{24} & C^*_{25} & C^*_{26} \\ C^*_{31} & C^*_{32} & C^*_{33} & C^*_{34} & C^*_{35} & C^*_{36} \\ C^*_{41} & C^*_{42} & C^*_{43} & C^*_{44} & C^*_{45} & C^*_{46} \\ C^*_{51} & C^*_{52} & C^*_{53} & C^*_{54} & C^*_{55} & C^*_{56} \\ C^*_{61} & C^*_{62} & C^*_{63} & C^*_{64} & C^*_{65} & C^*_{66} \end{bmatrix} \begin{Bmatrix} \varepsilon_{xx} \\ \varepsilon_{yy} \\ \varepsilon_{zz} \\ \varepsilon_{xy} \\ \varepsilon_{yz} \\ \varepsilon_{zx} \end{Bmatrix} \qquad (4\text{-}1)$$

where $C^*_{ij} = C^*_{ji}$ and are the elastic moduli of the equivalent material. Equation (4-1) can also be written in terms of the compliance matrix $[S^*]$, or

$$\begin{Bmatrix} \varepsilon_{xx} \\ \varepsilon_{yy} \\ \varepsilon_{zz} \\ \varepsilon_{xy} \\ \varepsilon_{yz} \\ \varepsilon_{zx} \end{Bmatrix} = \begin{bmatrix} S^*_{11} & S^*_{12} & S^*_{13} & S^*_{14} & S^*_{15} & S^*_{16} \\ S^*_{21} & S^*_{22} & S^*_{23} & S^*_{24} & S^*_{25} & S^*_{26} \\ S^*_{31} & S^*_{32} & S^*_{33} & S^*_{34} & S^*_{35} & S^*_{36} \\ S^*_{41} & S^*_{42} & S^*_{43} & S^*_{44} & S^*_{45} & S^*_{46} \\ S^*_{51} & S^*_{52} & S^*_{53} & S^*_{54} & S^*_{55} & S^*_{56} \\ S^*_{61} & S^*_{62} & S^*_{63} & S^*_{64} & S^*_{65} & S^*_{66} \end{bmatrix} \begin{Bmatrix} \sigma_{xx} \\ \sigma_{yy} \\ \sigma_{zz} \\ \sigma_{xy} \\ \sigma_{yz} \\ \sigma_{zx} \end{Bmatrix} \qquad (4\text{-}2)$$

where $S^*_{ij} = S^*_{ji}$ and are the compliances of the medium.

To solve for 21 unknowns, 21 equations from Equation (4-2) need be generated. For example, consider the simple compression test for the block specimen loaded along x-direction with the applied stress σ_{xx}. From Equation (4-2),

$$\begin{Bmatrix} \varepsilon_{xx} \\ \varepsilon_{yy} \\ \varepsilon_{zz} \\ \varepsilon_{xy} \\ \varepsilon_{yz} \\ \varepsilon_{zx} \end{Bmatrix} = \begin{bmatrix} & & \\ & S^*_{ij} & \\ & & \end{bmatrix} \begin{Bmatrix} \sigma_{xx} \\ 0 \\ 0 \\ 0 \\ 0 \\ 0 \end{Bmatrix} \tag{4-3}$$

Equation (4-3) gives 6 simple equations as shown in Equation (4-4)

$$\begin{Bmatrix} \varepsilon_{xx} \\ \varepsilon_{yy} \\ \varepsilon_{zz} \\ \varepsilon_{xy} \\ \varepsilon_{yz} \\ \varepsilon_{zx} \end{Bmatrix} = \sigma_{xx} \begin{Bmatrix} S^*_{11} \\ S^*_{21} \\ S^*_{31} \\ S^*_{41} \\ S^*_{51} \\ S^*_{61} \end{Bmatrix} \tag{4-4}$$

Similarly, the compression test loaded along y-direction with the applied load σ_{yy} gives additional relationship as shown in Equation (4-5).

$$\begin{Bmatrix} \varepsilon_{xx} \\ \varepsilon_{yy} \\ \varepsilon_{zz} \\ \varepsilon_{xy} \\ \varepsilon_{yz} \\ \varepsilon_{zx} \end{Bmatrix} = \sigma_{yy} \begin{Bmatrix} S^*_{21} \\ S^*_{22} \\ S^*_{23} \\ S^*_{24} \\ S^*_{25} \\ S^*_{26} \end{Bmatrix} \tag{4-5}$$

In Equation (4-4) and (4-5), the relationships for S^*_{12} and S^*_{21} are duplicated. Continuing to obtain such relationships as shown above by applying σ_{zz}, σ_{xy}, σ_{yz}, σ_{xz} respectively, one obtains 36 such relationships among which only 21 are independent. For each of 21 relationships, the strain components ε_{ij} have to be furnished in order to compute S^*_{ij}.

After obtaining all of the independent S^*_{ij} components, the matrix $[S^*]$ is inverted to obtain $[C^*]$, or

$$[C^*_{ij}] = [S^*_{ij}]^{-1} \tag{4-6}$$

To evaluate S^*_{ij} occurring in Equations (4-4) and (4-5), etc., the strain components ε_{ij} are needed. Since the strain components are given by

$$\varepsilon_{ij} = \frac{\partial U}{\partial \sigma_{ij}} \tag{4-7}$$

the numerical formulation may be written as

$$\varepsilon_{ij} = \frac{\Delta U}{\Delta \sigma_{ij}} \tag{4-8}$$

where $\Delta\sigma_{ij}$ is a small increment of the stress component and is given by

$$\Delta\sigma_{ij} = \sigma'_{ij} - \sigma_{ij} \tag{4-9}$$

and ΔU is the change in strain energy given by

$$\Delta U = U' - U \tag{4-10}$$

where U' and U are the strain energies corresponding to the applied loads which give rise to σ'_{ij} and σ_{ij} respectively. It is systematic and straightforward to use Equation (4-8) to evaluate the strain components. However, since the procedure of using Equation (4-8) requires two computer runs for each strain component, one with the applied load corresponding σ'_{ij} and another with the applied load corresponding σ_{ij}, the expense for the computer time increased more than several times compared with the other procedure that is described in Chapter V. There is another shortcoming of this procedure, i.e., since Equation (4-8) require the difference U'-U, both U' and U need be computed with seven to eight digits of accuracy. To obtain such accurate numbers for U' and U, it might require 30 to 40 degree of integration orders in the Gaussian quadrature integration increasing the computer time further. These requirements limit the further pursuance of this procedure. Therefore, a simple scheme which does not require a long computer execution time was sought, and it turned out that the weighted mean of the displacements gave reasonable results. The specific procedure of taking the weighted mean of the displacement is described in Chapter V.

CHAPTER V

UNIDIRECTIONAL FIBER COMPOSITES

Scope of the Investigation

The finite element procedure which is described in the previous chapters is subsequently applied to the unidirectional fiber composites. The unidirectional fiber composites whose cross-sections are square are investigated first because nearly exact solutions by the method of long-waves are available for comparison [20]. The procedure is then extended to two other unidirectional fiber composites of different fiber cross-sections to investigate the influence on the effective moduli due to the change of the shape of the fiber cross sections.

Unidirectional Fiber Composite with Square Cross-section Fibers

Consider the unidirectional fiber composite whose fiber cross-sections are square and the fibers are repeated periodically in the matrix material as shown in Figure 10. Due to the periodicity of the fibers, only the basic cell as shown in Figure 11 need be considered.

It can be shown that Hooke's law for the equivalent material contain five independent elastic constants C^*_{11}, C^*_{33}, C^*_{12}, C^*_{13}, and C^*_{66} for such geometry, as shown in Equation (5-1).

$$\begin{Bmatrix} \sigma_{xx} \\ \sigma_{yy} \\ \sigma_{zz} \\ \sigma_{xy} \\ \sigma_{yz} \\ \sigma_{zx} \end{Bmatrix} = \begin{bmatrix} C^*_{11} & C^*_{12} & C^*_{13} & 0 & 0 & 0 \\ C^*_{12} & C^*_{11} & C^*_{13} & 0 & 0 & 0 \\ C^*_{13} & C^*_{13} & C^*_{33} & 0 & 0 & 0 \\ 0 & 0 & 0 & C^*_{44} & 0 & 0 \\ 0 & 0 & 0 & 0 & C^*_{66} & 0 \\ 0 & 0 & 0 & 0 & 0 & C^*_{66} \end{bmatrix} \begin{Bmatrix} \varepsilon_{xx} \\ \varepsilon_{yy} \\ \varepsilon_{zz} \\ 2\varepsilon_{xy} \\ 2\varepsilon_{yz} \\ 2\varepsilon_{zx} \end{Bmatrix} \qquad (5\text{-}1)$$

where $C^*_{44} = \frac{1}{2}[C^*_{11} - C^*_{12}]$.

(i) Application of the Finite Element Method

Numerically it is advantageous to compute the elastic moduli C^*_{ij} directly instead of computing the compliance S^*_{ij} and then inverting them to obtain C^*_{ij}. Also, as one goes along computing the C^*_{ij} directly some judgement can be made as to whether the intermediate computations are reasonable and, if not, errors can be corrected immediately; otherwise, one must compute the entire set of S^*_{ij} and invert it to obtain five constants and then check the reliability.

For this particular case, Equation (5-1) can be written as two systems of equations and one single equation,

$$\begin{Bmatrix} \sigma_{xx} \\ \sigma_{yy} \\ \sigma_{zz} \end{Bmatrix} = \begin{bmatrix} C^*_{11} & C^*_{12} & C^*_{13} \\ C^*_{12} & C^*_{11} & C^*_{13} \\ C^*_{13} & C^*_{13} & C^*_{33} \end{bmatrix} \begin{Bmatrix} \varepsilon_{xx} \\ \varepsilon_{yy} \\ \varepsilon_{zz} \end{Bmatrix} \qquad (5\text{-}2)$$

$$\sigma_{xy} = C^*_{44} \; 2\varepsilon_{xy} \qquad (5\text{-}3)$$

$$\begin{Bmatrix} \sigma_{yz} \\ \sigma_{zx} \end{Bmatrix} = C^*_{66} \begin{Bmatrix} 2\varepsilon_{yz} \\ 2\varepsilon_{zx} \end{Bmatrix} \tag{5-4}$$

Consider the system of equations in Equation (5-2). Since there are four unknowns C^*_{11}, C^*_{12}, C^*_{13}, C^*_{33}, more than one test is needed. This can be seen, for example, by considering σ_{xx} only and then by considering σ_{zz} only as shown in Equations (5-5) and (5-6)

$$\begin{Bmatrix} \sigma_{xx} \\ 0 \\ 0 \end{Bmatrix} = \begin{bmatrix} C^*_{11} & C^*_{12} & C^*_{13} \\ C^*_{12} & C^*_{11} & C^*_{13} \\ C^*_{13} & C^*_{13} & C^*_{33} \end{bmatrix} \begin{Bmatrix} \varepsilon'_{xx} \\ \varepsilon'_{yy} \\ \varepsilon'_{zz} \end{Bmatrix} \tag{5-5}$$

$$\begin{Bmatrix} 0 \\ 0 \\ \sigma_{zz} \end{Bmatrix} = \begin{bmatrix} C^*_{11} & C^*_{12} & C^*_{13} \\ C^*_{12} & C^*_{11} & C^*_{13} \\ C^*_{13} & C^*_{13} & C^*_{33} \end{bmatrix} \begin{Bmatrix} \varepsilon_{xx} \\ \varepsilon_{yy} \\ \varepsilon_{zz} \end{Bmatrix} \tag{5-6}$$

where σ_{xx} and σ_{zz} are stresses and ε_{xx}, ε_{yy}, ε_{zz} and ε'_{xx}, ε'_{yy}, ε'_{zz} are the strains to be estimated from the result of the finite element program. In general, the set ε_{xx}, ε_{yy}, ε_{zz} are different from the set ε'_{xx}, ε'_{yy}, ε'_{zz}. Since the first two equations in Equation (5-6) are identical, because $\varepsilon'_{xx} = \varepsilon'_{yy}$ for tractions which result in the indicated stress state, Equations (5-5) and (5-6) give only five independent relationships any four of which may be used to compute the four unknowns.

In order to perform the tests which are implied in Equations (5-5) and (5-6) two simple problems are examined: the basic cell under

axial compression and the cell under lateral compression.

(1) The basic cell under uniform axial compression

Because of the physical, geometric, and loading symmetry only one octant of the basic cell need be considered. This problem is characterized by following boundary conditions:

(a) $T_{zz}(x,y,5) = -10{,}000$ psi and all other stresses on the boundary of the octant are zero.

(b) $u_x(0,y,z) = u_y(x,0,z) = u_z(x,y,0) = 0$

where T_{ij} are the applied traction in j^{th} direction on element area with normal in i^{th} direction.

(2) The basic cell under uniform lateral compression

The same symmetry prevail in this problem as the previous one and only one octant of the basic cell need be considered. The boundary conditions are:

(a) $T_{xx}(5,y,z) = -10{,}000$ psi and all other stresses on the boundary of the octant are zero.

(b) $u_x(0,y,z) = u_y(x,0,z) = u_z(x,y,0) = 0$

In applying finite element method to both problems, the octant is discretized as shown in Figure 12 where circled numbers refer to elements and plain numbers to nodal points. In this discretization there are 32 elements and 75 nodal points. The nodal points on the faces $x = 0$, $y = 0$, and $z = 0$ are properly constrained to conform to the boundary conditions stated above.

Two sets of finite element programs were executed and the resulting displacements of the nodal points of these tests are listed in Tables 2 and 3. To visualize the displacement fields in Table 3,

the v-component of the nodal points on the plane y = 5 is plotted in Figure 13. In the composite material considered, the tungsten fibers are embedded periodically in the steel matrix. The elastic constants of the constituents are $E_1 = 30 \times 10^6$ psi, $\nu_1 = 0.3$, $E_2 = 102 \times 10^6$ psi, and $\nu_2 = 0.22$ for the steel and tungsten respectively.

(ii) Evaluation of the Equivalent Strain for the Axially Loaded Tests

If there had been no or very relaxed restrictions on the computer memory size and the computer time, the computation of equivalent strain may be performed most ideally using Equation (4-8). However, due to the reasons stated in Chapter IV, a simpler scheme had been sought.

If the method discussed in Chapter IV is designated as the first method, then the second method which is applicable for some of the special cases of composites is as follows: Consider Figures 14 and 15, which represent the basic cell of the unidirectional fiber composite and the equivalent material. The initial shape of the two specimens are chosen to be a rectangular block of the same size. The dashed lines represent the schematic deformed position of the boundaries. Suppose that the same uniform compressive loads T_{zz} are applied on the two specimens. Due to inhomogeneity of the composite material and homogeneity of the equivalent material, they deform differently. One notes that the deformed boundary surfaces of the equivalent material remain plane after the deformation due to homogeneity and due to the original shape of the specimen. Under the requirements stated in Chapter IV, the quantities that must remain invariant between the two equivalent bodies are

$$V_0 = V_0^* \tag{5-7}$$

$$V_1 = V_1^* \tag{5-8}$$

$$m = m^* \tag{5-9}$$

$$U = U^* \tag{5-10}$$

where V_0, V_1, m, U and V_0^*, V_1^*, m^*, U^* are the undeformed volume, deformed volume, mass, strain energy of the composite and of the equivalent material respectively. The composite material in Figure 14 is simulated with the finite element method and V_1 and U are computed; hence V_1^* and U^* are known from Equations (5-8) and (5-10).

Since the geometry of the equivalent material has been chosen as a rectangular block, the equivalent material has been chosen to be homogeneous, and the loading which is applied on the two opposite faces is uniformly distributed, the strain or stress field inside the equivalent material is uniform throughout the material. In addition, $T_{ij} = \sigma_{ij}$ for the equivalent material. The strain energies stored in the two systems due to the loads can be written as

$$U = 1/2 \int_{\text{vol.}} \underset{\sim}{S}:\underset{\sim}{E}\, dV_1 = 1/2 \int_{\text{area}} \vec{F}\cdot\vec{u}\, dA \tag{5-11}$$

$$U^* = 1/2 \int_{\text{vol.}} \underset{\sim}{S}^*:\underset{\sim}{E}^*\, dV_1^* = 1/2 \int_{\text{area}} \vec{F}^*\cdot\vec{u}^*\, dA^* \tag{5-12}$$

$$= 1/2\, \underset{\sim}{S}^*:\underset{\sim}{E}^* \int_{\text{vol.}} dV_1 = 1/2\, \vec{F}^*\cdot\vec{u}^* \int_{\text{area}} dA^* \tag{5-13}$$

where S, E, $\vec{F}$, $\vec{u}$, A and S^*, E^*, $\vec{F}^*$, $\vec{u}^*$, A^* are the stress field, strain field, applied forces, displacement field, bounding surface of the material for the composite and for the equivalent material respectively. From Equations (5-11) and (5-13) it follows:

$$1/2\ \vec{F}^* \cdot \vec{u}^* \int_{\text{area}} dA^* = U \tag{5-14}$$

The strain energy U can be computed by means of the finite element method. Let the z-component of $\vec{F}^*$ be T^*_{zz}. One notices that

$$1/2\ \vec{F}^* \cdot \vec{u}^* \int_{\text{area}} dA^* = 1/2\ T^*_{zz}\vec{k}\, u^*_z\vec{k}\ (2ab) \tag{5-15}$$

$$= 1/2\ T^*_{zz}\ u^*_z\ (2ab)$$

therefore, from Equations (5-15) and (5-14),

$$u^*_z = \frac{2U}{T^*_{zz}(2ab)} = \frac{U}{T_{zz}(ab)} \tag{5-16}$$

From Equation (5-16), now, the strain field throughout the volume may be computed since the strain field is constant. For example, the strain component ε_{zz} is

$$\varepsilon^*_{zz} = \frac{u^*_z}{c} \tag{5-17}$$

To obtain the strain components ε_{xx} and ε_{yy} for this test, consider the schematic drawing shown in Figure 15.

$$V_0^* = (a)(b)(c) \tag{5-18}$$

$$V_1^* = (a+2u_x^*)(b+2u_y^*)(c+2u_z^*) \tag{5-19}$$

Due to the symmetry of the basic cell,

$$u_x^* = u_y^* \tag{5-20}$$

Substituting Equation (5-20) into Equation (5-19) gives

$$V_1^* = (a+2u_x^*)(a+2u_x^*)(a+2u_z^*) \tag{5-21}$$

Solving for u_x^*

$$u_x^* = (1/2)\left[\sqrt{V_1^*/(c+2u_z^*)} \quad -a\right] \tag{5-22}$$

After some manipulation, Equation (5-22) is rewritten as

$$u_x^* = (a/2)\ [\varepsilon - \varepsilon_{zz}^*] \tag{5-23}$$

where $\varepsilon = \varepsilon_{xx} + \varepsilon_{yy} + \varepsilon_{zz}$.

In order to compute the average displacement u_x^* using Equations (5-22) or (5-23), it is necessary to compute very accurately the deformed volume or the principal strains of the composite throughout the medium. In the former case, the integration order or the number of elements or both need be increased to obtain such an accuracy. In the latter case, since the strain field in the composite medium is not uniform, it is apparently necessary that the principal strain are computed in a sufficiently large number of points to assure the desired degree of accuracy. Thus, in both cases, a considerable amount of computer time and storage are anticipated.

The difficulty associated with the preceding method lies in expressing the volume change as the integral of nonuniform strain. To eliminate this problem, a third method is actually used in which the volume change is approximated from the normal displacements of the boundary surfaces.

Define

ΔV_i = change in volume due to displacements in i^{th} direction for surfaces with normal in the i^{th} direction

Then

$$\Delta V_i = \sum_{e=1}^{M} \int_{A^e} u_i^e \, dA_i^e$$

$$\simeq \sum_{e=1}^{M} \bar{u}_i^e \, A_i^e$$

where $\bar{u}_i^e$ is the average displacement for element e and is approximated as arithmetic mean of the four nodal points, A_i^e is the area of the element face which is normal to i^{th} direction, M is the number of elements whose faces are on the surface of interest.

Since the equivalent material is to have the same volume change, one requires

$$\sum_{e=1}^{M} \bar{u}_i^e \, A_i^e = \bar{u}_i \sum_{e=1}^{M} A_i^e$$

or

$$\bar{u}_i = \frac{\sum_{e=1}^{M} \bar{u}_i^e A_i^e}{\sum_{e=1}^{M} A_i^e} \qquad (5\text{-}24)$$

It is apparent that this method does not require any particular symmetry of the specimen.

The components of strain due to the uniformly distributed loads T_{xx} = -10,000 psi and T_{zz} = -10,000 psi are computed respectively according to Equation (5-24) and the results are tabulated in Table 4. Using the first and the second and the first and the third equation in Equations (5-5) and (5-6) respectively, for instance, the equivalent elastic moduli are computed by solving the four simultaneous equations. One obtains

$$\begin{aligned} C_{11}^* &= C_{22}^* = 0.4977 \times 10^8 \\ C_{33}^* &= 0.51679 \times 10^8 \\ C_{12}^* &= 0.20487 \times 10^8 \\ C_{13}^* &= C_{23}^* = 0.19688 \times 10^8 \end{aligned} \qquad (5\text{-}25)$$

The fifth equation, the third equation in Equation (5-5), that has not been used in the previous computation may be used to check the validity of the result obtained so far and it gives

$$C_{13}^*\varepsilon'_{xx} + C_{23}^*\varepsilon'_{yy} + C_{33}^*\varepsilon'_{zz} = 10^5 \left[(0.19688)(-0.2612) + (0.19688)(0.08023) + (0.51679)(0.06893)\right] = 0.703890 \qquad (5\text{-}26)$$

which is practically zero when compared to T_{xx} = 10,000 psi. Therefore one may conclude that the results obtained using the averaging procedure practically satisfy the system of equations in Equation (5-2).

(iii) Estimation of the Equivalent Strain in the Shear Tests

To obtain the remaining constants C^*_{44} and C^*_{66}, Equations (5-3) and (5-4) need be solved by performing the two shear tests. Due to the reasons stated in the previous subsections, the equivalent rotations are estimated by observing the displacement fields.

To suit this purpose, the basic cell shown in Figure 11 is rediscretized in two different ways: one to compute C^*_{44} and another to compute C^*_{66}.

To compute C^*_{44}, a thin section of the basic cell is discretized as shown in Figure 16 and the shear loads and the boundary conditions are applied to simulate the shear test. Following boundary conditions are applied for this test:

(a) $T_{xy}(\pm 5, y, z) = 10{,}000$ psi

(b) $T_{yx}(x, \pm 5, z) = 10{,}000$ psi

(c) All other stresses on the boundary are zero

(d) $u_x(0,0,0) = u_x(0,0,2) = 0$

The resulting deformation is shown with the dashed lines in Figure 17, and the displacements of the nodal points are listed in Table 5. From the deformed shape, the equivalent rotation, for instance $\bar{\theta}_1$ in Figure 17, is obtained by drawing the straight lines connecting the displaced positions of the nodal points 1 and 21 noticing that the displacement

components of this particular test are antisymmetric. With this approach, one may estimate

$$\bar{\theta}_1 \simeq \frac{\partial v}{\partial x} \tag{5-27}$$

$$\bar{\theta}_2 \simeq \frac{\partial u}{\partial y} \tag{5-28}$$

With these quantities, the strain component ε_{xy} can be computed using the strain displacement relationship,

$$\varepsilon_{xy} = (1/2) \left[\frac{\partial v}{\partial x} + \frac{\partial u}{\partial y} \right] \tag{5-29}$$

From Equation (5-3) with Equation (5-29) and Table 5, the shearing moduli C^*_{44} is computed.

$$C^*_{44} = \frac{\sigma_{xy}}{2\varepsilon_{xy}} \tag{5-30}$$

$$= \frac{10{,}000}{\frac{(2)(1.683)}{10} + \frac{(2)(1.712)}{10}}$$

$$= 0.147275 \times 10^8 \tag{5-31}$$

To compute the modulus $C^*_{66} = C^*_{55}$, tractions T_{yz} and T_{zy} are applied to the basic cell. Because of the physical and geometric symmetry of the basic cell and the symmetry of the imposed loading, only one half of the basic cell need be considered; therefore, one half of the basic cell shown in Figure 11 is discretized and shown in Figure 18. The computation of C^*_{66} is obtained by solving the problem characterized by the following boundary conditions.

(a) $T_{yz}(x,0,z) = T_{yz}(x,10,z) = 10{,}000$ psi

(b) $T_{zy}(x,y,0) = T_{zy}(x,y,10) = 10{,}000$ psi

(c) All other stresses on the boundary are zero

(d) $u_x(0,y,z) = 0$

(e) $u_x(0,5,5) = u_y(x,t,t) = u_z(x,5,5) = 0$

Symmetry characteristics of this problem permit employment of half the basic cell as shown in Figure 18 in which the discretization used is also indicated. The resulting displacements of the nodal points are listed in Table 6.

To compute the equivalent shearing strain, consider the schematic figure as shown in Figure 19.

Let

$$\begin{aligned}
\beta_1 &\simeq \left(\frac{\partial v}{\partial z}\right)_1 = \frac{1}{10}\,[v(5) - v(65)] \\
\beta_2 &\simeq \left(\frac{\partial v}{\partial z}\right)_2 = \frac{1}{10}\,[v(10) - v(70)] \\
\beta_3 &\simeq \left(\frac{\partial v}{\partial z}\right)_3 = \frac{1}{10}\,[v(15) - v(75)] \\
\beta_1 &\simeq \left(\frac{\partial w}{\partial y}\right)_1 = \frac{1}{10}\,[w(10) - w(6)] \\
\beta_2 &\simeq \left(\frac{\partial w}{\partial y}\right)_2 = \frac{1}{10}\,[w(10) - w(6)] \\
\beta_3 &\simeq \left(\frac{\partial w}{\partial y}\right)_3 = \frac{1}{10}\,[w(15) - w(11)]
\end{aligned} \tag{5-32}$$

where v(i) and w(i) are the components of the displacement vector corresponding to the nodal point i, and α and β are the angles as defined in Figure 19. Define the area spanned by the line connecting the nodal points 5, 10, and 15 due to deformation to be $(\text{Area})_1$. Then

$$(\text{Area})_1 = (1/2)\left[\left(\frac{\partial v}{\partial z}\right)_1 + \left(\frac{\partial v}{\partial z}\right)_2\right](5)\,[x(10) - x(5)]$$

$$+ (1/2)\left[\left(\frac{\partial v}{\partial z}\right)_2 + \left(\frac{\partial v}{\partial z}\right)_3\right](5)\,[x(15) - x(10)] \qquad (5\text{-}33)$$

The average $\frac{\partial v}{\partial z}$ of the plane y = 10 due to the deformation may be estimated by

$$\text{Ave.}\left(\frac{\partial v}{\partial z}\right) = \frac{(\text{Area})}{x(15) - x(5)}\left(\frac{1}{5}\right) \qquad (5\text{-}34)$$

where x(i) is the x-coordinate of nodal point i.

Similarly,

$$(\text{Area})_2 = (1/2)\left[\left(\frac{\partial w}{\partial y}\right)_1 + \left(\frac{\partial w}{\partial y}\right)_2\right](5)\,[x(10) - x(5)]$$

$$+ (1/2)\left[\left(\frac{\partial w}{\partial y}\right)_2 + \left(\frac{\partial w}{\partial y}\right)_3\right](5)\,[x(15) - x(10)] \qquad (5\text{-}35)$$

$$\text{Ave.}\left(\frac{\partial w}{\partial y}\right) = \frac{(\text{Area})}{x(15) - x(5)}\left(\frac{1}{5}\right) \qquad (5\text{-}36)$$

Hence the estimated strain is given by

$$\varepsilon_{yz} = (1/2)\ \text{Ave.}\left(\frac{\partial v}{\partial z}\right) + \text{Ave.}\left(\frac{\partial w}{\partial y}\right) \qquad (5\text{-}37)$$

Substituting the numerical results for the expression in Equation (5-37) into Equation (5-4), one obtains

$$C_{66}^{*} = \frac{10{,}000}{2\varepsilon_{yz}} = \frac{10{,}000}{[2.762 + 4.587]10^{-4}} \qquad (5\text{-}38)$$

$$= 0.13607 \times 10^{8}$$

Unidirectional Fiber Composites Whose Cross-Sections are not Square

As mentioned in the first section of this chapter, two different fibers whose cross-sections are not squares are investigated and their effective elastic moduli are computed. The problems analyzed for these composites are the same as those described for square fibers. The basic cells and the discretization of these two composites are shown in Figures 20 and 21. The shapes of the cross-section of the fibers in Figure 20 and 21 are right-crosses with one of them, Figure 20, running across the basic cell and the other, Figure 21, being inscribed within the cell. The former is referred to as the fixed-height cross and the latter as the varying-height cross composites. The cross-section of the basic cell shown in Figure 21 is composed of five equal squares. The cross sectional shape of the fibers is chosen so as to maintain the symmetry with respect to $x = 0$ and $y = 0$ planes. The volumetric ratio of fiber to the total basic cell depends upon the thickness of cross in Figure 20. In Figure 21 the variation of the volumetric ratio of the fiber to the total basic cell is obtained by varying the sides of the squares.

Results on the Unidirectional Fiber Composites

Three different unidirectional fiber composites were tested by using the finite element procedure for simple problems of elasticity. Several sets of tests were performed varying the volumetric ratio of fiber to the total volume of the basic cell for each of three unidirectional fiber composites.

The results for the square unidirectional fiber composite are compared with Behrens' results [20], and the results of the other two composites are also compared with the square fiber composite to seek meaningful conclusions. These are displayed in graphic form in Figures 22 through 27, and the numerical results are listed in Tables 7 through 8. It is evident in the figures that the effective moduli of unidirectional composites are practically the same regardless the shape of the cross-section except the shearing modulus C^*_{44} as displayed in Figure 26.

It is interesting to note in Figure 26 that the square shaped unidirectional fiber composite reveals the strongest shearing modulus C^*_{44}. Noticing that the varying-height cross-shape is a bit stronger than the fixed-height cross-section, it suggests that the shearing modulus C^*_{44} becomes stronger as the boundary of the fiber becomes smaller.

It is also noticed that the results of this method so far pursued agree well with the results obtained analytically by Behrens with the possible exception of C^*_{33}. The deviation of C^*_{33} from Behrens' result in Figure 23 might have been caused by the coarse discretization.

The numerical values of Behrens' results are listed in Table 10 and the closed forms are shown in Appendix A.

CHAPTER VI

LAMELLAR COMPOSITES

Description of the Problem

The lamellar composites considered in this investigation consist of layers, each of which is of uniform thickness and is a homogeneous isotropic elastic medium. The composites are constructed in such a manner as to have identical alternate layers. Such a composite as shown in Figure 28 is a periodic structure with the basic cell as shown in Figure 29. The chosen basic cell is transversely isotropic with respect to z-axis which is normal to the layers and is symmetric with respect to the middle plane of the basic cell which is parallel to the faces of the layers

This geometry implies that the basic cell behaves according to following Hookean law

$$\begin{Bmatrix} \sigma_{xx} \\ \sigma_{yy} \\ \sigma_{zz} \\ \sigma_{xy} \\ \sigma_{yz} \\ \sigma_{zx} \end{Bmatrix} = \begin{bmatrix} C_{11}^* & C_{12}^* & C_{13}^* & 0 & 0 & 0 \\ C_{12}^* & C_{11}^* & C_{13}^* & 0 & 0 & 0 \\ C_{13}^* & C_{13}^* & C_{33}^* & 0 & 0 & 0 \\ 0 & 0 & 0 & \frac{1}{2}(C_{11}^*-C_{12}^*) & 0 & 0 \\ 0 & 0 & 0 & 0 & C_{66}^* & 0 \\ 0 & 0 & 0 & 0 & 0 & C_{66}^* \end{bmatrix} \begin{Bmatrix} \varepsilon_{xx} \\ \varepsilon_{yy} \\ \varepsilon_{zz} \\ 2\varepsilon_{xy} \\ 2\varepsilon_{yz} \\ 2\varepsilon_{zx} \end{Bmatrix} \tag{6-1}$$

It is noticed that Hooke's law for the lamellar composite is the same as that of the unidirectional fiber composite studied in the previous

chapter. Therefore, the tests employed for the computation of the elastic moduli of the lamellar composite are the same as the ones used for the unidirectional fiber composite.

Results

The constants C^*_{11}, C^*_{33}, C^*_{12}, and C^*_{13} are obtained from the compression tests. An example of the discretization of an octant of the basic cell is shown in Figure 30. The elements 1 through 18 are matrix material and 19 through 27 are the fiber material. The average displacements and the average strain are computed exactly the same way as described in the previous chapter.

Examples of the discretization process employed for the shear tests to compute C^*_{44} and C^*_{66} are shown in Figures 31 and 32.

The results of this computation are listed in Tables 11 through 13 and also in Figures 33 through 38. The results are compared with the expressions obtained by method of long-waves by Behrens, whose numerical results are tabulated in Table 14.

It should be pointed out that the constant C^*_{44} is computed by means of a shear test while C^*_{11} and C^*_{12} are computed from the compression tests, which are completely independent of the shear test. However, for this particular composite, the constants C^*_{11}, C^*_{12}, and C^*_{44} are related by expression

$$C^*_{44} - (1/2)(C^*_{11} - C^*_{12}) = 0 \qquad (6\text{-}2)$$

The numerical result obtained from the above tests were substituted in Equation (6-2). This expression provides an extra means of

checking the finite element procedure employed in this work. The error exhibited by Equation (6-2) turns out to be very small, as shown in Figure 37.

CHAPTER VII

SHORT FIBER COMPOSITES

Description of the Problem

In this chapter, the method that has been developed, used, and checked in the previous chapters is used for a simple but truly three-dimensional problems.

The composite analyzed in this chapter consists of homogeneous isotropic elastic inclusions equally spaced in all directions in a homogeneous isotropic elastic matrix. This material is shown in Figure 39. The basic cell associated with this composite consists of two concentric cubes with their faces being normal to the coordinate axes as shown in Figure 40. Because of the symmetries exhibited by the basic cell, the Hooke's law becomes

$$\begin{Bmatrix} \sigma_{xx} \\ \sigma_{yy} \\ \sigma_{zz} \\ \sigma_{xy} \\ \sigma_{yz} \\ \sigma_{zx} \end{Bmatrix} = \begin{bmatrix} C^*_{11} & C^*_{12} & C^*_{12} & 0 & 0 & 0 \\ C^*_{12} & C^*_{11} & C^*_{12} & 0 & 0 & 0 \\ C^*_{12} & C^*_{12} & C^*_{11} & 0 & 0 & 0 \\ 0 & 0 & 0 & C^*_{66} & 0 & 0 \\ 0 & 0 & 0 & 0 & C^*_{66} & 0 \\ 0 & 0 & 0 & 0 & 0 & C^*_{66} \end{bmatrix} \begin{Bmatrix} \varepsilon_{xx} \\ \varepsilon_{yy} \\ \varepsilon_{zz} \\ 2\varepsilon_{xy} \\ 2\varepsilon_{yz} \\ 2\varepsilon_{zx} \end{Bmatrix} \qquad (7\text{-}1)$$

where $C^*_{66} = (1/2)\ (C^*_{11} - C^*_{12})$. Thus the equivalent material has only two independent constants, C^*_{11} and C^*_{12}, the same as an isotropic elastic medium for which Hooke's law, in terms of engineering constants,

is given by

$$\begin{Bmatrix} \sigma_{xx} \\ \sigma_{yy} \\ \sigma_{zz} \\ \sigma_{xy} \\ \sigma_{yz} \\ \sigma_{zx} \end{Bmatrix} = \frac{E^*}{(1+\nu^*)(1-2\nu^*)} \begin{bmatrix} 1-\nu^* & \nu^* & \nu^* & 0 & 0 & 0 \\ \nu^* & 1-\nu^* & \nu & 0 & 0 & 0 \\ \nu^* & \nu^* & 1-\nu^* & 0 & 0 & 0 \\ 0 & 0 & 0 & \frac{1-2\nu^*}{2} & 0 & 0 \\ 0 & 0 & 0 & 0 & \frac{1-2\nu^*}{2} & 0 \\ 0 & 0 & 0 & 0 & 0 & \frac{1-2\nu^*}{2} \end{bmatrix} \begin{Bmatrix} \varepsilon_{xx} \\ \varepsilon_{yy} \\ \varepsilon_{zz} \\ 2\varepsilon_{xy} \\ 2\varepsilon_{yz} \\ 2\varepsilon_{zx} \end{Bmatrix}$$

Results

The test problems employed in this chapter are the same as the ones used for the uniaxial fiber composites since the same symmetry of physical properties, geometry, and loading prevail. Again, the finite element procedure developed in Chapters IV and V is employed.

A typical discretization of one octant of the basic cell is shown in Figure 42 where the number of the elements along x-, y-, and z-directions are the same to maintain better symmetry of deformation. The element numbers 10, 11, 13, 14, 19, 20, 22, and 23 are the fiber and the remaining element numbers are the matrix materials. For the discretization shown in Figure 42, the volumetric ratio of fiber to the whole basic cell is 34.3%. By re-discretizing the one octant with different sizes of elements, different volumetric ratios can be attained without increasing the total number of elements.

Using only one compression test, the effective moduli C_{11}^* and C_{12}^* are obtained; they are plotted in Figures 43 and 44 for different volumetric ratios with numerical values shown in Table 15. C_{66}^*, ν^*,

and E^* are computed using the values of C^*_{11} and C^*_{12} and the relationships

$$C^*_{66} = (1/2)\ (C^*_{11} - C^*_{12}) \tag{7-3}$$

$$\nu^* = C^*_{12}/(C^*_{12} + C^*_{11}) \tag{7-4}$$

$$E^* = (C^*_{11} + 2C^*_{12})\,(C^*_{11}-C^*_{12})/(C^*_{11}+C^*_{12}) \tag{7-5}$$

These results are also shown in Table 15.

The engineering moduli E^* and ν^* obtained for 0% of fiber and for 100% fiber are 0.29995×10^8, 0.29993 and 1.020007×10^8, 0.021900 respectively. These values compare very well with the corresponding original values of 0.3000×10^8, 0.3000 and 1.02000×10^8, 0.22000.

The effective modulus C^*_{66} can also be obtained by the simple shear tests defined in Chapter V. This duplicate effort is made here in order to check the results of the compression test and to demonstrate the reliability of the procedure employed in the shear tests of earlier chapters. One half of the basic cell of the short fiber composite used in the shear test is discretized as shown in Figure 45. The values of C^*_{66} obtained by the shear test are found to be within less than 3% of the values shown in Table 15.

CHAPTER VIII

THE LAMINATED COMPOSITES

Description of the Problem

The composite medium under consideration in this chapter consists of a number of layers of identical composition, with each identical layer composed of a uniaxial fiber composite. The layers of the particular laminated composite examined here have the same thickness and are of mutually orthogonal orientations. A schematic view of this laminated composite is given in Figure 46 in which only the two layers which repeat themselves in y-direction are shown.

The conditions of periodicity limit the choice of the basic cell to the two cases as shown in Figure 47. The basic cell A is chosen as the basic cell for the rest of the analysis. The magnified three dimensional view of the basic cell is shown in Figure 48. It consists of two layers and is an orthogonal parallelepiped. The fact that this cell remains as an orthogonal parallelipiped for all orientations of two successive layers made it more desirable and the resulting computer program more flexible than the other choice.

Due to the symmetries exhibited by the basic cell the Hooke's law for the equivalent material becomes

$$\begin{Bmatrix} \sigma_{xx} \\ \sigma_{yy} \\ \sigma_{zz} \\ \sigma_{xy} \\ \sigma_{yz} \\ \sigma_{zx} \end{Bmatrix} = \begin{bmatrix} C^*_{11} & C^*_{12} & C^*_{13} & 0 & 0 & 0 \\ C^*_{12} & C^*_{22} & C^*_{12} & 0 & 0 & 0 \\ C^*_{13} & C^*_{12} & C^*_{11} & 0 & 0 & 0 \\ 0 & 0 & 0 & C^*_{44} & 0 & 0 \\ 0 & 0 & 0 & 0 & C^*_{44} & 0 \\ 0 & 0 & 0 & 0 & 0 & C^*_{66} \end{bmatrix} \begin{Bmatrix} \varepsilon_{xx} \\ \varepsilon_{yy} \\ \varepsilon_{zz} \\ 2\varepsilon_{xy} \\ 2\varepsilon_{yz} \\ 2\varepsilon_{zx} \end{Bmatrix} \tag{8-1}$$

Thus this laminated composite is specified by six independent elastic constants. Equation (8-1) may be expressed as

$$\begin{Bmatrix} \sigma_{xx} \\ \sigma_{yy} \\ \sigma_{zz} \end{Bmatrix} = \begin{bmatrix} C^*_{11} & C^*_{12} & C^*_{13} \\ C^*_{12} & C^*_{22} & C^*_{12} \\ C^*_{13} & C^*_{12} & C^*_{11} \end{bmatrix} \begin{Bmatrix} \varepsilon_{xx} \\ \varepsilon_{yy} \\ \varepsilon_{zz} \end{Bmatrix} \tag{8-2}$$

$$\begin{Bmatrix} \sigma_{xy} \\ \sigma_{yz} \end{Bmatrix} = C^*_{44} \begin{Bmatrix} 2\varepsilon_{xy} \\ 2\varepsilon_{yz} \end{Bmatrix} \tag{8-3}$$

$$\sigma_{zx} = C^*_{66}\ 2\varepsilon_{zx} \tag{8-4}$$

In order to compute the six elastic moduli the discretized basic cell as shown in Figure 49 is subjected to the following computer tests.

(i) Uniform Longitudinal Compression Test

(a) $T_{zz}(x,y,10) = -10{,}000$ psi

(b) $T_{zz}(x,y,0) = -10{,}000$ psi (8-5)

(c) All other stresses on the boundary of the basic cell are zero

(d) $u_x(5,3,z) = 0$

(e) $u_y(5,3,z) = u_y(x,3,5) = 0$

(f) $u_z(x,3,5) = 0$

(ii) Uniform Lateral Compression Test

(a) $T_{yy}(x,6,z) = -10{,}000$ psi

(b) $T_{yy}(x,0,z) = -10{,}000$ psi

(c) All other stresses on the boundary of the basic cell are zero

(d) $u_x(5,3,z) = 0$ (8-6)

(e) $u_y(5,3,z) = u_y(x,3,5) = 0$

(f) $u_z(x,3,5) = 0$

(iii) Simple Shear test to compute C^*_{66}

(a) $T_{xz}(0,y,z) = 10{,}000$ psi

(b) $T_{xz}(10,y,z) = 10{,}000$ psi

(c) $T_{zx}(x,y,0) = 10{,}000$ psi (8-7)

(d) $T_{zx}(x,y,10) = 10{,}000$ psi

(e) All other stresses on the boundary of the basic cell are zero

(f) $u_x(x,3,5) = 0$

(g) $u_y(x,3,z) = 0$

(h) $u_z(5,3,z) = 0$

(iv) Simple Shear Test to Compute C^*_{44}

(a) $T_{yz}(x,0,z) = 10{,}000$ psi

(b) $T_{yz}(x,6,z) = 10{,}000$ psi

(c) $T_{zy}(x,y,0) = 10{,}000$ psi

(d) $T_{zy}(x,y,10) = 10{,}000$ psi (8-8)

(e) All other stresses on the boundary of the basic cell are zero

(f) $u_x(5,y,z) = 0$

(g) $u_y(5,y,5) = 0$

(h) $u_z(5,3,z) = 0$

Result

To solve for C_{11}^*, C_{22}^*, C_{12}^*, and C_{13}^* from Equation (8-2), two compression tests stated in (i) and (ii) are utilized. As the results of the two compression tests, one obtains the following systems of equations using Equation (8-2):

$$\begin{Bmatrix} 0 \\ 0 \\ 10{,}000 \end{Bmatrix} = \begin{bmatrix} C_{11}^* & C_{12}^* & C_{13}^* \\ C_{12}^* & C_{22}^* & C_{12}^* \\ C_{13}^* & C_{12}^* & C_{11}^* \end{bmatrix} \begin{Bmatrix} \varepsilon_{xx} \\ \varepsilon_{yy} \\ \varepsilon_{zz} \end{Bmatrix} \tag{8-9}$$

$$\begin{Bmatrix} 0 \\ 10{,}000 \\ 0 \end{Bmatrix} = \begin{bmatrix} C_{11}^* & C_{12}^* & C_{13}^* \\ C_{12}^* & C_{22}^* & C_{12}^* \\ C_{13}^* & C_{12}^* & C_{11}^* \end{bmatrix} \begin{Bmatrix} \varepsilon'_{xx} \\ \varepsilon'_{yy} \\ \varepsilon'_{zz} \end{Bmatrix} \tag{8-10}$$

where, as before, ε_{xx}, ε_{yy}, ε_{zz} and ε'_{xx} ε'_{yy}, ε'_{zz} are the average strains from the two tests on the composite. To obtain the shear moduli C_{66}^* and C_{44}^*, the pure shear tests shown schematically in Figures 50 and 52 are performed using the boundary conditions stated in (iii) and (iv) respectively.

The displacements of the nodal points of the laminated composite of 13.3333% volumetric ratio shown in Figure 49 subjected to the above mentioned tests are listed in Tables 16 through 19. From the tables the average strains are computed and they are schematically shown in

Figures 54, 55, 51, and 53 respectively. With the average displacements of the boundary surfaces in Figures 54 and 55:

$$
\begin{aligned}
u_x &= 5.0987 \times 10^{-4} \\
u_y &= 2.4072 \times 10^{-4} \\
u_z &= -1.7951 \times 10^{-3} \\
u'_x &= 4.0331 \times 10^{-4} \\
u'_y &= -8.7312 \times 10^{-4} \\
u'_z &= 4.0331 \times 10^{-4}
\end{aligned}
\qquad (8\text{-}11)
$$

the constant strain fields are computed to be

$$
\begin{aligned}
\varepsilon_{xx} &= 1.0197 \times 10^{-4} \\
\varepsilon_{yy} &= 0.8024 \times 10^{-4} \\
\varepsilon_{zz} &= -3.5902 \times 10^{-4} \\
\varepsilon'_{xx} &= 0.8066 \times 10^{-4} \\
\varepsilon'_{yy} &= -2.9104 \times 10^{-4} \\
\varepsilon'_{zz} &= 0.8066 \times 10^{-4}
\end{aligned}
\qquad (8\text{-}12)
$$

The values in Equation (8-11) are substituted into Equations (8-9) and (8-10) and taking only first four relationships the four unknowns are computed to be

$$
\begin{aligned}
C^*_{11} &= C^*_{33} = 0.34367 \times 10^8 \\
C^*_{22} &= 0.41763 \times 10^8 \\
C^*_{12} &= C^*_{32} = 0.13037 \times 10^8 \\
C^*_{13} &= 0.12674 \times 10^8
\end{aligned}
\qquad (8\text{-}13)
$$

The remaining two equations, i.e.,

$$10{,}000 = C_{12}^{*}\,\varepsilon_{xx}^{'} + C_{22}^{*}\,\varepsilon_{yy}^{'} + C_{12}^{*}\,\varepsilon_{zz}^{'}$$

$$0 = C_{13}^{*}\,\varepsilon_{xx}^{'} + C_{12}^{*}\,\varepsilon_{yy}^{'} + C_{11}^{*}\,\varepsilon_{zz}^{'} \qquad (8\text{-}14)$$

are checked to see their agreements by substituting the values in Equation (8-12) and (8-13):

$$C_{12}^{*}\,\varepsilon_{xx}^{'} + C_{22}^{*}\,\varepsilon_{yy}^{'} + C_{12}^{*}\,\varepsilon_{zz}^{'} = 1.00457 \times 10^{4}$$

$$\simeq 10{,}000 \qquad (8\text{-}15)$$

$$C_{13}^{*}\,\varepsilon_{xx}^{'} + C_{12}^{*}\,\varepsilon_{yy}^{'} + C_{11}^{*}\,\varepsilon_{zz}^{'} = 0.04$$

$$\simeq 0 \qquad (8\text{-}16)$$

Equations (8-15) and (8-16) show a good agreement.

Using the average shearing strain shown in Figure 51, the modulus C_{66}^{*} is computed as

$$C_{66}^{*} = \sigma_{xz}/(2\varepsilon_{xz}) = 0.22779 \times 10^{8} \qquad (8\text{-}17)$$

Similarly, using the average strain shown in Figure 53, the modulus C_{44}^{*} is computed as

$$C_{44}^{*} = \sigma_{yz}/(2\varepsilon_{yz}) = 0.12081 \times 10^{8} \qquad (8\text{-}18)$$

In order to demonstrate the significance of the results obtained for the laminated composite, the effective moduli C_{11}^{*}, C_{22}^{*}, C_{12}^{*}, C_{13}^{*}, C_{66}^{*}, and C_{44}^{*} are plotted in Figures 56 through 61. In the figures the dashed lines are for the lamellar composites that have been shown in Figures 33 through 38 and are redrawn here for comparison. The values for the laminated composites are indicated with small circles.

The values of the effective moduli of the laminated composites at the volumetric ratio 0% and 100% are the same as the lamellar composites.

In all of the results in Chapters V through VII, it has been noticed that the values of the effective moduli increase as the volumetric ratios increase. However, for the laminated composites, the values of the effective moduli C_{11}^*, C_{12}^*, C_{13}^* are decreased as the volumetric ratios are varied from 0% to, for instance, 13.3333%. On the other hand, the values of the effective shearing modulus C_{66}^* increases considerably. C_{22}^* and C_{44}^* show very small changes with respect to the values at the volumetric ratio 0%. The essential nature of this phenomenon has been experimentally found by Toy and Dickerson [28].

To illustrate the ways of changing the volumetric ratio, the cross section z = 10 inches in Figure 49 is shown in Figure 62 with various volumetric ratios. In Figure 62a through 62e, the heights of the fibers are initially kept constant, 1 inch, and the widths are changed from zero to 5 inches as shown in Figure 62a through 62c. When the width become 5 inches the laminated composite degenerates to the lamellar composite. Once this point is reached, the volumetric ratio can be increased by starting to increase the height of the fibers as shown in Figures 62c through 62e. Hence the material becomes the lamellar composite from the point on. The interpolated lines passing through these points are shown with solid lines in Figures 56 through 61.

The change of the volumetric ratio can also take place in another

way, as an example, the widths of the fibers are initially kept constant, 2 inches, the heights are changed from zero to 3 inches as shown in Figures 62f through 62h. Once this point is reached, the volumetric ratio can be increased by increasing the widths of the fibers as shown in Figure 62h through 62j. The intuitive values are drawn with broken lines in Figures 56 through 61.

As illustrated, the values of the effective moduli will follow different paths depending upon the geometric shapes of the constituents as well as the volumetric ratios.

CHAPTER IX

DISCUSSIONS AND CONCLUSIONS

In the previous chapters it is demonstrated that the finite element procedure can effectively and reasonably accurately determine the effective elastic moduli of various composites. The procedure was checked by the method of long-waves in the cases of unidirectional composites and lamellar composites, thus establishing its capability for accuracy with relatively small number of elements. The self-consistancy of the method is also demonstrated by computing C^*_{44} of the unidirectional fiber composites and the lamellar composites independently and comparing them with the values by $C^*_{44} = (1/2)\ (C^*_{11} - C^*_{12})$. A similar demonstration is made for the short fiber composites.

It is believed that the deviations of C^*_{33} from the results of Behrens' in Figures 23 and 33 are due to the simplified scheme of obtaining the average displacements. Consequently, the results may be further improved by elaborating further the estimation of the equivalent displacements without increasing the number of elements. Of course, the results will be improved by just increasing the number of elements without changing any procedures already described.

With the procedure employed it is possible that one can analyze any practical composites with some idealization of the boundaries.

The importance of the results of this investigation is summarized as follows:

(1) The effective moduli of the unidirectional fiber composites with different shapes of the fiber cross sections are all the same, except C^*_{44}, as long as their volumetric ratios are equal. As shown in Figure 26, the shearing modulus C^*_{44} becomes larger as the boundary between the constituents becomes smaller suggesting how to design the constituents.

(2) The effective moduli of the short fiber composites are computed and, as expected, they exhibit the homogeneous isotropic behavior in the large.

(3) For the laminated composite, all of the six effective moduli are obtained. With the conventional analysis [16, 17] only four of them can be calculated for such composites since they are treated as plates.

(4) It is well known that, particularly for the laminated composites, due to inhomogeneity and the geometric configuration of constituents, the scissoring effect occurs which causes high concentration of stresses. The conventional composite plate analysis [16, 17] has no way of recognizing such a phenomenon. With the finite element method it is possible to calculate the stress and strain fields of the heterogeneous material throughout the body. The equivalent material, which by construction is homogeneous material, cannot exhibit the scossoring effect per se. However, the weakening of elastic constants C^*_{11}, C^*_{12}, C^*_{13} and strengthening of C^*_{66} in small volumetric ratios as shown in Figures 56 through 60 seem to be consistent with the scissoring effect occurring in the actual material.

(5) For the specific case of the laminated composite of cross-ply

of $\pm 45^{0}$ and relatively small volumetric ratios, it was found that all of the effective moduli, except C^{*}_{66}, become smaller (or do not change their values much) than in the original matrix material. On the other hand, however, the effective shearing moduli C^{*}_{66} becomes considerably larger.

There are drawbacks in adopting this procedure. The results are numerical, not functional, although interpolation or extrapolation of the desired values at any points in the region of interest are possible. With the capability to analyze more complicated composites, the necessity of increasing the number of elements results in increase of computer time and storage.

In closing this investigation it should be pointed out that it is quite possible to test a given composite material in the computer lab by means of the finite element method instead of actual experimenting with the actual specimens. It is also conceivable that this computer technique may be used for actually designing the composites to perform according to needs prior to being manufactured.

TABLES

Table 1. Values of the Argument and the Weighting Factors for Gauss-Legendre Formula

l,m,n	x_i, y_j, z_k	A_i, A_j, A_k
2	$\pm$ .57735027	1.00000000
4	$\pm$ .86113631	.34785485
	$\pm$ .33998104	.65214515
6	$\pm$ .93246951	.17132449
	$\pm$ .66120939	.36076157
	$\pm$ .23861919	.46791393
8	$\pm$ .96028986	.10122854
	$\pm$ .79666648	.22381034
	$\pm$ .52553241	.31370665
	$\pm$ .18343464	.36268378
.	.	.
.	.	.
.	.	.

Table 2. Displacements of the Nodal Points for the Discretized Model Shown in Figure 12 Which is Loaded with T_{xx}=-10,000 psi (u, v, w are given in inches.)

Nodal point	u	v	w	Nodal point	u	v	w
1	0.000	0.000	1.164-04	39	-6.927-04	2.559-04	1.518-04
2	0.000	-2.206-05	1.289-04	40	-8.432-04	3.743-04	1.806-04
3	0.000	-1.652-05	1.742-04	41	-6.116-04	0.000	1.281-04
4	0.000	2.218-05	2.861-04	42	-6.614-04	1.451-04	1.338-04
5	0.000	1.308-04	3.601-04	43	-8.261-04	3.013-04	1.512-04
6	-1.297-04	0.000	1.190-04	44	-1.055-03	4.282-04	1.747-04
7	-1.545-04	-7.482-06	1.320-04	45	-1.265-03	5.499-04	1.950-04
8	-2.187-04	-5.962-07	1.795-04	46	-1.052-03	0.000	1.751-04
9	-3.441-04	6.165-05	2.946-04	47	-1.109-03	2.390-04	1.782-04
10	-4.480-04	1.856-04	3.674-04	48	-1.261-03	4.463-04	1.860-04
11	-2.752-04	0.000	1.721-04	49	-1.465-03	6.152-04	1.971-04
12	-2.993-04	4.824-05	1.946-04	50	-1.679-03	7.498-04	2.119-04
13	-4.487-04	1.035-04	2.381-04	51	0.000	0.000	0.000
14	-7.270-04	2.009-04	3.258-04	52	0.000	3.017-06	0.000
15	-8.755-04	3.194-04	3.769-04	53	0.000	2.567-05	0.000
16	-6.737-04	0.000	3.189-04	54	0.000	9.454-05	0.000
17	-7.218-04	1.278-04	3.287-04	55	0.000	2.137-04	0.000
18	-8.787-04	2.697-04	3.459-04	56	-1.034-04	0.000	0.000
19	-1.095-03	3.887-04	3.612-04	57	-1.275-04	1.825-05	0.000
20	-1.302-03	5.024-04	3.954-04	58	-1.919-04	4.123-05	0.000
21	-1.102-03	0.000	3.339-04	59	-3.210-04	1.319-04	0.000
22	-1.158-03	2.216-04	3.429-04	60	-4.232-04	2.645-04	0.000
23	-1.305-03	4.162-04	3.631-04	61	-2.324-04	0.000	0.000
24	-1.503-03	5.787-04	3.884-04	62	-2.562-04	7.381-05	0.000
25	-1.716-03	7.126-04	4.163-04	63	-4035-04	1.479-04	0.000
26	0.000	0.000	5.334-05	64	-6.847-04	2.642-04	0.000
27	0.000	1.581-06	6.193-05	65	-8.322-04	3.876-04	0.000
28	0.000	2.466-05	7.951-05	66	-6.005-04	0.000	0.000
29	0.000	8.942-05	1.259-04	67	-6.504-04	1.498-04	0.000
30	0.000	2.006-04	1.644-04	68	-8.145-04	3.113-04	0.000
31	-1.053-04	0.000	6.413-05	69	-1.042-03	4.408-04	0.000
32	-1.297-04	1.674-05	7.320-05	70	-1.250-03	5.580-04	0.000
33	-1.940-04	4.052-05	9.002-05	71	-1.026-03	0.000	0.000
34	-3.255-04	1.266-04	1.327-04	72	-1.085-03	2.442-04	0.000
35	-4.295-04	2.513-04	1.692-04	73	-1.240-03	4.566-04	0.000
36	-2.311-04	0.000	8.266-05	74	-1.449-03	6.279-04	0.000
37	-2.553-04	7.266-05	9.128-05	75	-1.633-03	7.619-04	0.000
38	-4.043-04	1.453-04	1.114-04				

Table 3. Displacements of the Nodal Points for the Discretized Model Shown in Figure 12 Which is Loaded with T_{zz}=-10,000 psi (u, v, w are given in inches.)

Nodal point	u	v	w	Nodal point	u	v	w
1	0.000	0.000	-4.505-04	39	1.289-04	1.784-04	-5.362-04
2	0.000	1.018-04	-4.758-04	40	1.306-04	3.171-04	-6.412-04
3	0.000	1.922-04	-6.475-04	41	1.366-04	0.000	-4.616-04
4	0.000	3.575-04	-1.093-03	42	1.461-04	5.829-05	-4.798-04
5	0.000	4.882-04	-1.243-03	43	1.784-04	1.289-04	-5.362-04
6	1.018-04	0.000	-4.758-04	44	2.233-04	2.233-04	-6.082-04
7	1.062-04	1.062-04	-5.027-04	45	2.323-04	3.466-04	-6.763-04
8	1.081-04	1.961-04	-6.738-04	46	2.804-04	0.000	-6.082-04
9	1.115-04	3.585-04	-1.116-03	47	2.899-04	5.791-05	-6.175-04
10	1.117-04	4.863-04	-1.257-03	48	3.171-04	1.306-04	-6.412-04
11	1.922-04	0.000	-6.475-04	49	3.466-04	2.323-04	-6.763-04
12	1.961-04	1.081-04	-6.738-04	50	3.566-04	3.566-04	-7.240-04
13	2.125-04	2.125-04	-8.515-04	51	0.000	0.000	0.000
14	2.300-04	3.559-04	-1.178-03	52	0.000	1.512-05	0.000
15	2.256-04	4.811-04	-1.294-03	53	0.000	4.832-05	0.000
16	3.575-04	0.000	-1.093-03	54	0.000	1.090-04	0.000
17	3.585-04	1.115-04	-1.116-03	55	0.000	2.138-04	0.000
18	3.559-04	2.300-04	-1.178-03	56	1.512-05	0.000	0.000
19	3.468-04	3.468-04	-1.253-03	57	1.837-05	1.837-05	0.000
20	3.459-04	4.733-04	-1.347-03	58	2.181-05	5.393-05	0.000
21	4.882-04	0.000	-1.243-03	59	4.193-05	1.189-04	0.000
22	4.863-04	1.117-04	-1.257-03	60	3.711-05	2.261-04	0.000
23	4.811-04	2.256-04	-1.294-03	61	4.532-05	0.000	0.000
24	4.733-04	3.459-04	-1.347-03	62	5.393-05	2.181-05	0.000
25	4.897-04	4.697-04	-1.417-03	63	6.540-05	6.540-05	0.000
26	0.000	0.000	-2.090-04	64	9.865-05	1.463-04	0.000
27	0.000	2.031-05	-2.424-04	65	9.369-05	2.615-04	0.000
28	0.000	4.680-05	-3.036-04	66	1.090-04	0.000	0.000
29	0.000	1.366-04	-4.616-04	67	1.189-04	4.193-05	0.000
30	0.000	2.804-04	-6.082-04	68	1.463-04	9.866-05	0.000
31	2.031-05	0.000	-2.424-04	69	1.816-04	1.816-04	0.000
32	2.431-05	2.431-05	-2.766-04	70	1.872-04	3.001-04	0.000
33	2.848-05	5.303-05	-3.350-04	71	2.138-04	0.000	0.000
34	5.829-05	1.461-04	-4.798-04	72	2.261-04	3.711-05	0.000
35	5.791-05	2.899-04	-6.175-04	73	2.615-05	9.369-05	0.000
36	4.680-05	0.000	-3.036-04	74	3.001-04	1.872-04	0.000
37	5.303-05	2.848-05	-3.350-04	75	3.127-04	3.127-04	0.000
38	7.140-05	7.140-05	-4.040-04				

Table 4. Average Displacements and Strain
(Displacements are given in inches.)

	Applied load	
	σ_{zz}=-10,000 psi	σ_{xx}=-10,000 psi
Equivalent Displacement	$\bar{u}_x = 0.3447 \times 10^{-3}$ $\bar{u}_y = 0.3447 \times 10^{-3}$ $\bar{u}_z = -0.9841 \times 10^{-3}$	$\bar{u}'_x = -0.1306 \times 10^{-2}$ $\bar{u}'_y = 0.4011 \times 10^{-3}$ $\bar{u}'_z = 0.2757 \times 10^{-3}$
Equivalent Strain	$\bar{\varepsilon}_{xx} = 0.6893 \times 10^{-4}$ $\bar{\varepsilon}_{yy} = 0.6893 \times 10^{-4}$ $\bar{\varepsilon}_{zz} = -0.2460 \times 10^{-4}$	$\bar{\varepsilon}'_{xx} = -0.2612 \times 10^{-3}$ $\bar{\varepsilon}'_{yy} = 0.8023 \times 10^{-4}$ $\bar{\varepsilon}'_{zz} = 0.6893 \times 10^{-4}$

Table 5. Displacements of the Nodal Points for the Discretized Model Shown in Figure 16 Loaded by Pure Shear T_{xy}=-10,000 psi (u, v, w are given in inches.)

Nodal point	u	v	w	Nodal point	u	v	w
1	-1.712-03	-1.683-03	4.294-05	26	-1.712-03	-1.683-03	-4.295-05
2	-5.335-04	-1.902-03	-4.699-06	27	-5.355-04	-1.902-03	4.693-06
3	2.140-10	-2.028-03	2.386-10	28	8.672-11	-2.028-03	2.962-10
4	5.335-04	-1.902-03	4.699-06	29	5.335-04	-1.902-03	-4.692-06
5	1.712-03	-1.683-03	-4.294-05	30	1.712-03	-1.683-03	4.295-05
6	-1.931-03	-5.221-04	-4.699-06	31	-1.931-03	-5.221-04	4.692-06
7	-3.102-04	-2.988-04	-3.077-05	32	-3.102-04	-2.988-04	3.077-05
8	9.852-11	-2.435-04	7.443-11	33	2.891-11	-2.435-04	8.018-11
9	3.102-04	-2.988-04	3.077-05	34	3.102-04	-2.988-04	-3.077-05
10	1.931-03	-5.221-04	4.700-06	35	1931-03	-5.221-04	-4.692-06
11	-2.057-03	-4.131-10	-4.123-10	36	-2.057-03	-9.199-11	-4.657-10
12	-2.550-04	-1.848-10	-4.226-11	37	-2.550-04	-7.673-11	-1.371-12
13	0.000	0.000	5.704-11	38	0.000	0.000	0.000
14	2.550-04	-2.185-10	1.715-10	39	2.550-04	-6.248-11	1.749-10
15	2.057-03	-3.764-10	5.166-10	40	2.057-03	-9.696-11	5.753-10
16	-1.931-03	5.221-04	4.699-06	41	-1.931-03	5.221-04	-4.693-06
17	-3.102-04	2.988-04	3.077-05	42	-3.102-04	2.988-04	-3.077-05
18	-2.827-11	2.435-04	1.743-10	43	1.728-10	2.435-04	1.942-10
19	3.102-04	2.988-04	-3.077-05	44	3.102-04	2.988-04	3.077-05
20	1.931-03	5.221-04	-4.699-06	45	1.931-03	5.221-04	4.693-06
21	-1.712-03	1.683-03	-4.294-05	46	-1.712-03	1.683-03	4.295-05
22	-5.335-04	1.902-03	4.700-06	47	-5.335-04	1.902-03	-4.692-06
23	-3.896-11	2.028-03	7.036-10	48	3.722-10	2.028-03	6.721-10
24	5.335-04	1.902-03	-4.698-06	49	5.335-04	1.902-03	4.693-06
25	1.712-03	1.683-03	4.294-05	50	1.712-03	1.683-03	-4.295-05

Table 6. Displacements of the Nodal Points for the Discretized Model Shown in Figure 16 Loaded by Pure Shear T_{yz}=-10,000 psi (u, v, w are given in inches.)

Nodal point	u	v	w	Nodal point	u	v	w
1	0.000	1.197-03	-2.252-03	39	4.820-11	2.242-10	3.362-04
2	0.000	1.010-03	-1.796-04	40	1.055-10	3.670-10	2.234-03
3	0.000	9.791-04	1.164-10	41	-1.612-10	3.431-10	-2.339-03
4	0.000	1.010-03	1.796-04	42	-5.602-11	2.542-10	-8.992-04
5	0.000	1.197-03	2.252-03	43	-5.343-12	0.000	0.000
6	2.579-04	1.317-03	-2.258-03	44	5.821-11	2.692-10	8.992-04
7	1.754-04	1.202-03	-3.650-04	45	1.774-10	4.002-10	2.339-03
8	-3.638-12	1.166-03	1.128-10	46	0.000	-6.095-04	-2.194-03
9	-1.754-04	1.202-03	3.650-04	47	0.000	-5.812-04	-1.483-04
10	-2.579-04	1.317-03	2.258-03	48	0.000	-5.838-04	8.140-11
11	3.899-04	1.611-03	-2.380-03	49	0.000	-5.812-04	1.483-04
12	2.926-04	1.760-03	-9.642-04	50	0.000	-6.095-04	2.194-03
13	-3.763-11	1.861-10	1.830-10	51	-1.016-04	-6.575-04	-2.234-03
14	-2.926-04	1.760-03	9.642-04	52	-2.120-05	-6.135-04	-3.416-04
15	-3.899-04	1.611-03	2.380-03	53	2.160-12	-6.043-04	7.594-11
16	0.000	6.095-04	-2.194-03	54	2.120-05	-6.135-04	3.416-04
17	0.000	5.812-04	-1.483-04	55	1.016-04	-6.575-04	2.235-03
18	0.000	5.838-04	9.823-11	56	-1.627-04	-7.743-04	-2.343-03
19	0.000	5.812-04	1.483-04	57	-5.215-05	-7.698-04	-9.111-04
20	0.00	6.095-04	2.194-03	58	8.832-12	-7.621-04	9.260-11
21	1.016-04	6.575-04	-2.235-03	59	5.215-05	-7.698-04	9.111-04
22	2.120-05	6.136-04	-3.416-04	60	1.627-04	-7.743-04	2.343-03
23	-3.411-12	6.043-04	1.073-10	61	0.000	-1.197-03	-2.252-03
24	-2.120-05	6.136-04	3.416-04	62	0.000	-1.010-03	-1.796-04
25	-1.016-04	6.575-04	2.235-03	63	0.000	-9.790-04	9.413-11
26	1.627-04	7.743-04	-2.343-03	64	0.000	-1.010-03	1.796-04
27	5.215-05	7.698-04	-9.111-04	65	0.000	-1.197-03	2.252-03
28	-2.652-11	7.621-04	1.067-10	66	-2.579-04	-1.317-03	-2.258-03
29	-5.215-05	7.698-04	9.111-04	67	-1.754-04	-1.202-03	-3.650-04
30	-1.627-04	7.743-04	2.343-03	68	-8.924-12	-1.166-03	9.777-11
31	0.000	4.038-10	-2.182-03	69	1.754-04	-1.202-03	3.650-04
32	0.000	2.029-10	-1.400-04	70	2.579-04	-1.317-03	2.258-03
33	0.000	0.000	0.000	71	-3.899-04	-1.611-03	-2.380-03
34	0.000	2.078-10	1.400-04	72	-2.926-04	-1.760-03	-9.642-04
35	0.000	3.761-10	2.182-03	73	-9.095-13	-1.861-03	9.913-11
36	-1.414-10	3.547-10	-2.234-03	74	2.926-04	-1.760-03	9.642-04
37	-3.136-11	2.572-10	-3.362-04	75	3.899-04	-1.611-03	2.380-03
38	-3.524-12	0.000	0.000				

Table 7. Effective Moduli of Unidirectional Fiber Composites at Various Volumetric Ratios (C^*_{ij} are given in psi.)

Shape of fiber	Volumetric ratio (%)	C^*_{11} ($\times 10^8$)	C^*_{33} ($\times 10^8$)	C^*_{12} ($\times 10^8$)	C^*_{13} ($\times 10^8$)
square	0.00	0.40374	0.40394	0.17301	0.17307
	25.00	0.49777	0.51679	0.20487	0.19688
	49.00	0.62594	0.66558	0.23852	0.22607
	81.00	0.90738	0.97055	0.28027	0.27916
	100.00	1.16400	1.16420	0.32826	0.32821
Fixed-height cross	0.00	0.40374	0.40394	0.17301	0117307
	19.00	0.48410	0.50546	0.19097	0.19114
	36.00	0.55704	0.58995	0.21276	0.21025
	64.00	0.72146	0.77407	0.25768	0.25082
	75.00	0.81516	0.87326	0.27732	0.27038
	100.00	1.16400	1.16420	0.32826	0.32821
Varying-height cross	0.00	0.40374	0.40394	0.17301	0.17307
	27.00	0.50642	0.52797	0.20901	0.19948
	48.00	0.61426	0.65645	0.24062	0.22578
	60.75	0.70151	0.75731	0.25702	0.24513
	75.00	0.81516	0.87326	0.27732	0.27038
	100.00	1.16400	1.16420	0.32826	0.32821

Table 8. Effective Modulus C^*_{44} of Unidirectional Fiber Composites at Various Volumetric Ratios (C^*_{44} are given in psi.)

Shape of fiber	Volumetric ratio (%)	C^*_{44} ($\times 10^8$)
square	0.00	0.11420
	16.00	0.14727
	36.00	0.19516
	49.00	0.21422
	64.00	0.27294
	100.00	0.41802
Fixed-height cross	0.00	0.11420
	36.00	0.14029
	64.00	0.19260
	84.00	0.24526
	91.00	0.27451
	96.00	0.32222
	100.00	0.41802
Varying-height cross	0.00	0.11420
	20.00	0.13368

Table 9. Effective Modulus C_{66}^* of Unidirectional Fiber Composites at Various Volumetric Ratios (C_{66}^* are given in psi.)

Shape of fiber	Volumetric ratio (%)	C_{66}^* ($\times 10^8$)
Square	0.00	0.11500
	16.00	0.13607
	36.00	0.16903
	49.00	0.19786
	64.00	0.22172
	81.00	0.30670
	100.00	0.41373
Fixed-height cross	0.00	0.11500
	36.00	0.17211
	64.00	0.22172
	84.00	0.31328
	100.00	0.41373
Varying-height cross	0.00	0.11500

Table 10. Effective Moduli of Unidirectional Fiber Composites from Behrens' Results (C^*_{ij} are given in psi.)

Volumetric ratio (%)	C^*_{11} ($\times 10^8$)	C^*_{33} ($\times 10^8$)	C^*_{12} ($\times 10^8$)	C^*_{13} ($\times 10^8$)	C^*_{66} ($\times 10^8$)	C^*_{44} ($\times 10^8$)
0	0.4038	0.4038	0.1731	0.1731	0.1154	0.1154
5	0.4235	0.4418	0.1755	0.1768	0.1221	0.1214
10	0.4438	0.4796	0.1784	0.1808	0.1293	0.1288
15	0.4648	0.5174	0.1821	0.1849	0.1369	0.1370
20	0.4865	0.5550	0.1865	0.1894	0.1449	0.1462
25	0.5091	0.5925	0.1916	0.1941	0.1535	0.1561
30	0.5327	0.6299	0.1974	0.1991	0.1627	0.1669
35	0.5573	0.6673	0.2041	0.2044	0.1726	0.1784
40	0.5833	0.7047	0.2117	0.2101	0.1831	0.1909
45	0.6107	0.7420	0.2201	0.2161	0.1945	0.2041
50	0.6399	0.7794	0.2293	0.2227	0.2068	0.2182
55	0.6711	0.8168	0.2394	0.2297	0.2201	0.2333
60	0.7047	0.8543	0.2503	0.2372	0.2345	0.2494
65	0.7412	0.8920	0.2620	0.2454	0.2502	0.2663
70	0.7811	0.9298	0.2742	0.2542	0.2674	0.2843
75	0.8253	0.9678	0.2869	0.2639	0.2863	0.3034
80	0.8747	1.0060	0.2996	0.2744	0.3074	0.3237
85	0.9307	1.0450	0.3117	0.2859	0.3303	0.3453
90	0.9953	1.0840	0.3221	0.2987	0.3562	0.3681
95	1.0720	1.1240	0.3289	0.3128	0.3852	0.3923
100	1.1650	1.1650	0.3285	0.3285	0.4180	0.4180

Table 11. Effective Moduli of Lamellar Composites at Various Volumetric Ratios (C^*_{ij} are given in psi.)

Volumetric ratio (%)	C_{11} ($\times 10^8$)	C_{33} ($\times 10^8$)	C_{12} ($\times 10^8$)	C_{13} ($\times 10^8$)
0.00	0.40374	0.40374	0.17301	0.17307
30.00	0.55155	0.50097	0.20519	0.20073
70.00	0.83866	0.74040	0.26256	0.25617
100.00	1.16440	1.16420	0.32826	0.32821

Table 12. Effective Modulus C^*_{66} of Lamellar Composites at Various Volumetric Ratios (C^*_{66} is given in psi.)

Volumetric ratio (%)	C^*_{66} ($\times 10^8$)
0.00	0.11420
20.00	0.12559
40.00	0.16242
60.00	0.20402
70.00	0.23394
100.00	0.41802

Table 13. Effective Modulus C^*_{44} Of Lamellar Composites at Various Volumetric Ratios (C^*_{44} is given in psi.)

Volumetric ration (%)	C^*_{44} ($\times 10^8$)
0.00	0.11420
50.00	0.21886
80.00	0.32754
100.00	0.41802

Table 14. Effective Moduli of Lamellar Composites from Behrens' Results (C^*_{ij} are given in psi.)

Volumetric ratio (%)	C^*_{11} ($\times 10^8$)	C^*_{33} ($\times 10^8$)	C^*_{12} ($\times 10^8$)	C^*_{13} ($\times 10^8$)	C^*_{66} ($\times 10^8$)	C^*_{44} ($\times 10^8$)
0	0.4038	0.4038	0.1731	0.1731	0.1154	0.1154
5	0.4409	0.4175	0.1798	0.1759	0.1197	0.1305
10	0.4779	0.4321	0.1866	0.1788	0.1244	0.1456
15	0.5150	0.4477	0.1935	0.1820	0.1294	0.1608
20	0.5522	0.4645	0.2003	0.1855	0.1349	0.1759
25	0.5894	0.4827	0.2073	0.1892	0.1409	0.1910
30	0.6266	0.5023	0.2143	0.1932	0.1474	0.2062
35	0.6640	0.5235	0.2213	0.1975	0.1545	0.2213
40	0.7014	0.5467	0.2285	0.2023	0.1624	0.2364
45	0.7389	0.5720	0.2357	0.2074	0.1711	0.2516
50	0.7765	0.5997	0.2431	0.2131	0.1809	0.2667
55	0.8142	0.6303	0.2505	0.2193	0.1917	0.2818
60	0.8521	0.6641	0.2581	0.2262	0.2040	0.2970
65	0.8901	0.7018	0.2659	0.2339	0.2179	0.3121
70	0.9283	0.7441	0.2738	0.2426	0.2339	0.3272
75	0.9667	0.7917	0.2820	0.2523	0.2525	0.3424
80	1.0050	0.8459	0.2904	0.2634	0.2742	0.3575
85	1.0440	0.9080	0.2992	0.2761	0.3000	0.3726
90	1.0840	0.9799	0.3084	0.2908	0.3312	0.3878
95	1.1240	1.0640	0.3181	0.3080	0.3696	0.4029
100	1.1650	1.1650	0.3285	0.3285	0.4180	0.4180

Table 15. Effective Moduli of Short Fiber Composites at Various Volumetric Ratios (C^*_{ij} and E^* are given in psi.)

Volumetric ratio (%)	C^*_{11} ($\times 10^8$)	C^*_{12} ($\times 10^8$)	C^*_{66} ($\times 10^8$)	ν^*	E^* ($\times 10^8$)
0.00	0.40370	0.17296	0.11537	0.29993	0.29995
34.30	0.55892	0.21498	0.17197	0.27778	0.43950
72.90	0.85042	0.26584	0.29229	0.23815	0.72381
100.00	1.16440	0.32824	0.41808	0.21990	1.02007

Table 16. Displacements of the Nodal Points for the Discretized Model Shown in Figure 49 Loaded by T_{zz}=-10,000 psi (u, v, w are given in inches.)

Nodal point	u	v	w	Nodal point	u	v	w
1	-7.334-04	-3.904-04	-2.722-03	43	9.085-05	-2.258-04	-4.119-04
2	-7.197-04	-2.630-04	-2.707-03	44	3.125-05	-1.375-04	-3.375-04
3	-7.171-04	-1.693-04	-2.638-03	45	-3.327-06	-8.829-05	-3.606-04
4	-7.510-04	0.000	-2.510-03	46	0.000	0.000	-5.634-04
5	-6.883-04	8.354-05	-2.019-03	47	-1.269-04	9.594-05	-4.118-04
6	-6.713-04	1.351-04	-2.002-03	48	-1.359-04	1.455-04	-4.141-04
7	-6.456-04	2.484-04	-2.304-03	49	-1.370-04	2.250-04	-4.404-04
8	-5.310-04	-3.677-04	-1.847-03	50	1.462-05	-2.174-04	3.223-05
9	-5.449-04	-2.573-04	-1.900-03	51	-8.845-06	-1.441-04	1.668-04
10	-5.447-04	-1.168-04	-1.882-03	52	-1.596-05	-8.923-05	1.660-04
11	-5.914-04	0.000	-1.586-03	53	-1.360-05	0.000	0.000
12	-5.707-04	4.076-05	-1.399-03	54	-2.206-05	8.487-05	-1.526-04
13	-5.514-04	8.933-05	-1.295-03	55	-1.560-05	1.410-04	-1.748-04
14	-5.208-04	1.850-04	-1.509-03	56	-2.179-06	2.110-04	-1.567-05
15	5.064-04	-1.167-04	-1.422-03	57	-4.910-05	-1.974-04	4.818-05
16	4.812-04	-5.759-05	-1.250-03	58	-3.088-05	-1.321-04	-1.095-04
17	4.657-04	-2.082-05	-1.245-03	59	-3.417-05	-8.266-05	-1.224-04
18	6.043-04	0.000	-1.929-03	60	-6.419-05	0.000	0.000
19	5.717-04	8.968-05	-1.846-03	61	-2.743-05	8.310-05	1.745-04
20	5.697-04	1.932-04	-1.852-03	62	-6.517-05	1.213-04	1.729-04
21	5.316-04	2.610-04	-1.756-03	63	-7.228-05	1.926-04	3.382-05
22	6.386-04	-2.074-04	-1.822-03	64	-1.412-04	-2.571-04	1.704-04
23	5.799-04	-9.629-05	-1.578-03	65	-1.074-04	-1.518-04	1.614-04
24	6.147-04	-5.259-05	-1.603-03	66	-8.366-05	-1.007-04	1.633-04
25	6.977-04	0.000	-1.889-03	67	0.000	0.000	1.993-04
26	7.495-04	1.750-04	-2.092-03	68	6.764-06	9.982-05	1.099-05
27	7.565-04	2.440-04	-2.157-03	69	6.188-05	1.638-04	6.848-05
28	7.496-04	3.348-04	-2.136-03	70	1.261-04	2.789-04	1.314-04
29	-5.048-04	-4.104-04	-1.483-03	71	-3.987-04	-2.110-04	1.082-03
30	-5.153-04	-2.730-04	-1.518-03	72	-4.417-04	-1.304-04	1.214-03
31	-5.087-04	-1.027-04	-1.479-03	73	-4.644-04	-9.292-05	1.240-03
32	-4.752-04	0.000	-1.384-03	74	-5.285-04	0.000	1.172-03
33	-4.120-04	1.137-04	-1.412-03	75	-5.884-04	1.004-04	1.241-03
34	-4.086-04	1.565-04	-1.399-03	76	-5.933-04	2.783-04	1.246-03
35	-3.635-04	2.370-04	-1.312-03	77	-5.732-04	4.150-04	1.193-03
36	2.961-04	-1.973-04	-1.196-03	78	5.411-04	-3.937-04	1.270-03
37	3.153-04	-1.040-04	-1.274-03	79	5.610-04	-2.650-04	1.321-03
38	3.375-04	-6.193-05	-1.276-03	80	5.718-04	-1.081-04	1.314-03
39	4.886-04	0.000	-1.202-03	81	5.023-04	0.000	1.235-03
40	5.082-04	1.301-04	-1.466-03	82	4.617-04	7.999-05	1.364-03
41	4.739-04	3.089-04	-1.505-03	83	4.515-04	1.269-04	1.323-03
42	4.180-04	4.573-04	-1.482-03	84	4.161-04	2.097-04	1.203-03

Table 16. Continued

Nodal point	u	v	w	Nodal point	u	v	w
85	-6.347-04	-1.267-04	2.062-03	99	3.689-04	-2.084-04	2.009-03
86	-5.437-04	-6.192-05	1.663-03	100	3.898-04	-1.589-04	2.041-03
87	-5.507-04	-4.536-05	1.694-03	101	4.198-04	-7.676-05	1.999-03
88	-6.217-04	0.000	2.168-03	102	4.669-04	0.000	1.892-03
89	-5.670-04	1.223-04	2.240-03	103	5.547-04	2.946-05	1.567-03
90	-5.361-04	1.555-04	2.253-03	104	5.806-04	6.147-05	1.515-03
91	-5.379-04	1.824-04	2.162-03	105	5.382-04	9.767-05	1.710-03
92	-4.226-04	-9.209-05	1.676-03	106	6.276-04	-2.065-04	2.254-03
93	-4.469-04	-5.165-05	1.441-03	107	6.275-04	-1.642-04	2.310-03
94	-4.407-04	-1.574-05	1.489-03	108	6.517-04	-1.178-04	2.295-03
95	-4.005-04	0.000	1.872-03	109	7.086-04	0.000	2.265-03
96	-3.454-04	8.766-05	2.118-03	110	6.528-04	3.383-05	1.821-03
97	-2.837-04	1.464-04	2.140-03	111	6.605-04	5.023-05	1.796-03
98	-2.930-04	2.011-04	2.002-03	112	7.609-04	1.224-04	2.186-03

Table 17. Displacements of the Nodal Points for the Discretized Model Shown in Figure 49 Loaded by T_{yy}=-10,000 psi (u, v, w are given in inches.)

Nodal point	u	v	w	Nodal point	u	v	w
1	-4.425-04	1.033-03	4.512-04	43	-4.759-05	7.963-04	1.820-04
2	-4.622-04	6.816-04	4.784-04	44	4.081-05	4.748-04	1.052-04
3	-4.291-04	4.174-04	4.525-04	45	3.805-05	3.181-04	8.641-05
4	-3.543-04	0.000	3.959-04	46	0.000	0.000	1.478-04
5	-2.767-04	-2.932-04	3.086-04	47	-3.490-05	-3.303-04	1.129-04
6	-3.180-04	-3.819-04	2.768-04	48	-1.131-05	-4.972-04	1.037-04
7	-4.089-04	-7.071-04	2.757-04	49	8.075-05	-8.056-04	1.373-04
8	-2.567-04	1.083-03	4.896-04	50	-1.729-04	7.848-04	5.400-05
9	-2.406-04	7.491-04	4.760-04	51	-1.039-04	4.659-04	-4.548-05
10	-2.178-04	2.914-04	4.487-04	52	-9.774-05	3.154-04	-4.698-05
11	-1.976-04	0.000	3.916-04	53	-1.523-04	0.000	0.000
12	-2.148-04	-1.982-04	2.924-04	54	-1.206-04	-3.130-04	1.219-05
13	-2.239-04	-2.733-04	2.379-04	55	-1.153-04	-4.633-04	-6.144-06
14	-1.724-04	-5.928-04	2.872-04	56	-1.592-04	-7.836-04	-1.060-04
15	1.882-04	8.701-04	4.579-04	57	1,965-04	7.973-04	-6.969-05
16	2.476-04	5.580-04	3.229-04	58	1.377-04	4.797-04	1.068-05
17	2.670-04	4.332-04	2.982-04	59	1.168-04	3.247-04	7.332-06
18	2.169-04	0.000	3.782-04	60	1.823-04	0.000	0.000
19	2.167-04	-3.358-04	4.071-04	61	1.277-04	-3.126-04	-5.234-05
20	2.481-04	-7.892-04	4.494-04	62	1.126-04	-4.592-04	-5.426-05
21	3.010-04	-1.123-03	4.821-04	63	1.624-04	-7.843-04	3.481-05
22	4.150-04	8.386-04	3.995-04	64	7.062-05	7.870-04	-2.101-04
23	3.205-04	4.756-04	3.207-04	65	-1.983-05	4.713-04	-1.479-04
24	3.547-04	3.667-04	3.166-04	66	-2.362-05	3.185-04	-1.399-04
25	4.424-04	0.000	3.727-04	67	0.000	0.000	-1.917-04
26	4.588-04	-4.435-04	4.084-04	68	4.538-05	-4.012-04	-1.167-04
27	4.907-04	-7.409-04	4.605-04	69	3.008-05	-5.804-04	-1.601-04
28	4.814-04	-1.103-03	4.505-04	70	-5.516-05	-8.797-04	-2.233-04
29	-4.904-04	1.102-03	2.801-04	71	-4.210-04	7.664-04	-1.903-04
30	-4.701-04	7.694-04	2.596-04	72	-3.110-04	4.503-04	-2.562-04
31	-4.306-04	3.212-04	2.303-04	73	-3.207-04	3.119-04	-2.611-04
32	-3.686-04	0.000	2.084-04	74	-4.281-04	0.000	-2.126-04
33	-2.834-04	-3.197-04	2.274-04	75	-4.482-04	-3.219-04	-2.291-04
34	-3.124-04	-4.778-04	1.891-04	76	-4.747-04	-7.763-04	-2.526-04
35	-4.460-04	-7.872-04	1.144-04	77	-4.947-04	-1.110-03	-2.802-04
36	4.030-04	7.938-04	1.890-04	78	5.080-04	1.096-03	-2.923-04
37	3.053-04	4.817-04	2.336-04	79	4.891-04	7.597-04	-2.572-04
38	3.191-04	3.373-04	2.349-04	80	4.604-04	3.102-04	-2.393-04
39	3.956-04	0.000	1.236-04	81	4.415-04	0.000	-2.091-04
40	4.571-04	-3.127-04	1.824-04	82	3.351-04	-3.084-04	-2.694-04
41	4.939-04	-7.617-04	2.290-04	83	3.225-04	-4.454-04	-2.635-04
42	5.077-04	-1.094-03	2.718-04	84	4.274-04	-7.583-04	-2.031-04

Table 17. Continued

Nodal point	u	v	w	Nodal point	u	v	w
85	-3.806-04	7.701-04	-4.332-04	99	3.052-04	1.107-03	-5.206-04
86	-3.256-04	4.162-04	-3.326-04	100	2.776-04	7.703-04	-4.857-04
87	-3.330-04	3.272-04	-3.387-04	101	2.520-04	3.242-04	-4.520-04
88	-4.210-04	0.000	-4.308-04	102	2.296-04	0.000	-4.492-04
89	-4.736-04	-4.134-04	-4.655-04	103	2.690-04	-2.944-04	-3.605-04
90	-4.998-04	-6.974-04	-4.831-04	104	2.427-04	-4.303-04	-3.211-04
91	-4.749-04	-1.051-03	-4.574-04	105	1.611-04	-7.497-04	-4.099-04
92	-1.726-04	7.699-04	-4.358-04	106	4.806-04	1.077-03	-4.857-04
93	-2.361-04	4.541-04	-3.218-04	107	5.092-04	7.185-04	-4.921-04
94	-2.493-04	3.137-04	-3.321-04	108	4.809-04	4.270-04	-4.584-04
95	-2.182-04	0.000	-4.485-04	109	4.260-04	0.000	-4.326-04
96	-2.626-04	-3.089-04	-4.944-04	110	3.426-04	-3.101-04	-3.518-04
97	-2.715-04	-7.267-04	-4.813-04	111	3.361-04	-3.946-04	-3.368-04
98	-2.822-04	-1.067-03	-4.880-04	112	3.807-04	-7.451-04	-4.282-04

Table 18. Displacements of the Nodal Points for the Discretized Model Shown in Figure 49 Loaded by T_{xz}=10,000 psi (u, v, w are given in inches.)

Nodal point	u	v	w	Nodal point	u	v	w
1	3.234-03	-1.645-04	-2.750-03	43	1.134-03	4.315-05	-6.131-05
2	3.246-03	-1.374-04	-2.778-03	44	9.857-04	3.973-05	1.500-04
3	3.148-03	-1.583-04	-2.784-03	45	1.003-03	1.774-05	1.733-04
4	2.892-03	0.000	-2.527-03	46	1.239-03	0.000	9.203-05
5	2.320-03	1.747-05	-2.014-03	47	1.080-03	1.068-05	-2.452-05
6	2.318-03	1.048-04	-2.025-03	48	1.096-03	2.727-05	-2.146-05
7	2.708-03	2.650-04	-2.429-03	49	1.158-03	1.081-05	2.084-04
8	2.639-03	-2.306-04	-1.248-03	50	5.138-04	6.991-05	-7.082-04
9	2.728-03	-1.587-04	-1.313-03	51	3.071-04	6.475-05	-5.522-04
10	2.680-03	-4.685-05	-1.277-03	52	3.087-04	3.596-05	-5.413-04
11	2.336-03	0.000	-1.144-03	53	4.364-04	0.000	-6.604-04
12	2.044-03	1.961-05	-1.195-03	54	5.917-04	-8.848-07	-5.954-04
13	1.964-03	3.631-05	-1.177-03	55	5.711-04	2.074-05	-5.922-04
14	2.303-03	5.366-05	-1.152-03	56	3.312-04	1.251-05	-6.626-04
15	2.082-03	6.472-05	9.761-04	57	2.530-04	2.267-05	6.423-04
16	1.758-03	3.646-05	1.144-03	58	4.917-04	3.686-05	5.611-04
17	1.714-03	1.630-05	1.161-03	59	5.069-04	1.394-05	5.575-04
18	2.465-03	0.000	8.709-04	60	4.659-04	0.000	6.564-04
19	2.493-03	-5.371-05	1.015-03	61	3.409-04	3.564-05	5.144-04
20	2.509-03	-1.629-04	1.055-03	62	3.599-04	8.852-05	5.624-04
21	2.392-03	-2.320-04	1.054-03	63	5.903-04	1.209-04	7.065-04
22	2.187-03	2.544-04	2.249-03	64	-1.559-04	5.509-05	8.539-05
23	1.801-03	1.157-04	1.909-03	65	-6.406-05	5.711-05	-1.395-04
24	1.831-03	3.940-05	1.870-03	66	-4.826-05	2.421-05	-1.439-04
25	2.366-03	0.000	2.219-03	67	-1.041-04	0.000	-3.334-05
26	2.621-03	-1.499-04	2.317-03	68	7.762-03	7.180-05	3.077-04
27	2.620-03	-1.121-04	2.404-03	69	7.000-05	1.032-04	2.431-04
28	2.563-03	-1.142-04	2.375-03	70	-1.008-04	7.655-05	-5.641-05
29	1.740-03	-2.519-04	-2.159-03	71	-5.702-04	7.720-05	-1.538-03
30	1.793-03	-1.782-04	-2.248-03	72	-7.394-04	5.313-05	-1.220-03
31	1.737-03	-7.179-05	-2.195-03	73	-7.352-04	3.530-05	-1.241-03
32	1.163-03	0.000	-2.007-03	74	-5.491-04	0.000	-1.579-03
33	1.648-03	1.400-05	-1.716-03	75	-5.856-04	-4.678-05	-1.729-03
34	1.660-03	3.185-05	-1.712-03	76	-6.096-04	-1.711-04	-1.789-03
35	1.632-03	6.816-05	-2.010-03	77	-6.271-04	-2.329-04	-1.677-03
36	1.448-03	9.536-05	2.170-03	78	-6.348-04	-2.126-04	1.742-03
37	1.471-03	6.504-05	1.864-03	79	-6.426-04	-1.564-04	1.841-03
38	1.459-03	4.381-05	1.851-03	80	-5.869-04	-6.531-05	1.773-03
39	1.482-03	0.000	2.017-03	81	-5.269-04	0.000	1.623-03
40	1.713-03	-3.754-05	2.264-03	82	-6.990-04	2.892-05	1.238-03
41	1.757-03	-1.398-04	2.347-03	83	-6.853-04	3.935-05	1.205-03
42	1.712-03	-2.127-04	2.265-03	84	-4.973-04	5.378-05	1.531-03

Table 18. Continued

Nodal point	u	v	w	Nodal point	u	v	w
85	-2.017-03	2.072-04	-1.599-03	99	-2.042-03	-1.856-04	1.140-03
86	-1.696-03	6.889-05	-1.245-03	100	-2.146-03	-1.327-04	1.165-03
87	-1.697-03	7.583-06	-1.251-03	101	-2.111-03	-4.375-05	1.135-03
88	-2.155-03	0.000	-1.664-03	102	-1.995-03	0.000	1.063-03
89	-2.372-03	-1.558-04	-1.850-03	103	-1.733-03	1.555-06	1.046-03
90	-2.435-03	-9.176-05	-1.863-03	104	-1.718-03	3.189-05	1.054-03
91	-2.379-03	-7.076-05	-1.779-03	105	-2.022-03	5.741-05	9.611-04
92	-1.960-03	6.114-05	-9.364-04	106	-2.156-03	-1.012-04	1.865-03
93	-1.648-03	3.978-05	-1.031-03	107	-2.194-03	-9.283-05	1.902-03
94	-1.671-03	1.421-05	-1.055-03	108	-2.180-03	-1.182-04	1.858-03
95	-2.014-03	0.000	-1.045-03	109	-2.085-03	0.000	1.701-03
96	-2.344-03	-9.533-05	-1.427-03	110	-1.736-03	4.821-06	1.230-03
97	-2.440-03	-1.433-04	-1.360-03	111	-1.751-03	5.912-05	1.216-03
98	-2.229-03	-2.142-04	-1.230-03	112	-2.073-03	1.914-04	1.565-03

Table 19. Displacements of the Nodal Points for the Discretized Model Shown in Figure 49 Loaded by T_{yz}=10,000 psi (u, v, w are given in inches.)

Nodal point	u	v	w	Nodal point	u	v	w
1	-6.600-04	2.394-03	-1.847-03	43	0.000	6.370-05	-2.119-03
2	-3.139-04	2.288-03	-1.315-03	44	0.000	4.319-05	-1.174-03
3	-2.329-04	2.138-03	-6.696-04	45	0.000	4.780-05	-8.234-04
4	-1.088-04	2.072-03	1.479-04	46	0.000	4.110-05	1.534-04
5	-1.120-04	1.944-03	9.621-04	47	0.000	-3.053-05	9.300-04
6	2.971-04	1.975-03	8.366-04	48	0.000	-2.957-05	1.276-03
7	5.923-04	2.045-03	1.485-03	49	0.000	-1.845-06	2.172-03
8	-5.401-04	1.299-03	-1.905-03	50	2.362-04	-5.445-05	-2.263-03
9	-2.134-04	1.177-03	-1.458-03	51	2.995-05	-3.824-05	-1.281-03
10	-1.237-04	1.117-03	-4.819-04	52	-1.763-05	-3.707-05	-9.149-04
11	-5.384-05	9.761-04	-3.456-05	53	-8.178-05	-9.520-06	-2.026-05
12	-7.957-05	9.295-04	8.666-04	54	-1.451-05	2.890-05	8.447-04
13	1.829-04	8.955-04	8.843-04	55	-1.139-05	5.809-05	1.231-03
14	4.302-04	9.711-04	1.587-03	56	-1.271-04	7.421-05	2.271-03
15	7.071-04	1.652-04	-2.632-03	57	-2.035-04	5.601-05	-2.453-03
16	3.465-04	1.991-04	-1.413-03	58	-7.284-05	6.681-05	-1.390-03
17	2.509-04	2.353-04	-1.061-03	59	-7.690-05	4.666-05	-9.964-04
18	1.148-05	4.698-04	6.308-04	60	-1.255-04	-3.519-05	-4.015-05
19	4.938-06	4.530-04	8.789-04	61	-5.493-05	-1.165-04	9.805-04
20	-2.278-04	4.139-04	1.899-03	62	4.857-05	-1.219-04	1.429-03
21	-6.394-04	3.457-04	2.847-03	63	3.070-04	-1.411-04	2.537-03
22	5.445-04	5.544-04	-2.383-03	64	0.000	5.232-04	-2.055-03
23	3.878-04	5.565-04	-1.557-03	65	0.000	5.440-04	-1.397-03
24	1.981-04	5.339-04	-1.277-03	66	0.000	5.534-04	-8.980-04
25	2.234-04	5.012-04	-4.741-04	67	0.000	5.800-04	-1.526-04
26	-2.186-05	5.603-04	7.214-04	68	0.000	6.850-04	9.393-04
27	-1.656-04	6.897-04	1.618-03	69	0.000	6.825-04	1.521-03
28	-4.351-04	7.704-04	2.520-03	70	0.000	6.453-04	2.132-03
29	-4.261-04	1.091-03	-1.938-03	71	7.097-04	-5.929-04	-2.354-03
30	-1.399-04	1.062-03	-1.532-03	72	2.922-04	-5.704-04	-1.381-03
31	-1.095-04	1.032-03	-5.676-04	73	9.498-05	-5.348-04	-1.142-03
32	-4.766-05	1.002-03	9.300-05	74	-2.459-05	-5.052-04	-1.075-04
33	-8.000-05	1.018-03	8.801-04	75	-2.049-04	-5.555-04	7.678-04
34	1.532-04	1.042-03	9.831-04	76	-4.252-04	-5.870-04	1.906-03
35	3.744-04	1.104-03	1.557-03	77	-8.545-04	-5.778-04	2.670-03
36	4.277-04	7.274-04	-2.240-03	78	-8.540-04	-4.400-04	-2.893-03
37	2.314-04	6.650-04	-1.583-03	79	-4.310-04	-4.462-04	-2.064-03
38	2.202-05	6.261-04	-1.320-03	80	-2.119-04	-3.911-04	-8.371-04
39	-4.063-06	5.526-04	-4.653-04	81	-3.617-05	-2.964-04	1.266-04
40	-1.495-04	6.431-04	6.162-04	82	9.585-05	-3.258-04	1.159-03
41	-2.183-04	7.020-04	1.812-03	83	2.431-04	-3.755-04	1.411-03
42	-5.361-04	7.360-04	2.334-03	84	6.678-04	-4.026-04	2.486-03

Table 19. Continued

Nodal point	u	v	w	Nodal point	u	v	w
85	7.124-04	-9.097-04	-2.777-03	99	-6.517-04	-2.912-04	-3.350-03
86	3.519-04	-9.099-04	-1.350-03	100	-3.996-04	-3.027-04	-1.990-03
87	7.433-05	-9.152-04	-1.170-03	101	-2.058-04	-2.910-04	-8.450-04
88	-1.089-04	-1.024-03	-1.348-04	102	-8.174-05	-2.293-04	1.798-04
89	-2.952-04	-1.079-03	8.236-04	103	9.936-06	-1.744-04	1.125-03
90	-5.097-04	-1.157-03	1.843-03	104	2.713-04	-1.305-04	1.486-03
91	-8.473-04	-1.220-03	3.117-03	105	4.049-04	-1.289-04	2.969-03
92	5.549-04	-3.264-04	-2.833-03	106	-7.955-04	-8.907-04	-3.348-03
93	3.433-04	-3.271-04	-1.349-03	107	-4.544-04	-8.331-04	-1.975-03
94	4.788-05	-3.592-04	-1.130-03	108	-2.675-04	-7.544-04	-8.923-04
95	-3.667-05	-4.562-04	-9.143-05	109	-1.189-04	-7.334-04	1.494-04
96	-2.251-04	-5.800-04	6.627-04	110	3.600-05	-6.339-04	1.171-03
97	-4.456-04	-6.434-04	1.867-03	111	2.699-04	-6.218-04	1.406-03
98	-7.525-04	-6.220-04	3.121-03	112	5.721-04	-6.191-04	2.869-03

FIGURES

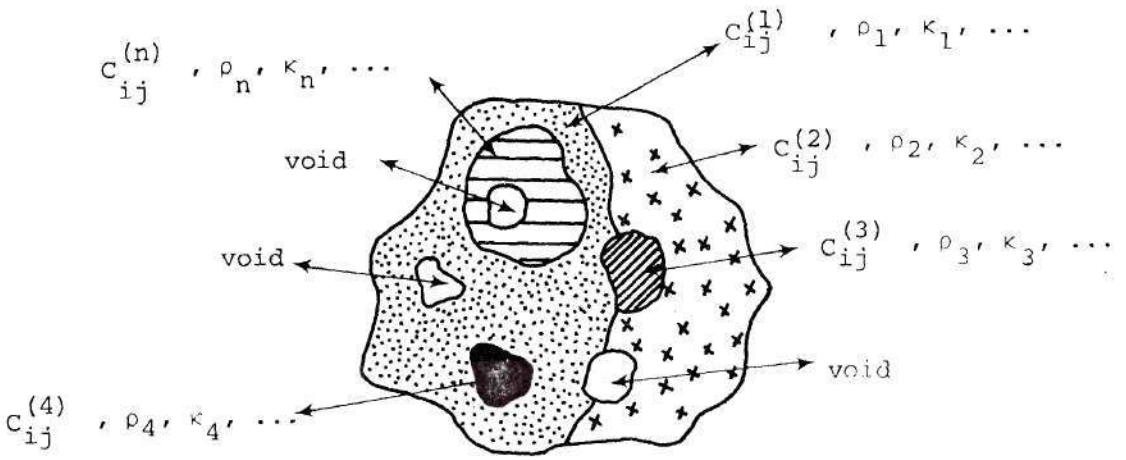

Figure 1. Composite Material

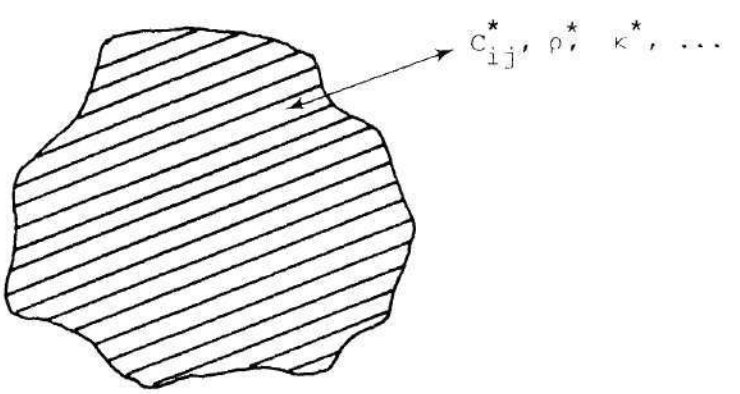

Figure 2. Equivalent Material

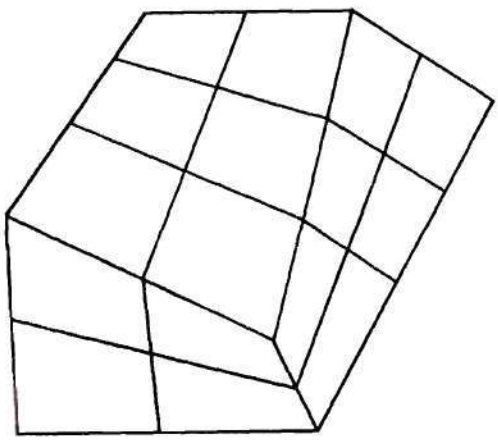

Figure 3. Discretization of a Continuum

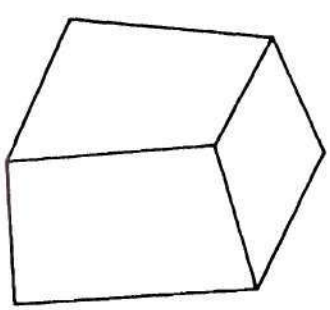

Figure 4. An Element

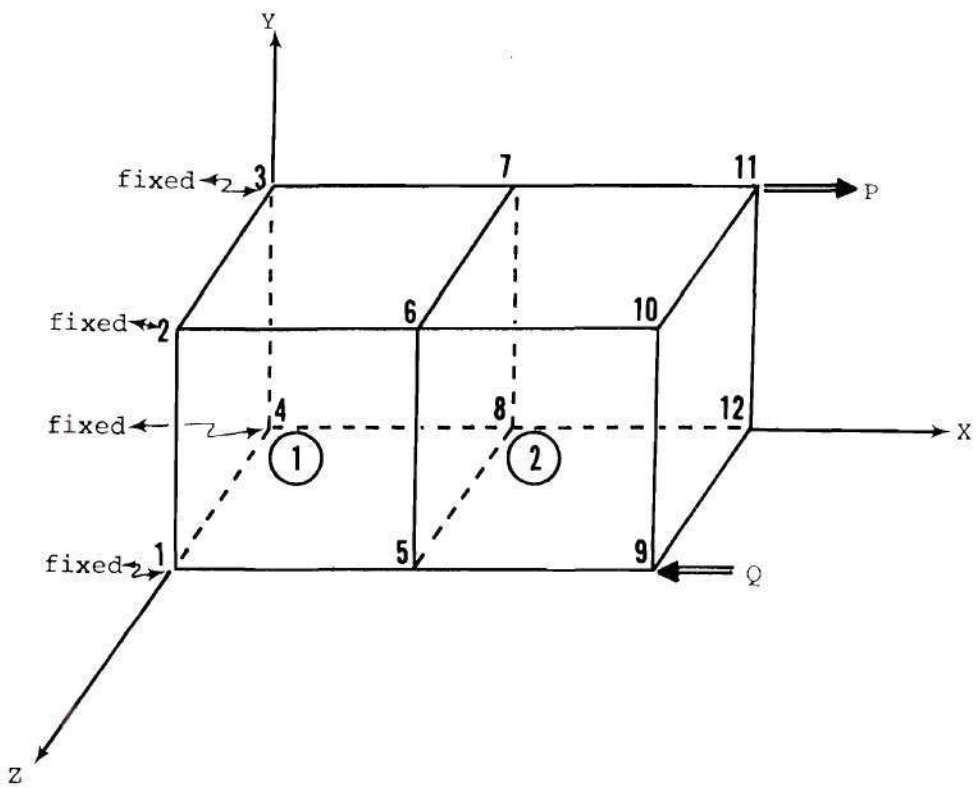

Figure 5. An Example of a Total Structure

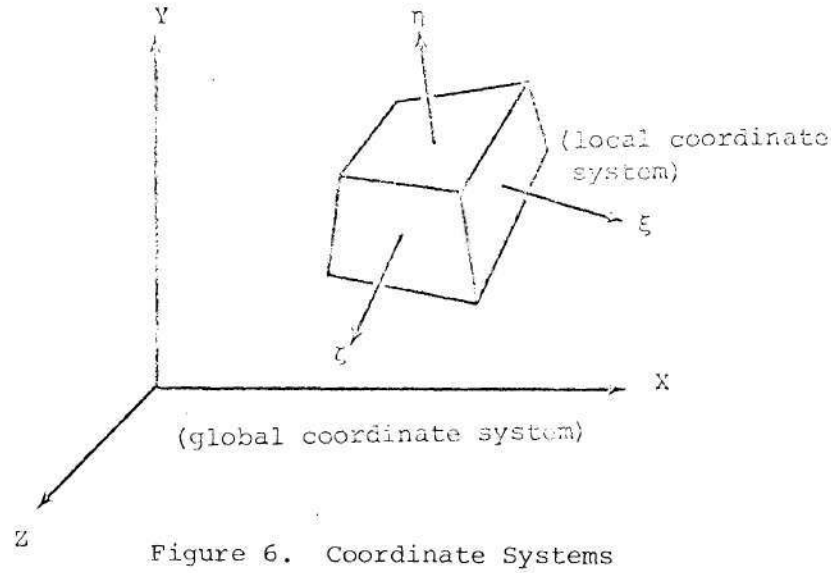

Figure 6. Coordinate Systems

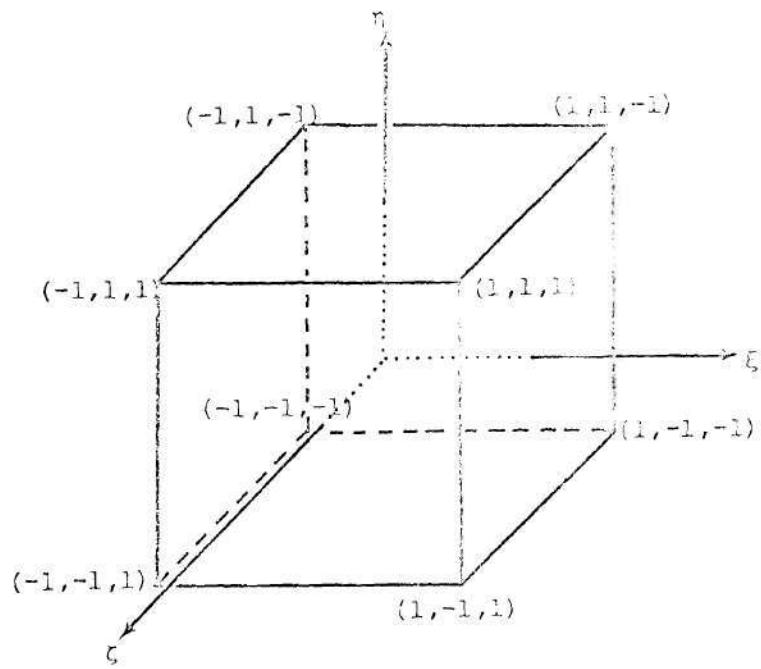

Figure 7. Coordinates of the Nodal Points in Local Coordinate System

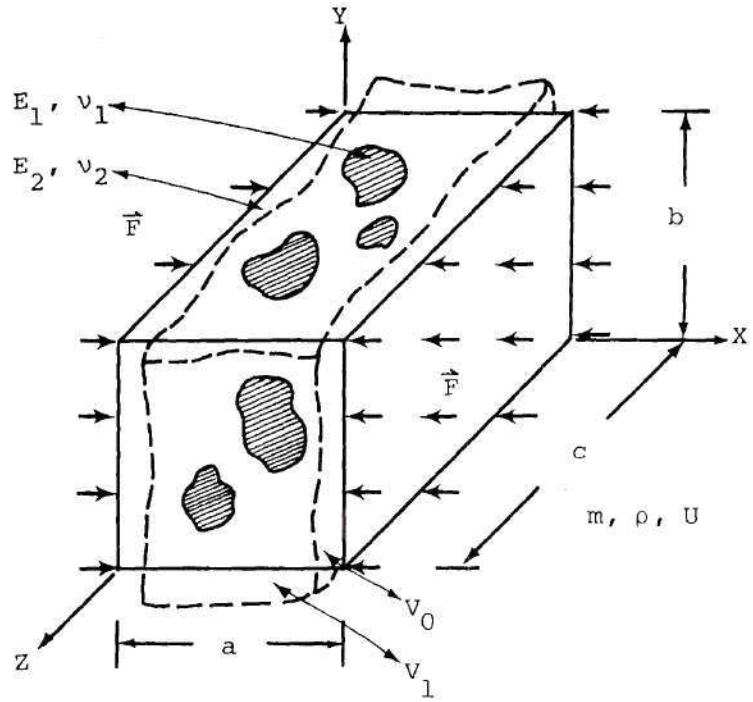

Figure 8. Actual Composite

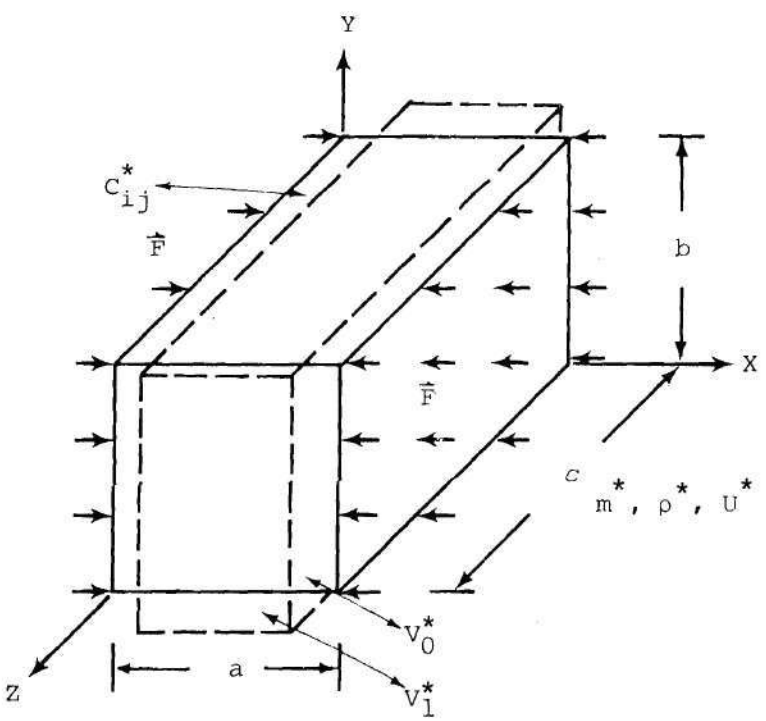

Figure 9. Equivalent Material

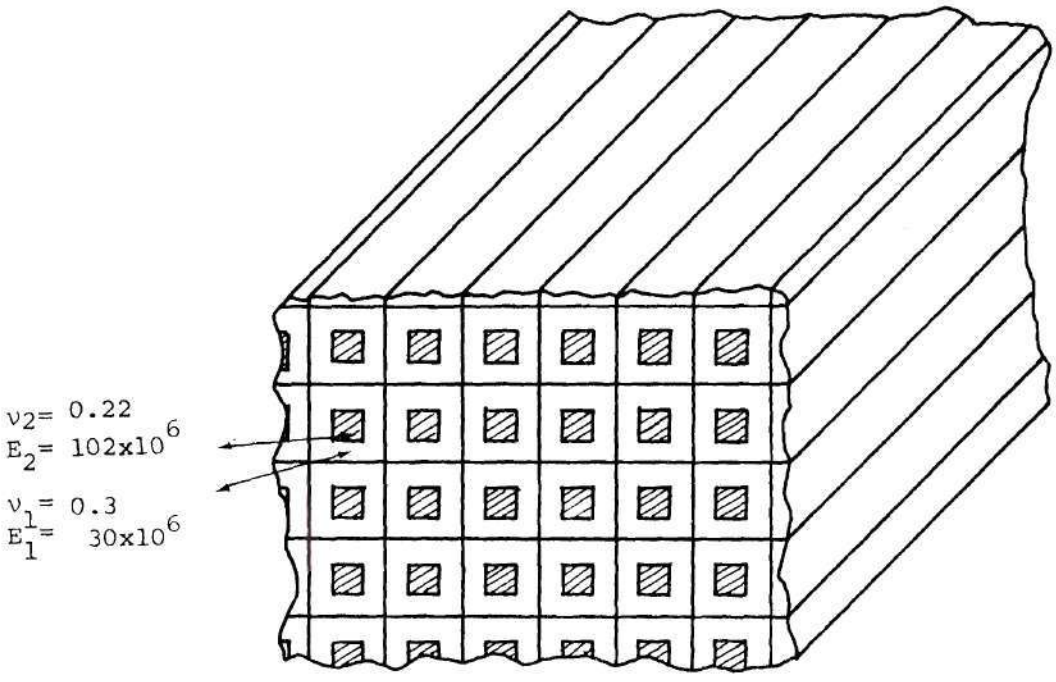

Figure 10. Unidirectional Square-Fiber Composite

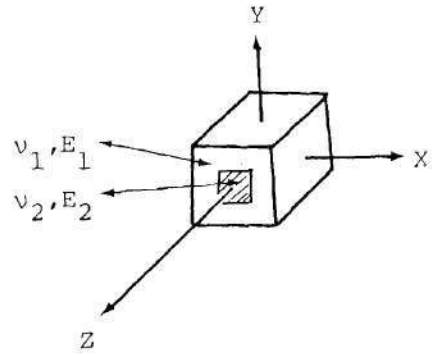

Figure 11. A Representative Basic Cell for the Composite Shown in Figure 10

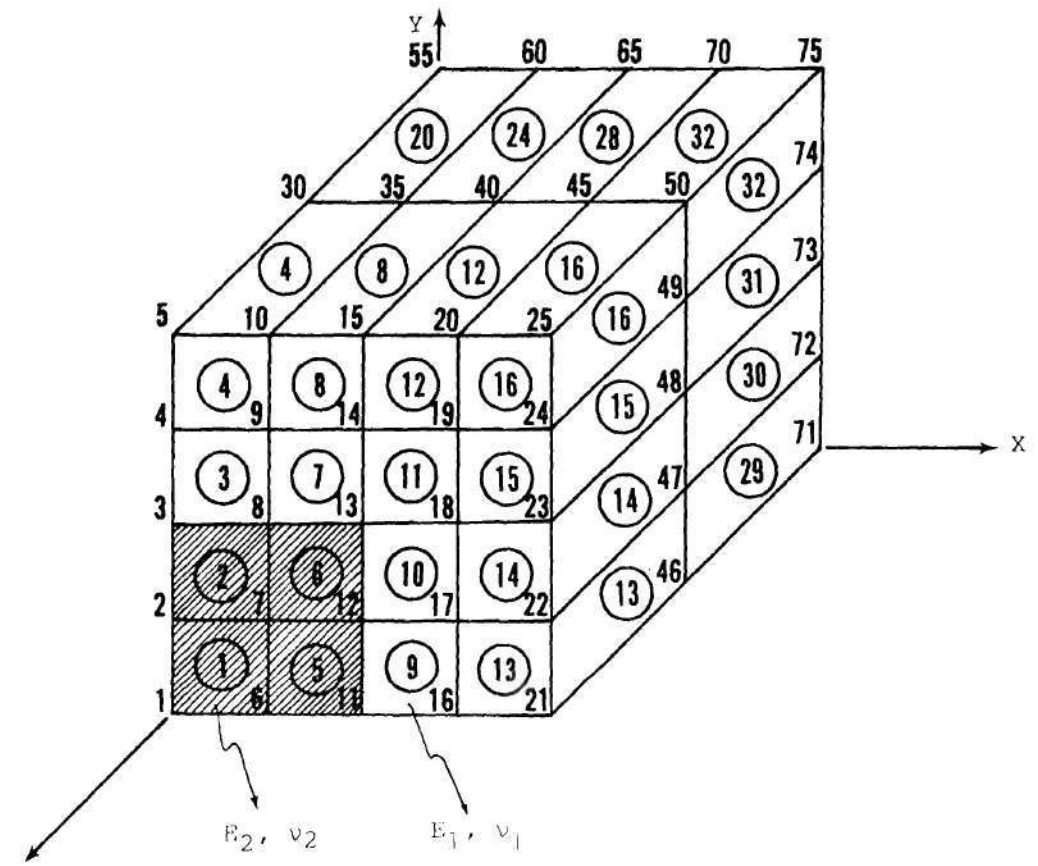

Figure 12. Discretization of One Octant of the Basic Cell Shown in Figure 11 (Volumetric Ratio of Fiber to Entire Basic Cell: 25%)

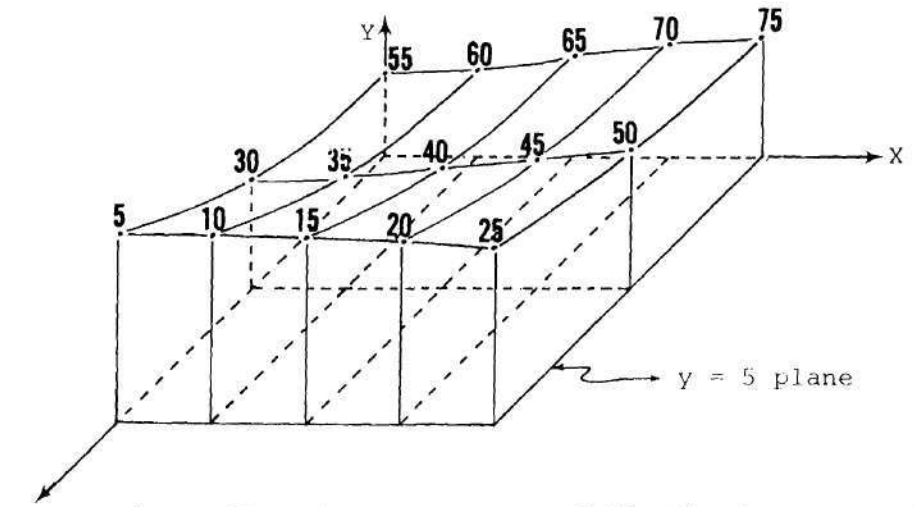

Figure 13. The v-Component of the Displacements of the Nodal Points on the Plane y = 5

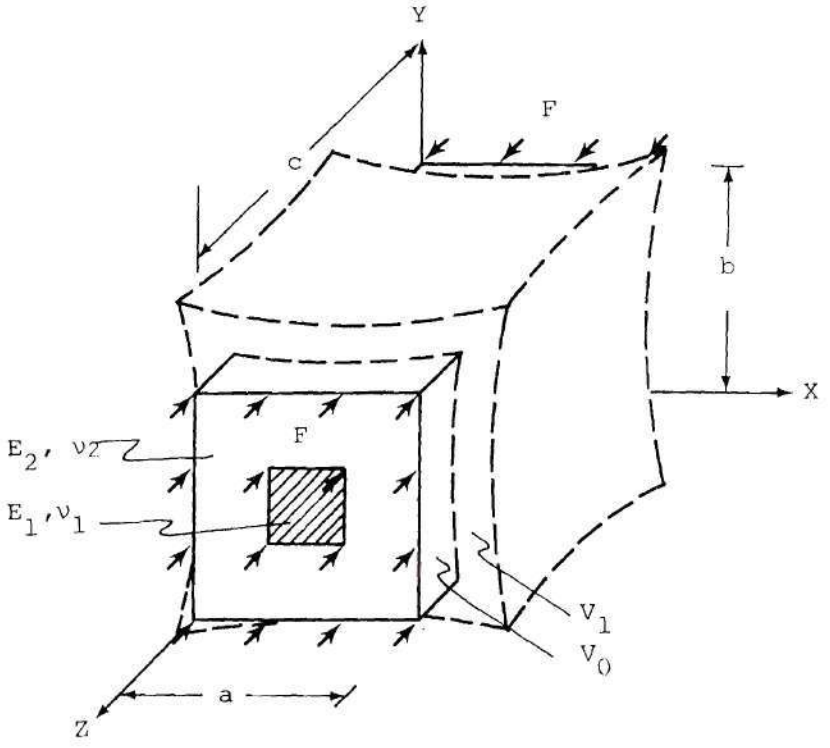

Figure 14. Schematic Deformation of the Unidirectional Fiber Composite

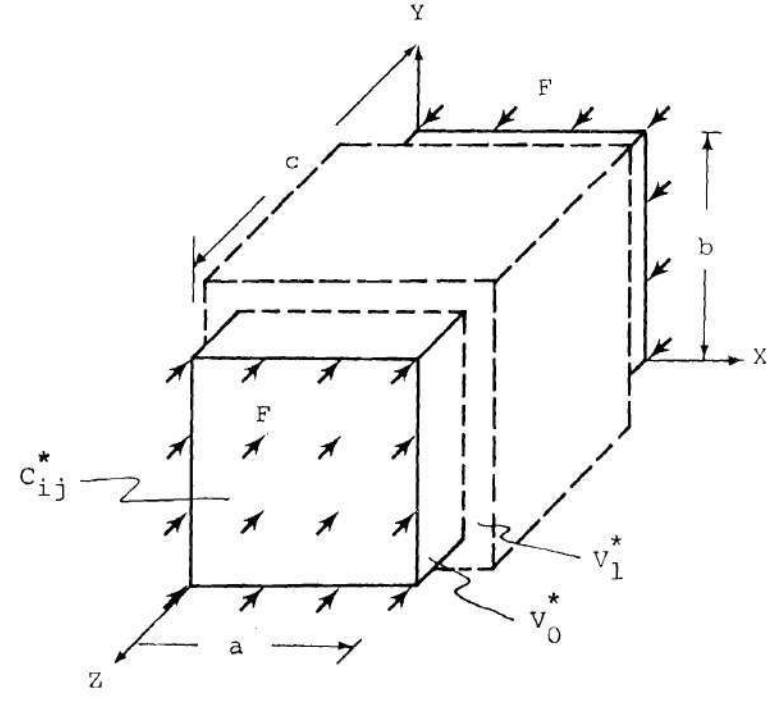

Figure 15. Schematic Deformation of the Equivalent Material

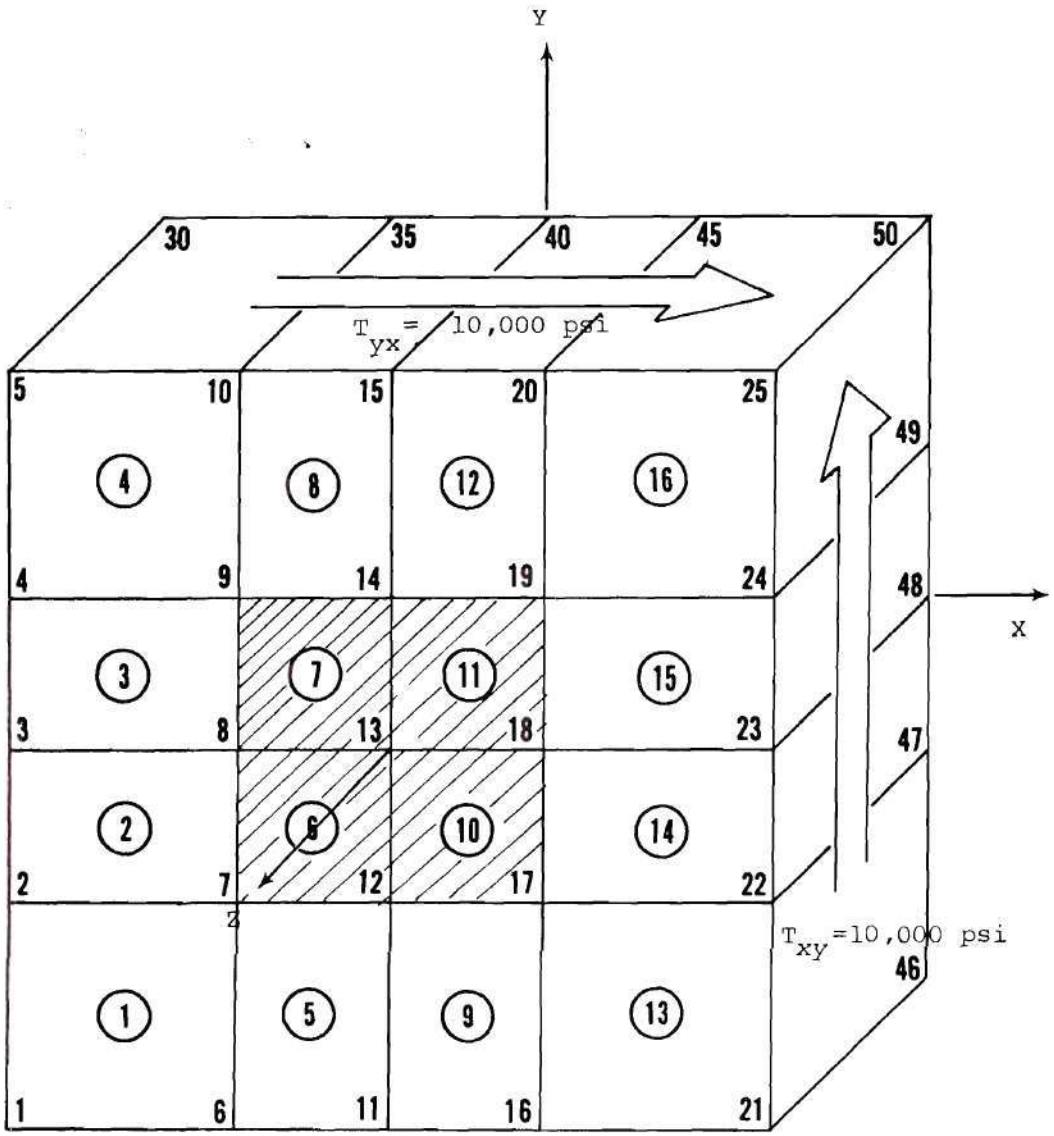

Figure 16. Discretization of the Basic Cell for the Shear Test

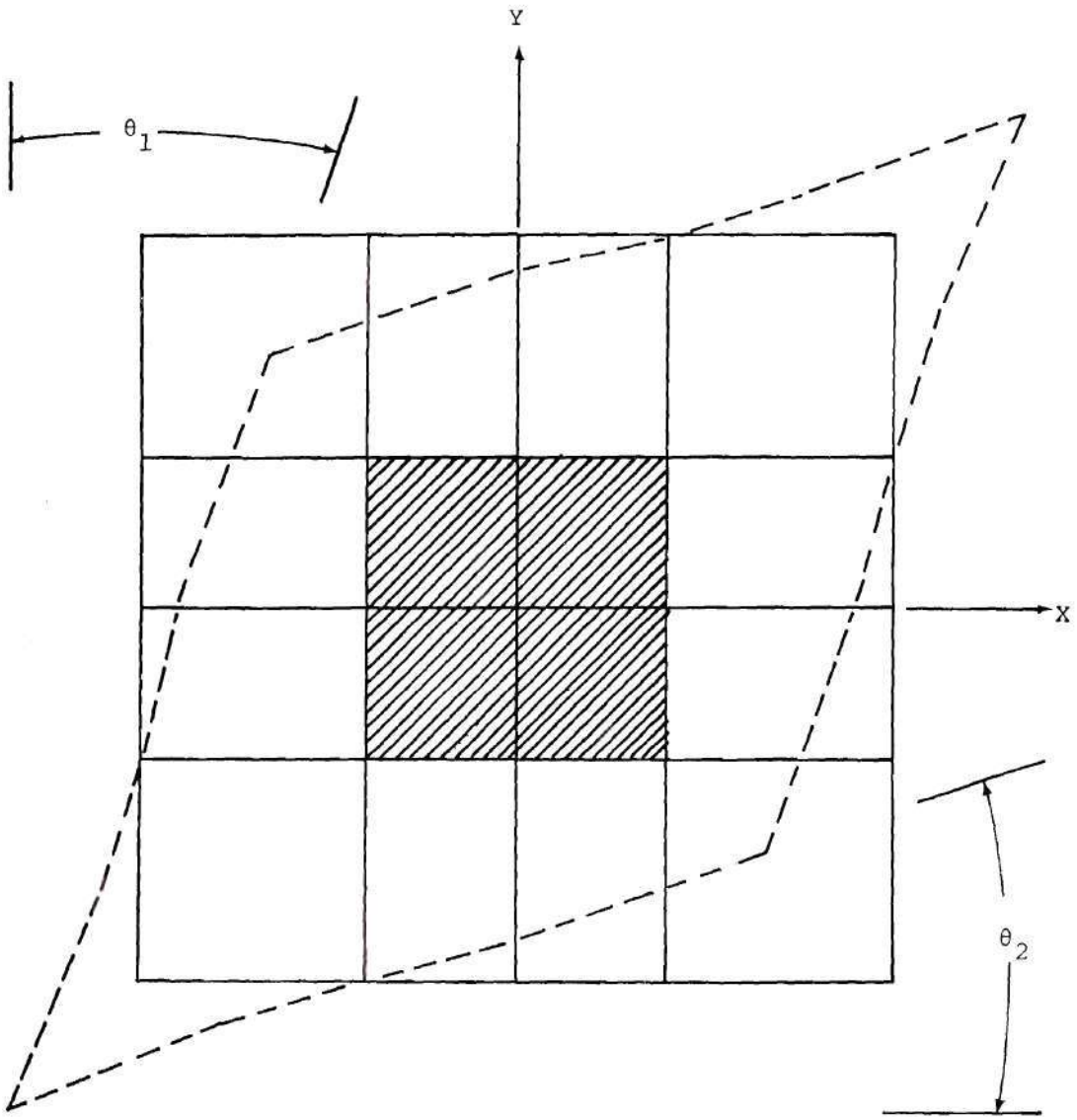

Figure 17. The Deformed Shape Due to the Shear Test (The displacements are magnified by 1,000 times.)

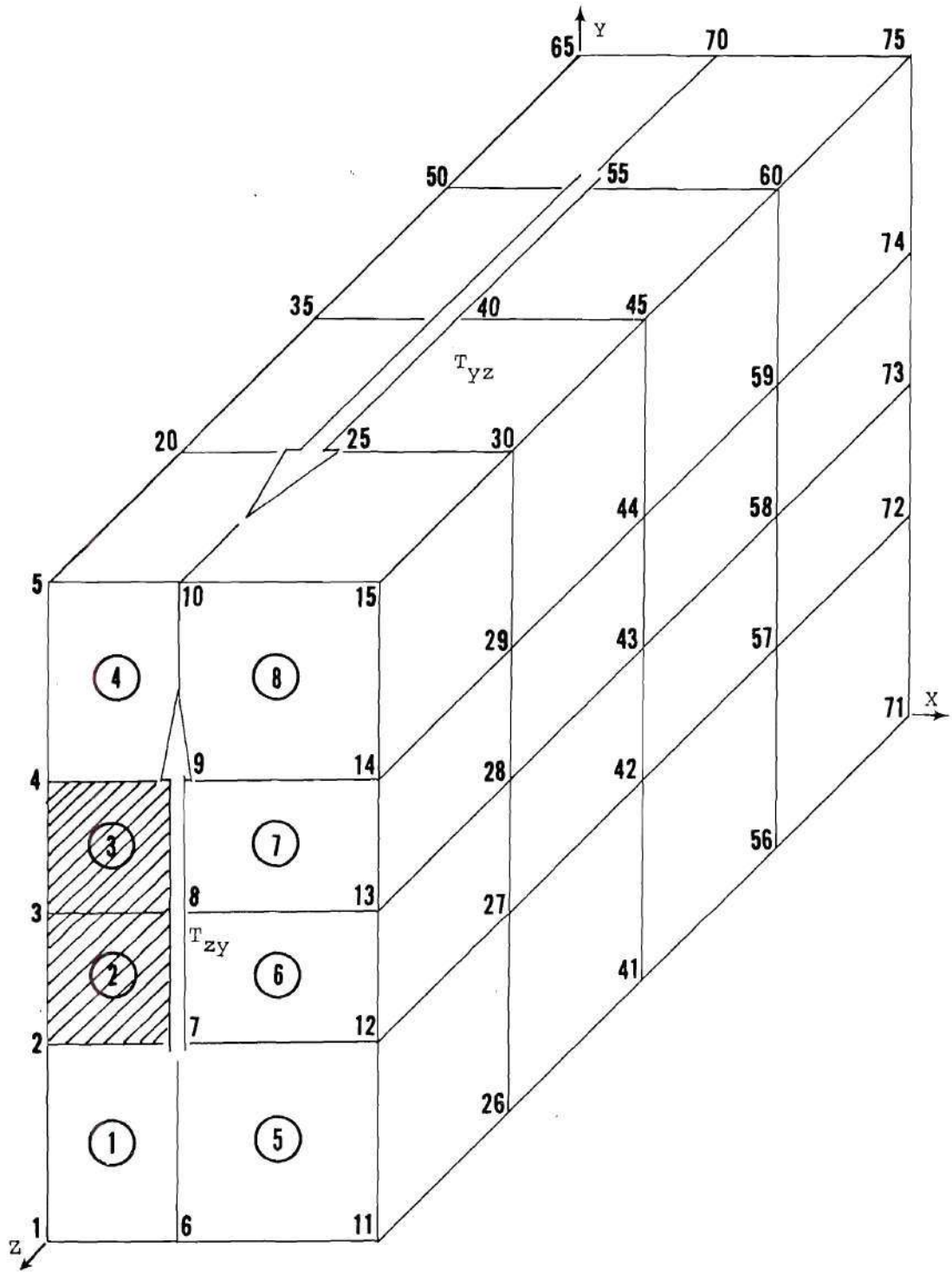

Figure 18. Discretization of One Half of the Basic Cell for the Shear Test

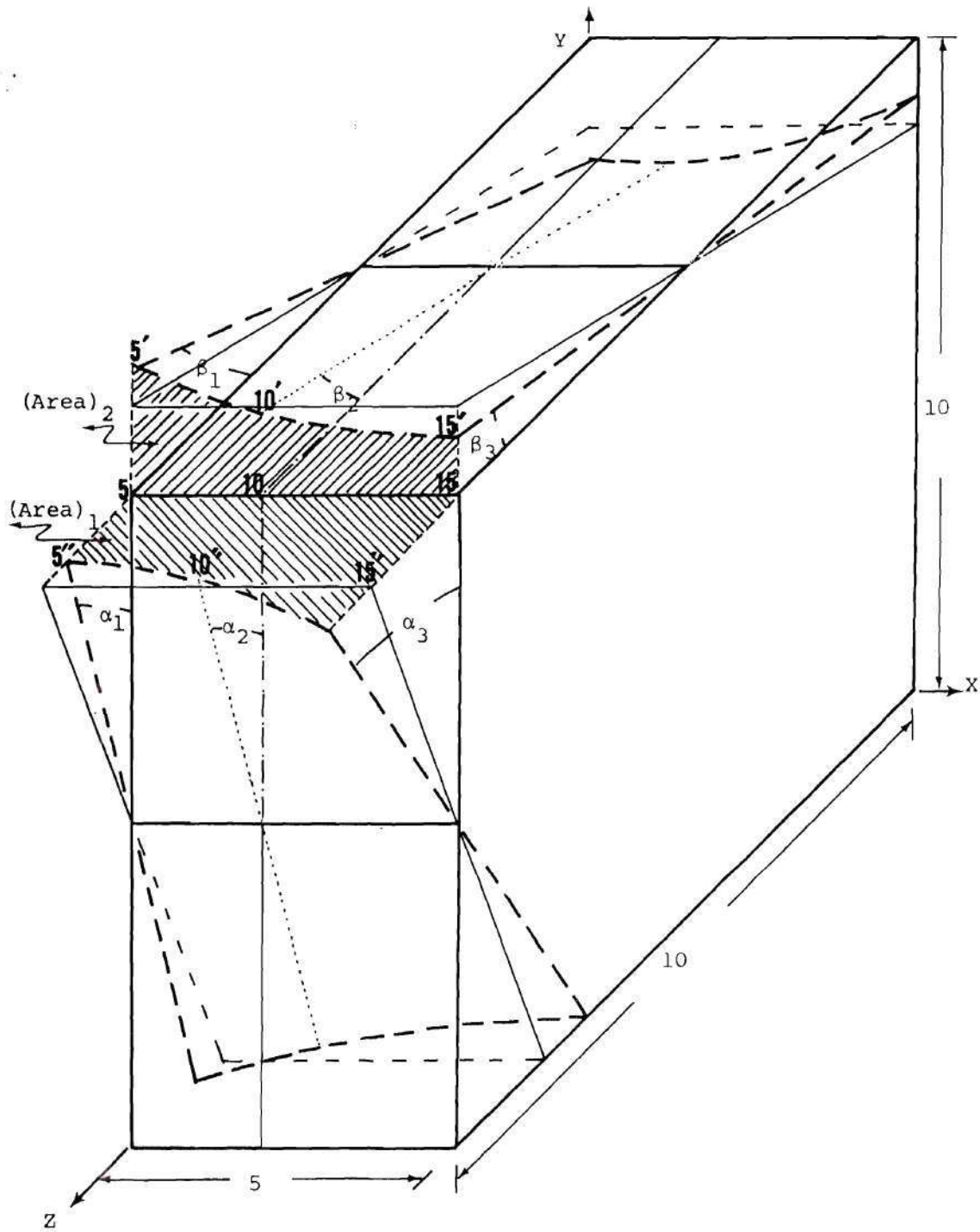

Figure 19. Schematic Drawing of the Displacement Due to the Shear Test Loaded by T_{yz}

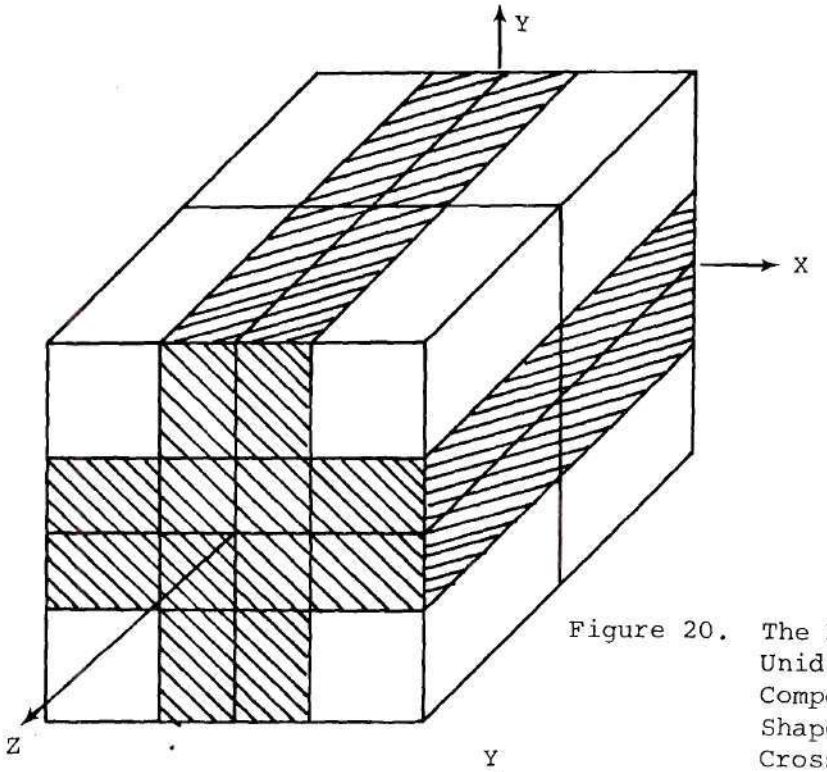

Figure 20. The Basic Cell of the Unidirectional Fiber Composite Whose Fiber Shape is Fixed-Height Cross

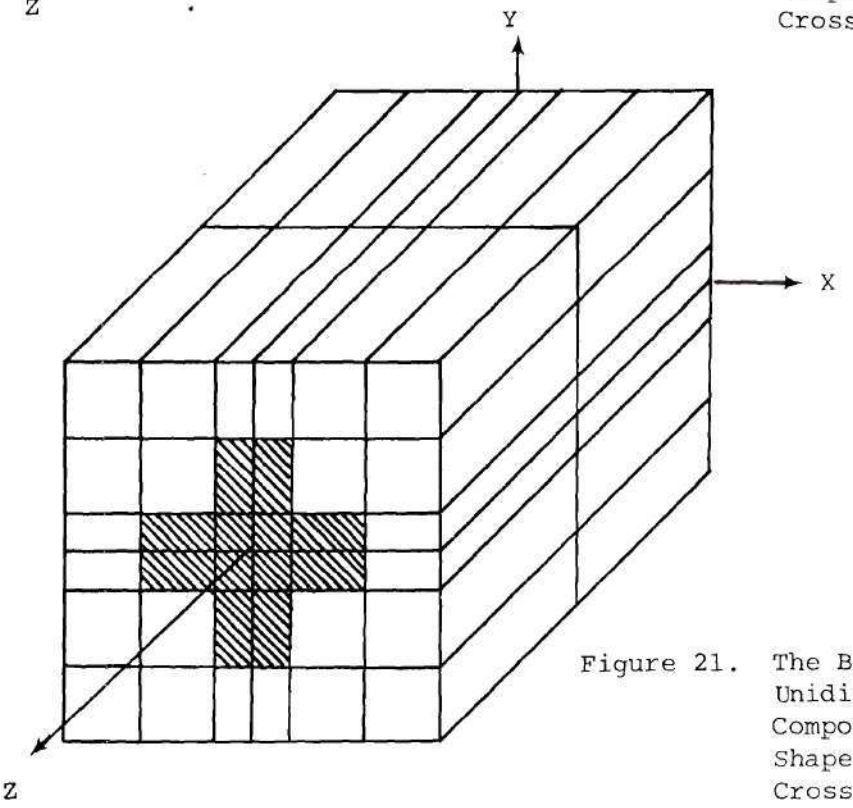

Figure 21. The Basic Cell of the Unidirectional Fiber Composite Whose Fiber Shape is Varying-Height Cross

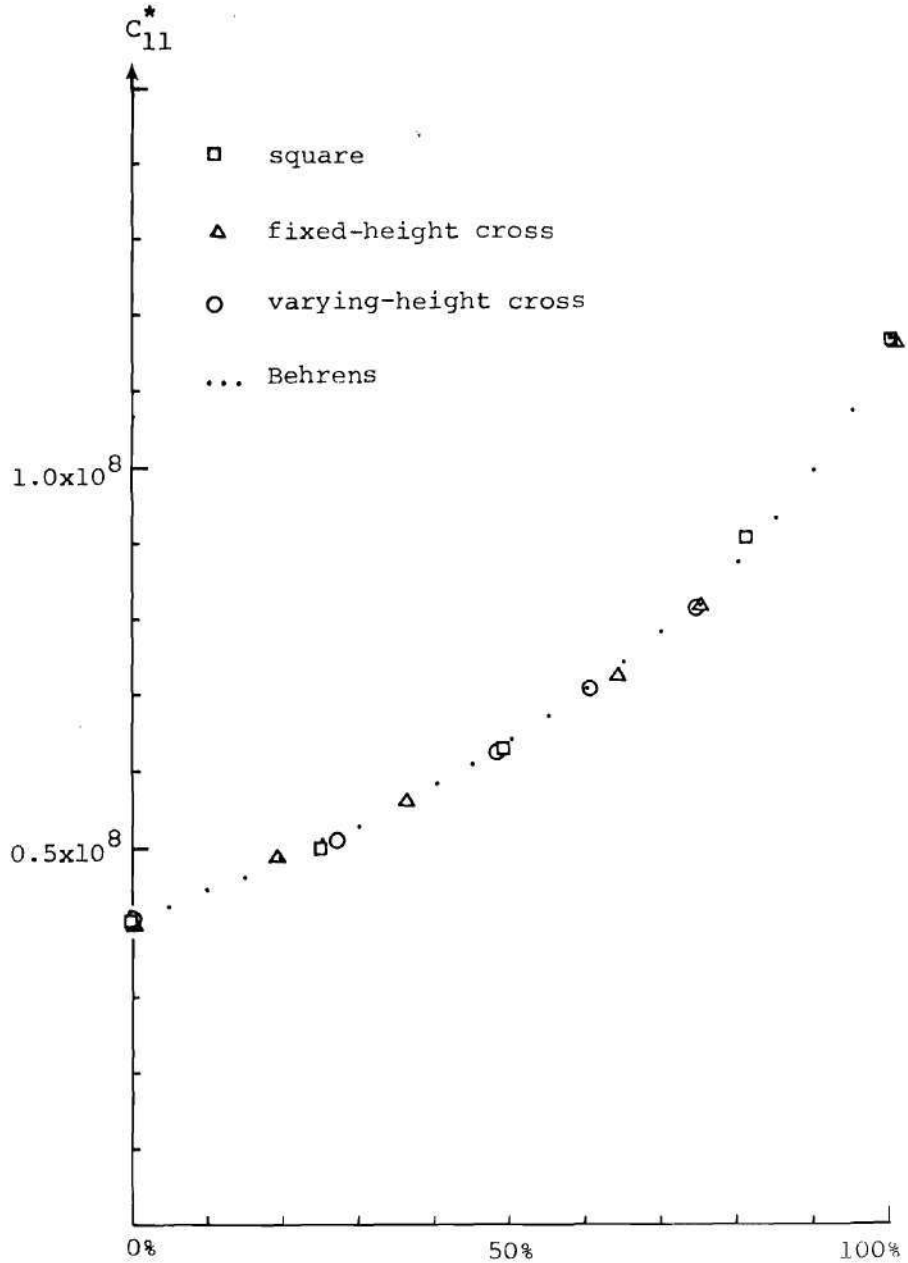

Figure 22. The Effective Modulus C^*_{11} of the Unidirectional Fiber Composites

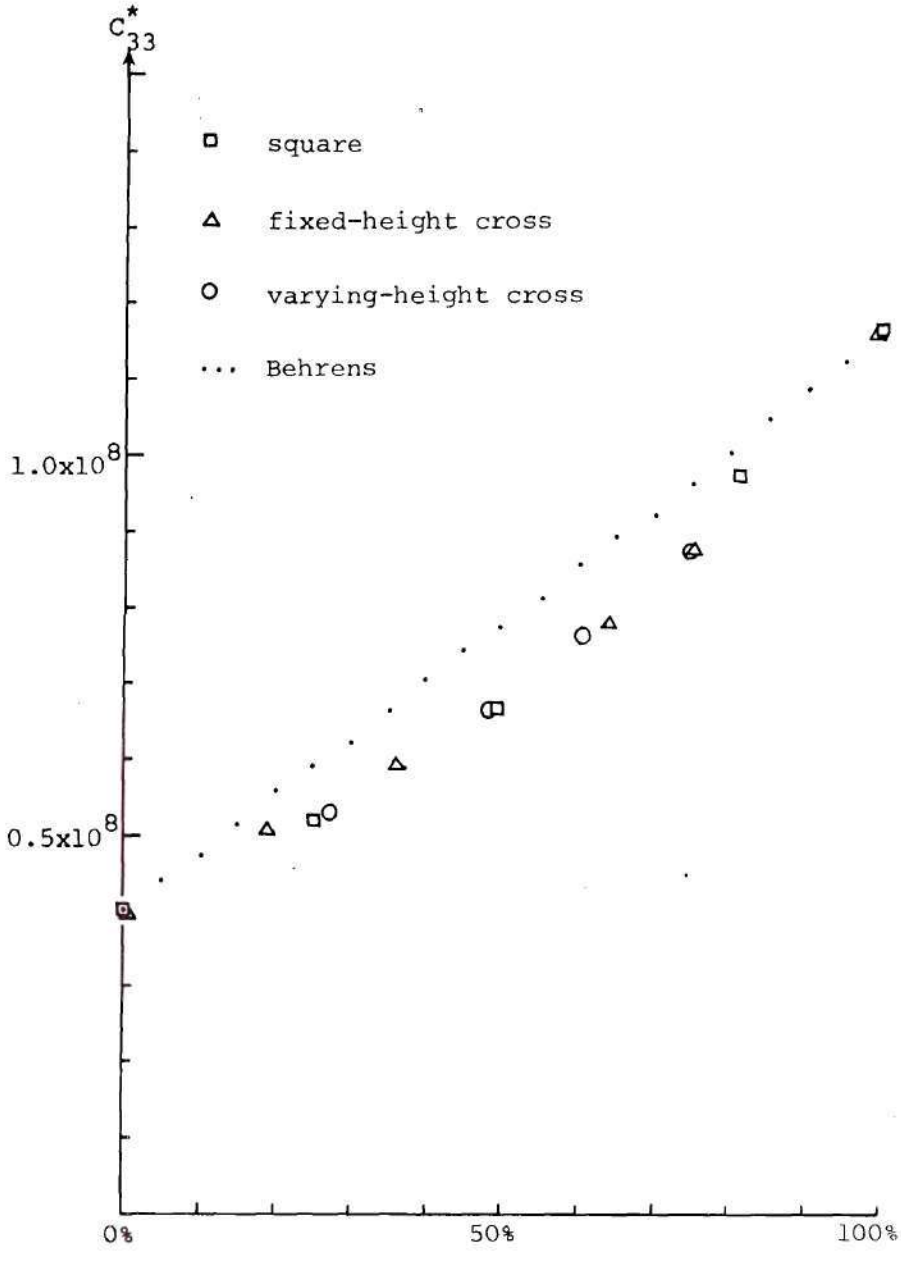

Figure 23. The Effective Modulus C^*_{33} of the Unidirectional Fiber Composites

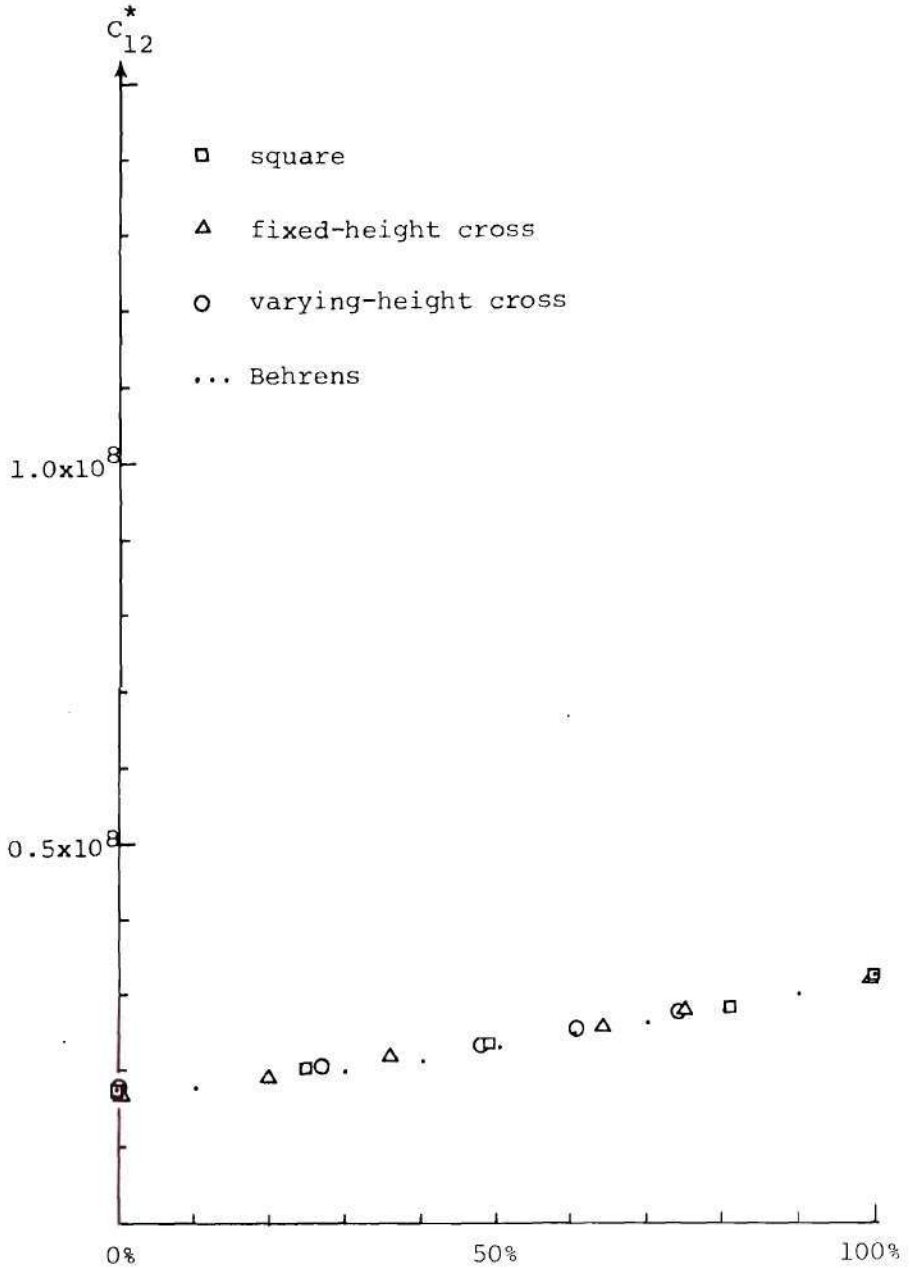

Figure 24. The Effective Modulus C^*_{12} of the Unidirectional Fiber Composites

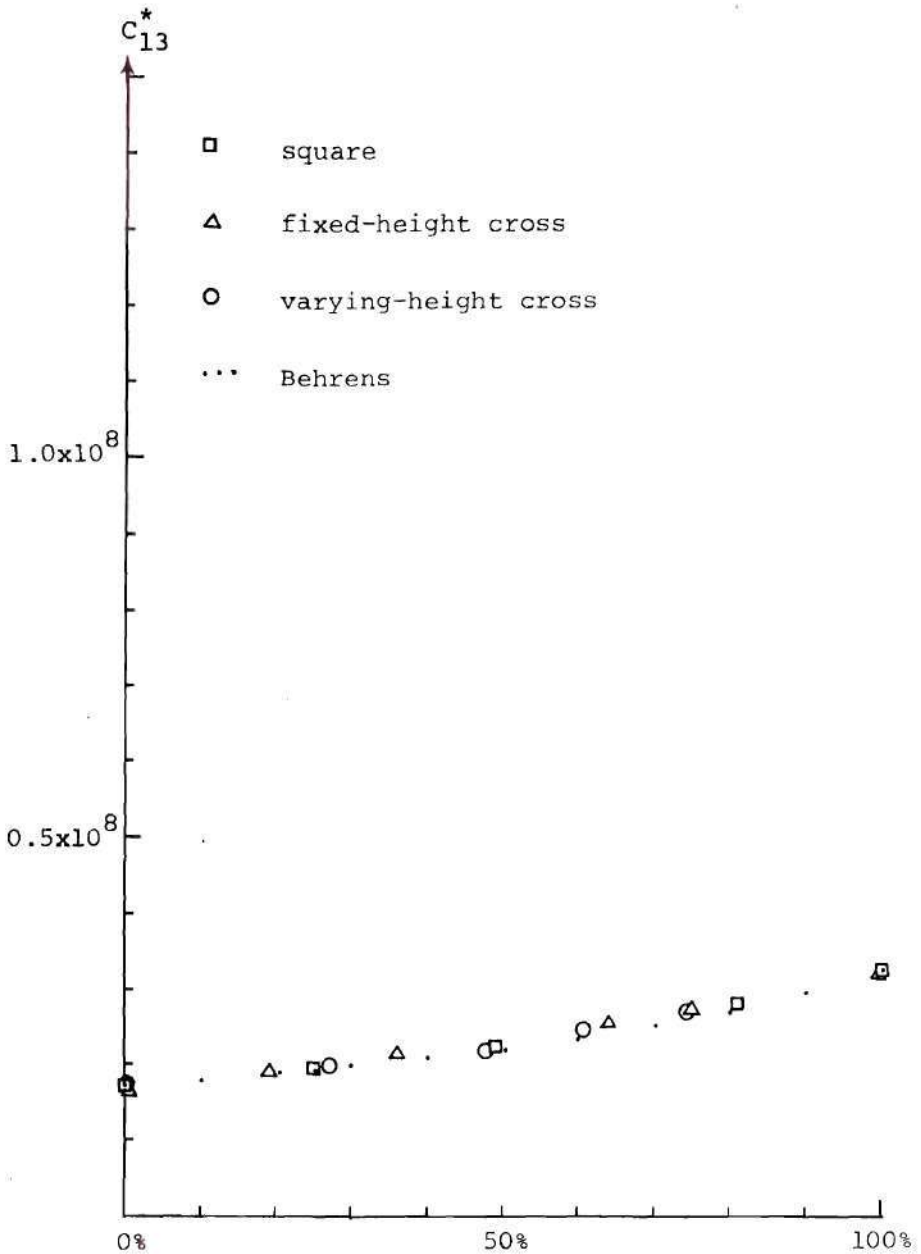

Figure 25. The Effective Modulus C_{13}^* of the Unidirectional Fiber Composites

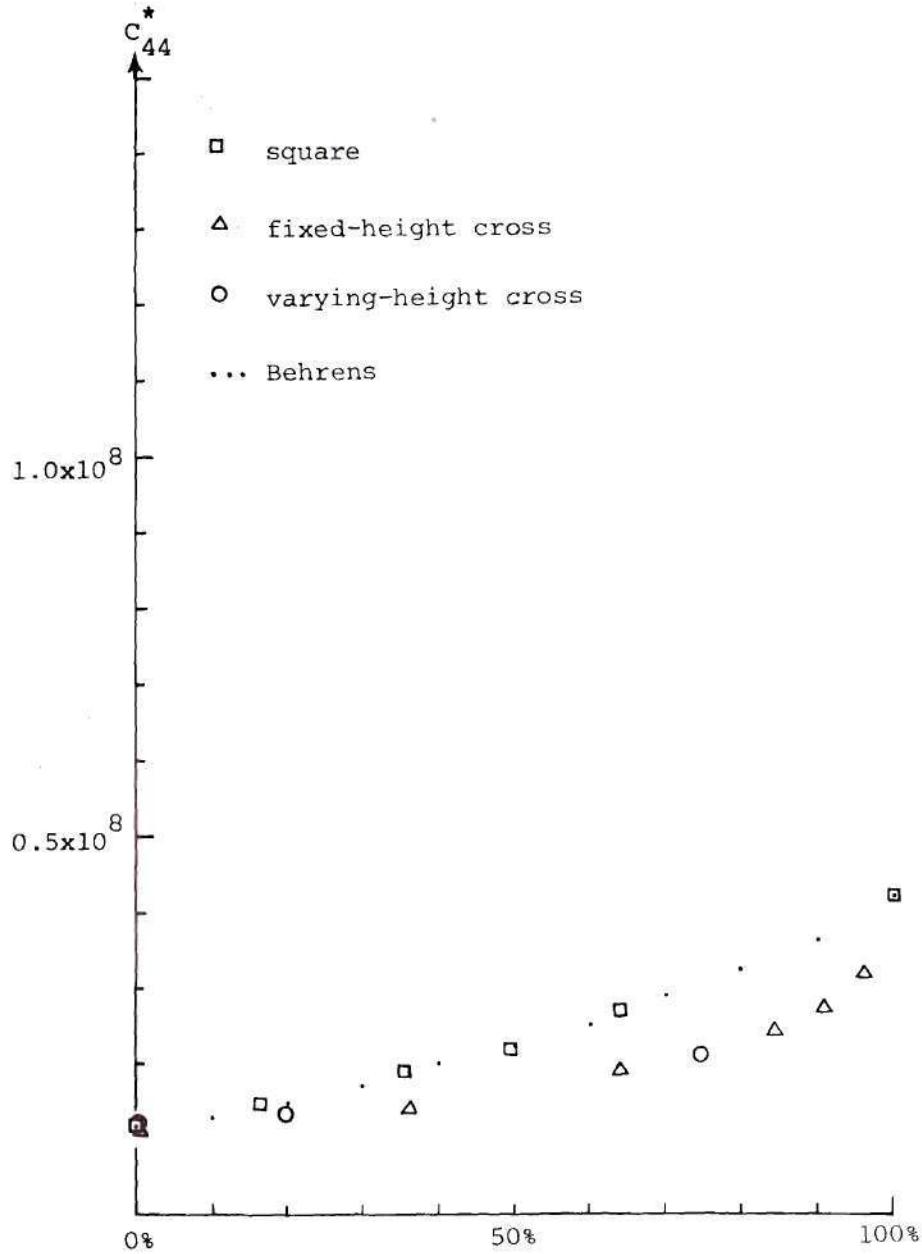

Figure 26. The Effective Modulus C^*_{44} of the Unidirectional Fiber Composites

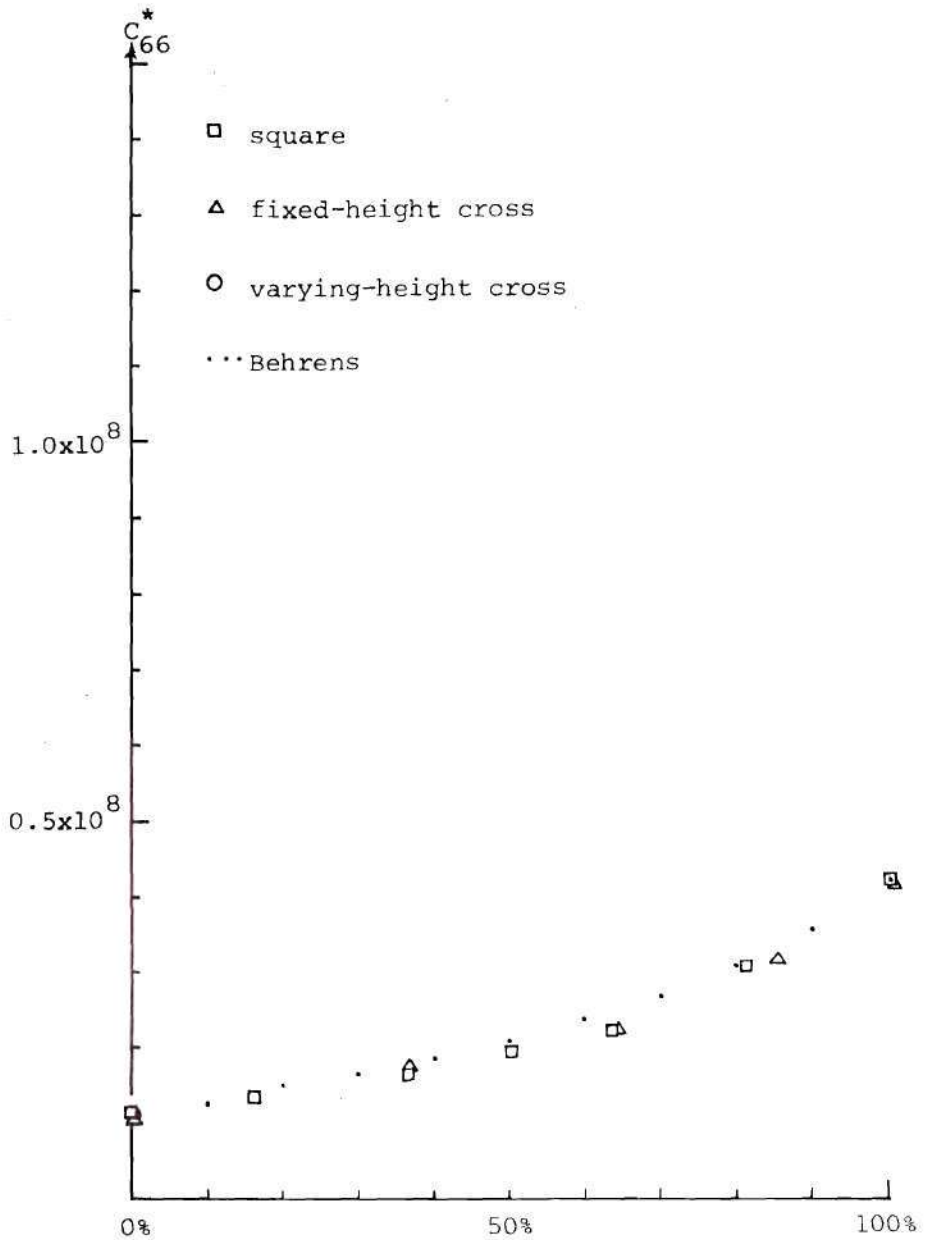

Figure 27. The Effective Modulus C^*_{66} of the Unidirectional Fiber Composites

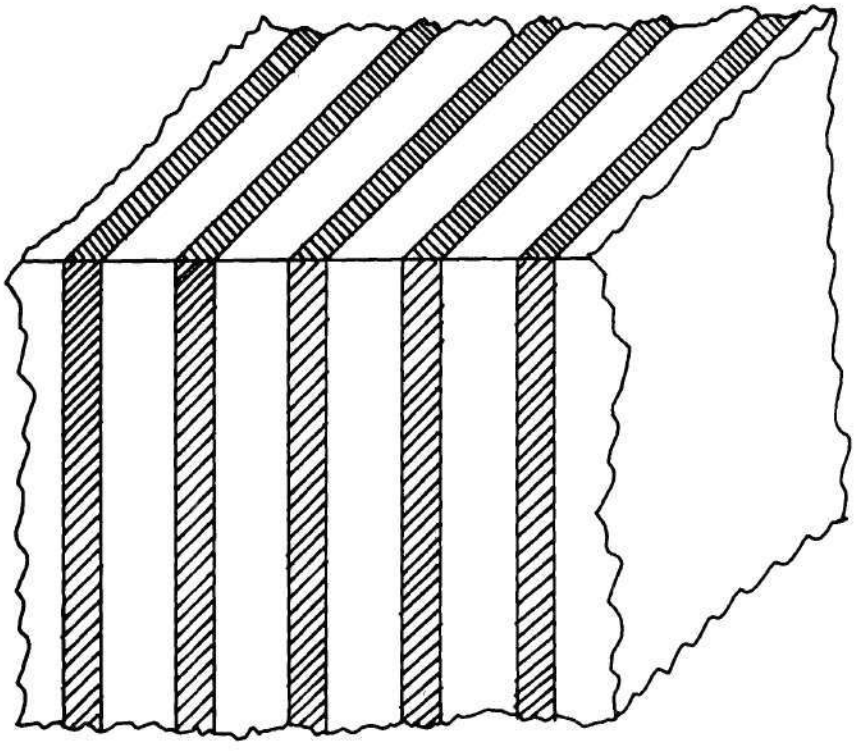

Figure 28. Lamellar Composite

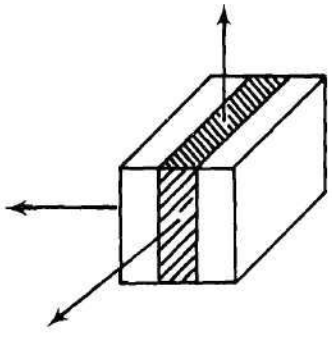

Figure 29. Basic Cell

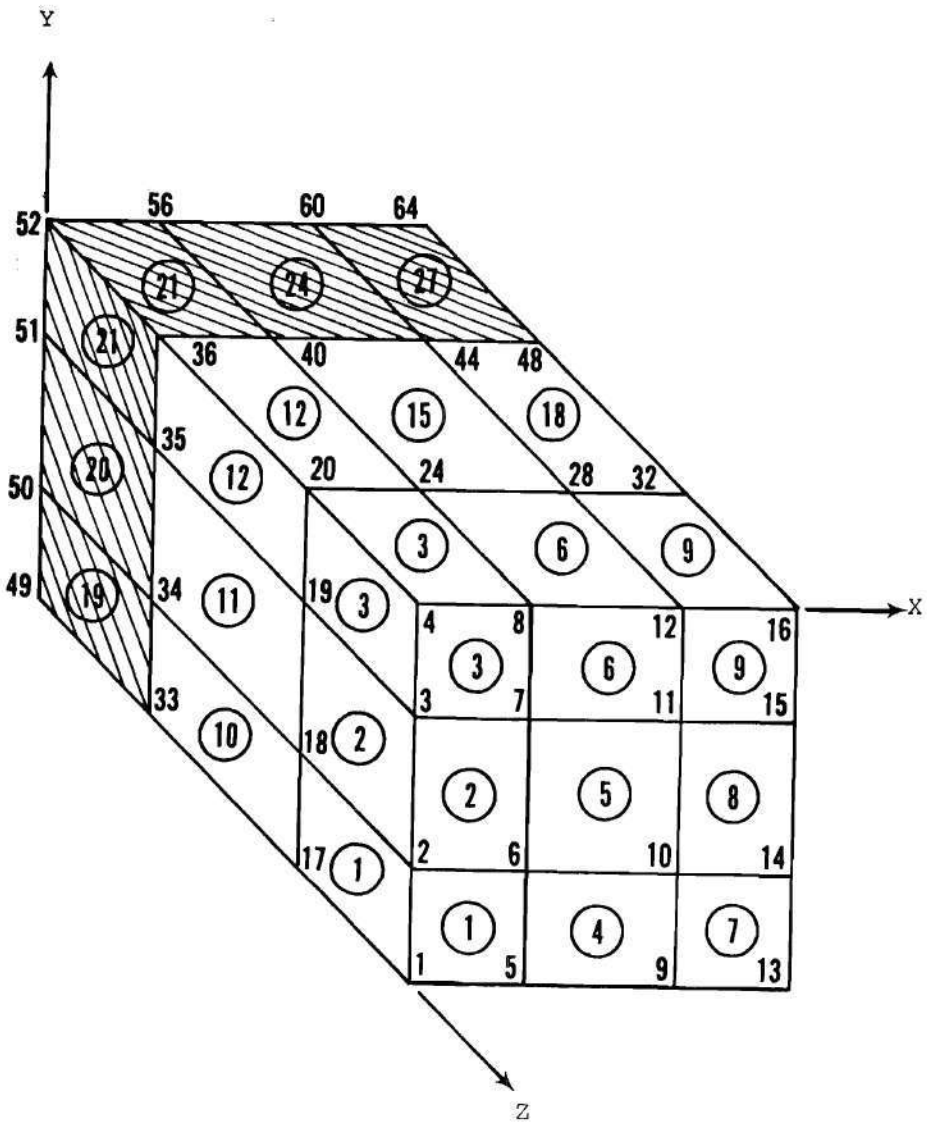

Figure 30. Discretization of One Octant of the Basic Cell of the Lamellar Composite

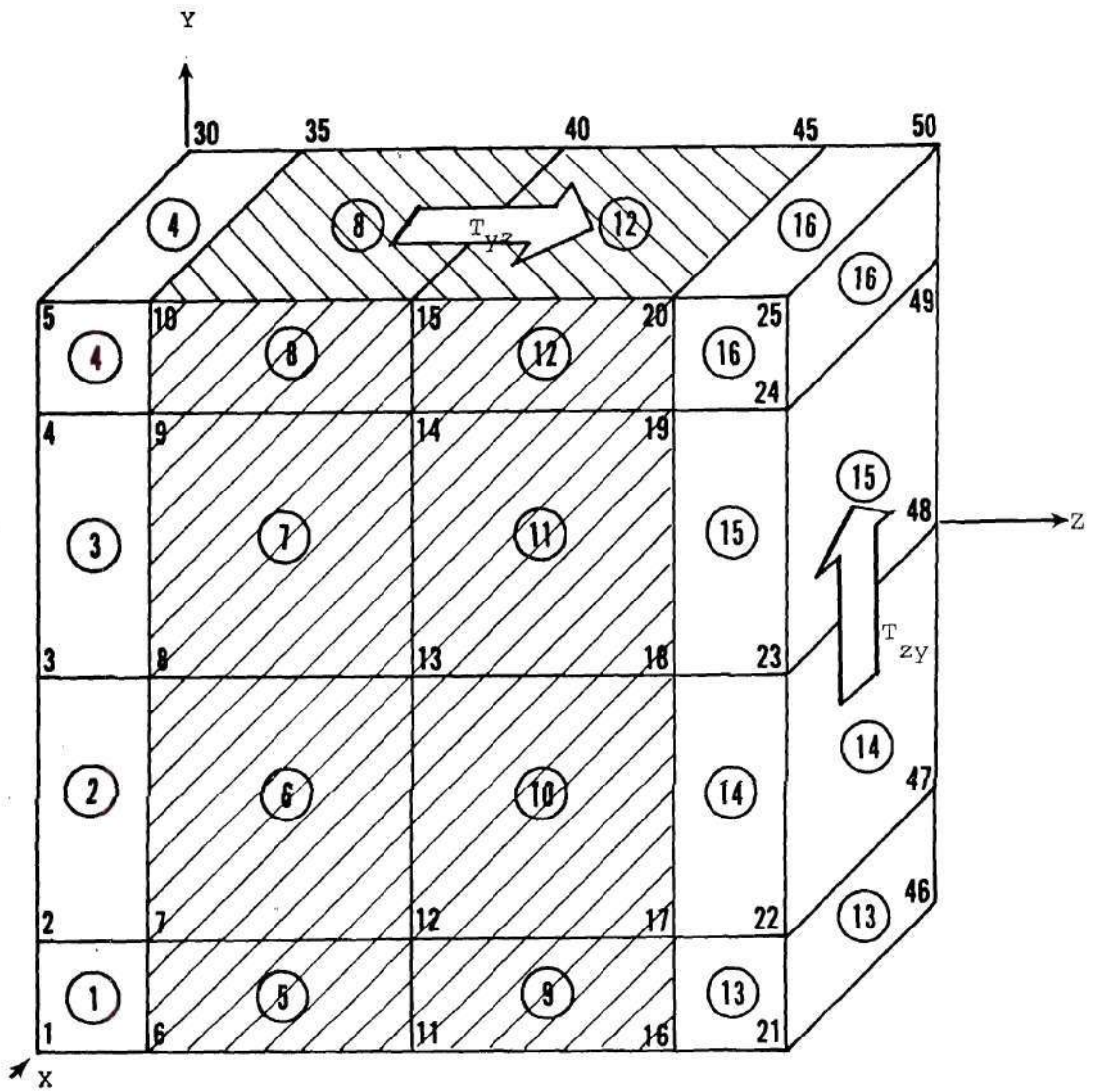

Figure 31. Discretization of a Basic Cell of a Lamellar Composite for the Shear Test Loaded by T_{yz}

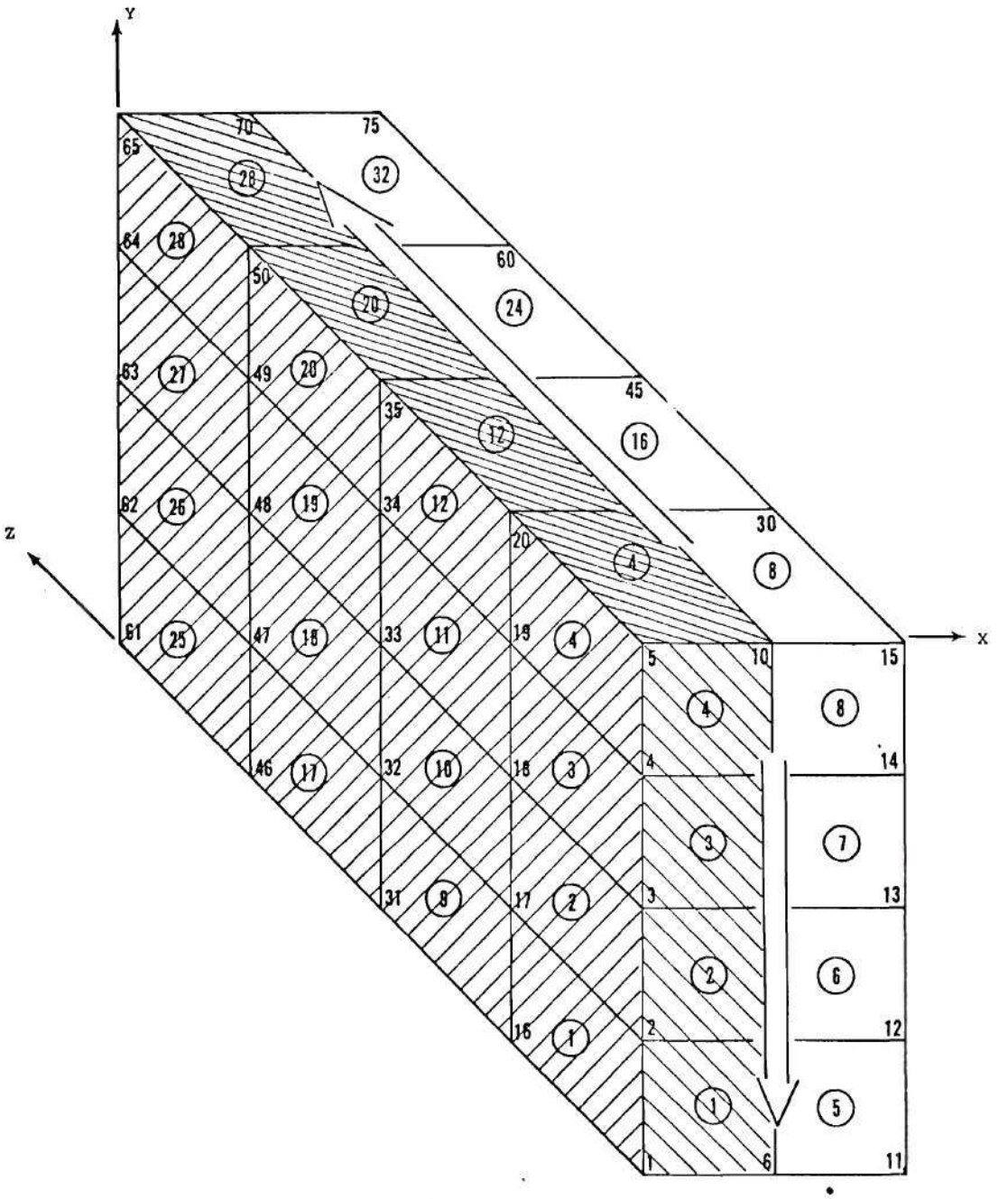

Figure 32. The Discretization of One Half of the Basic Cell of a Lamellar Composite for the Shear Test Loaded by T_{yz}

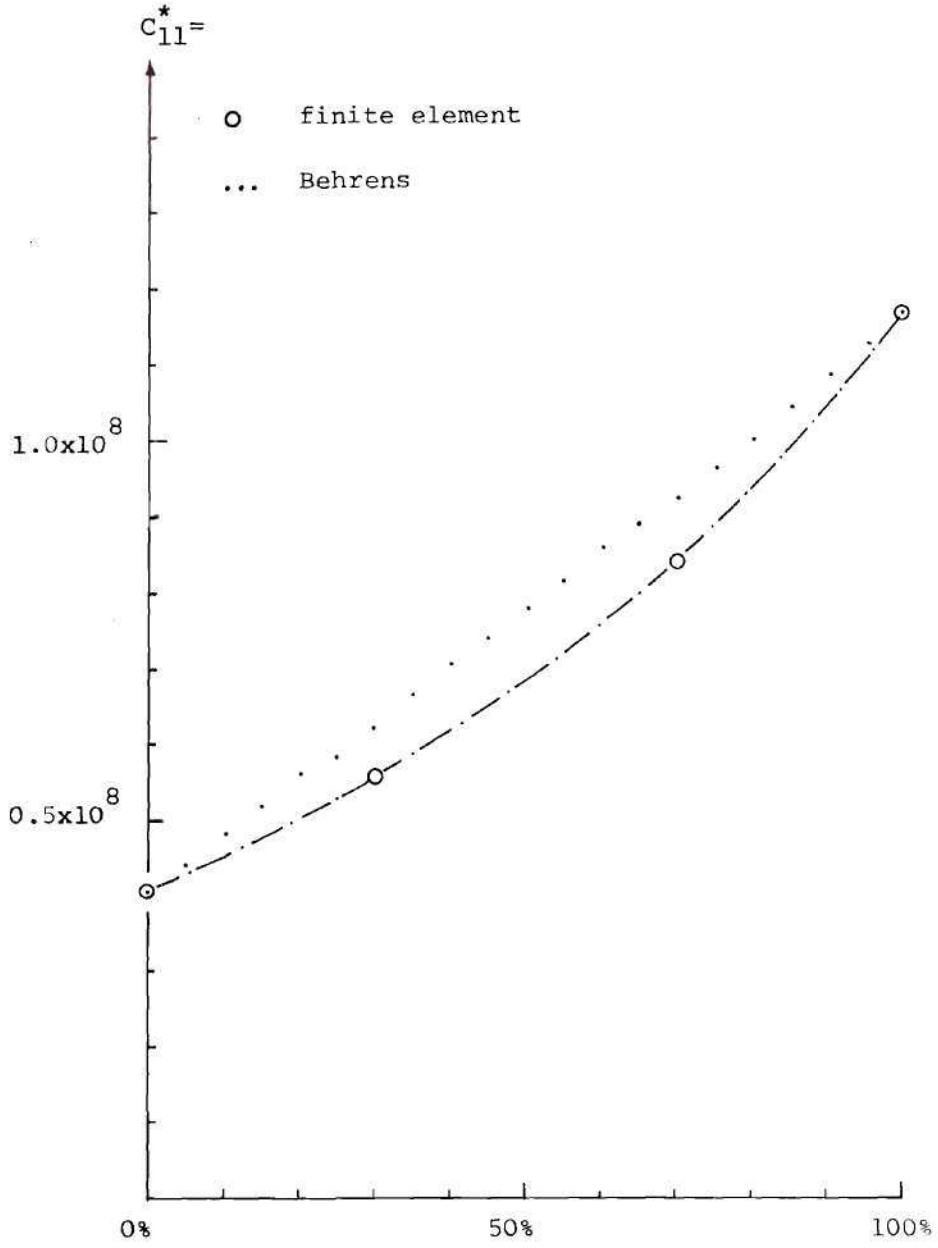

Figure 33. The Effective Modulus C^*_{11} of the Lamellar Composites

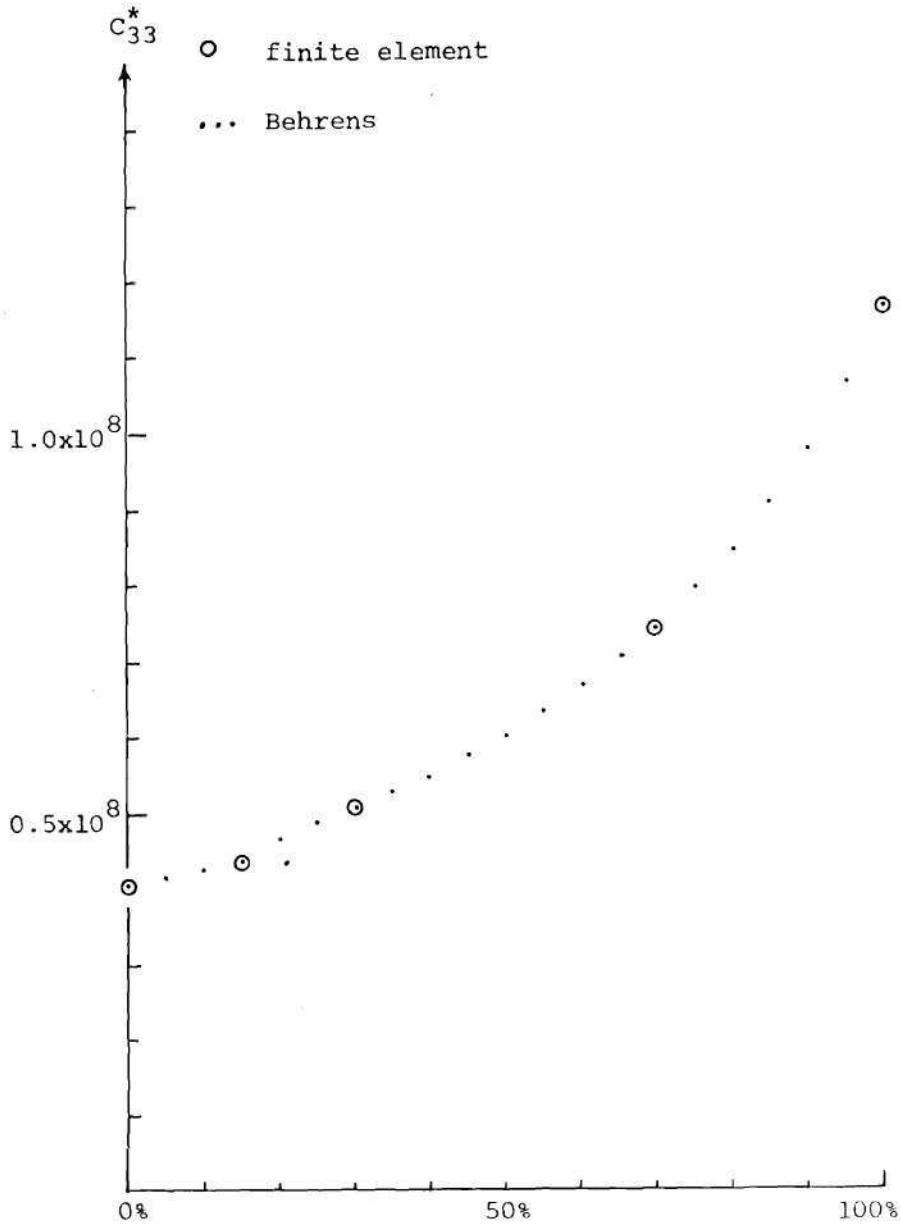

Figure 34. The Effective Modulus C_{33}^* of the Lamellar Composites

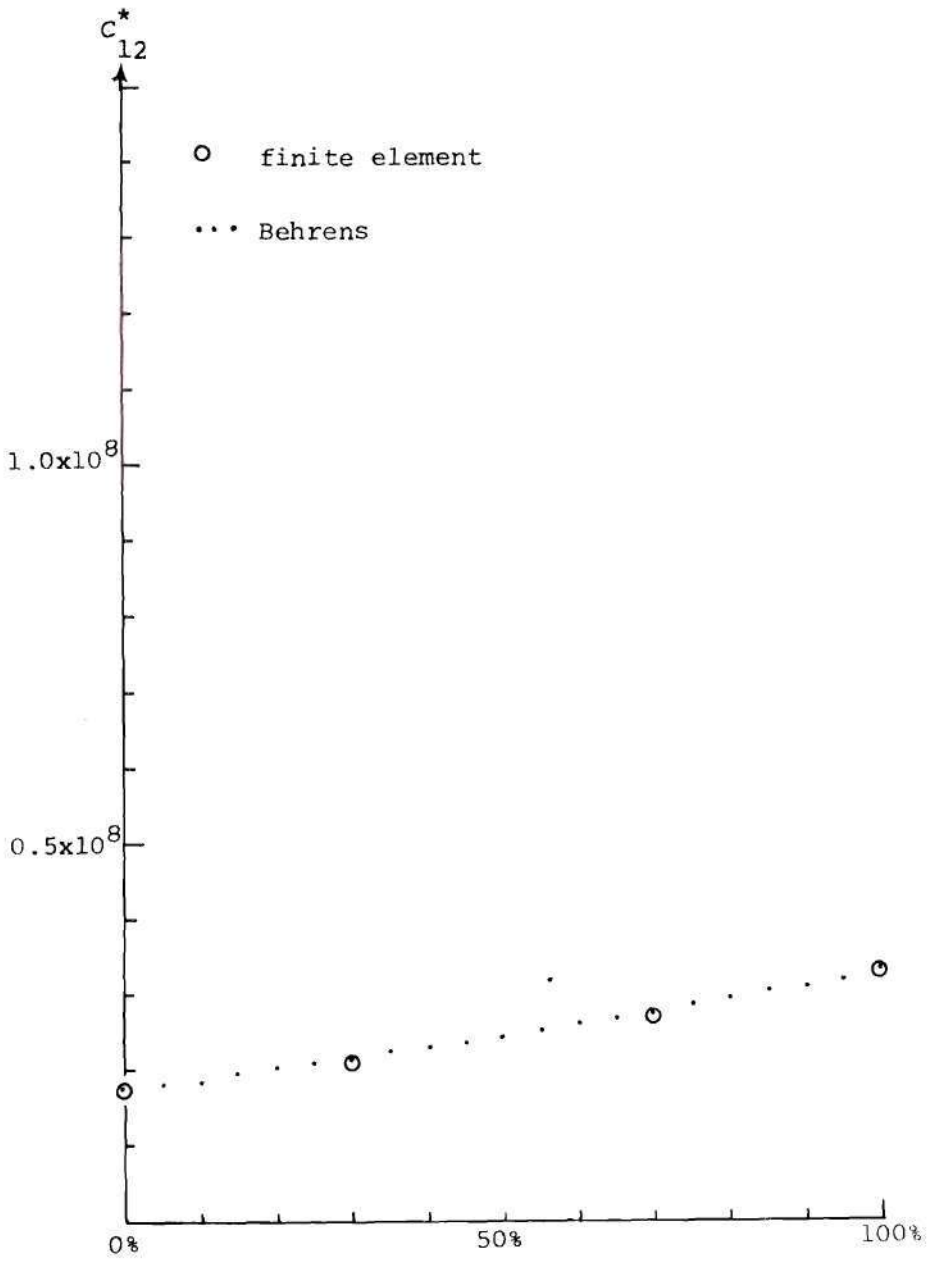

Figure 35. The Effective Modulus C^*_{12} of the Lamellar Composites

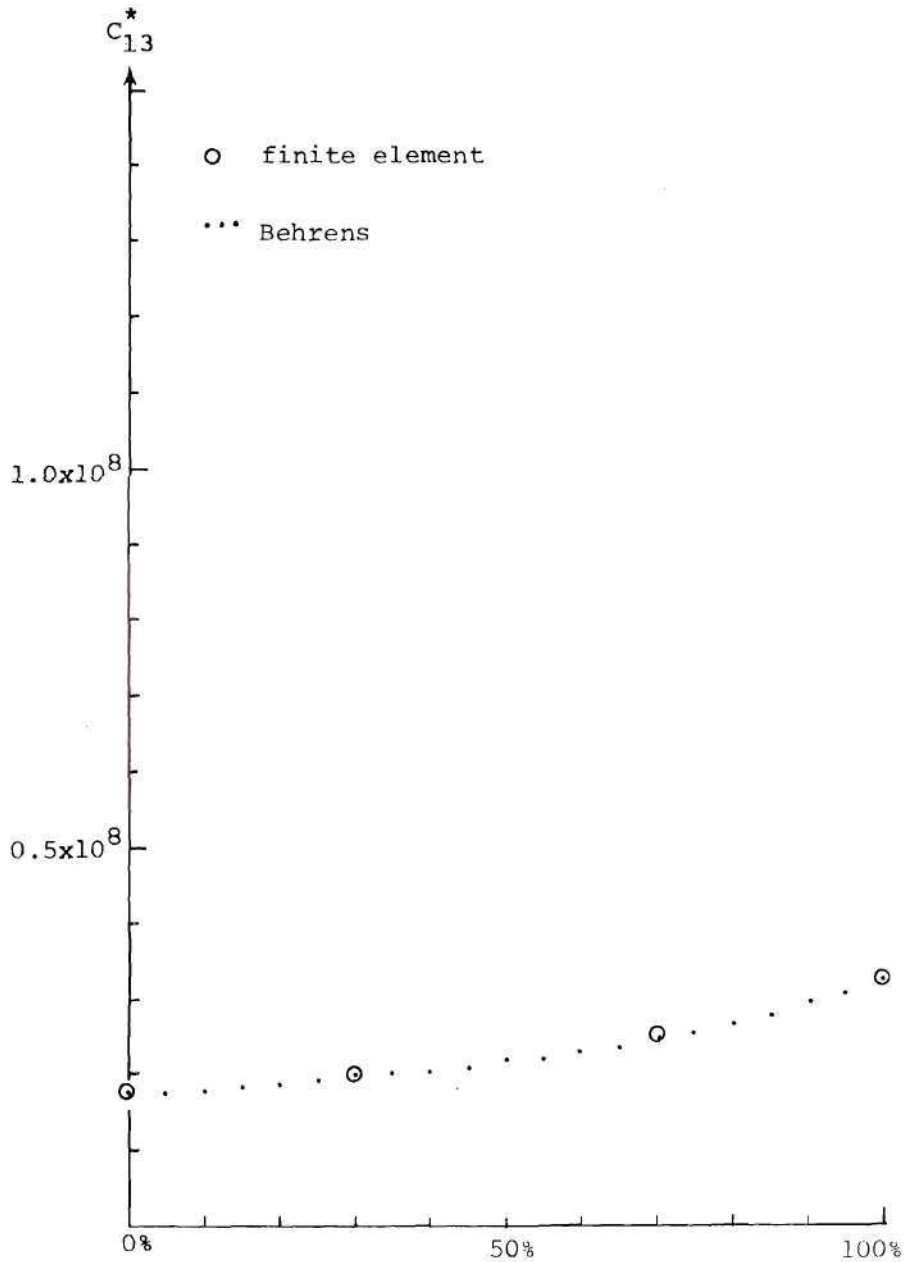

Figure 36. The Effective Modulus C^*_{13} of the Lamellar Composites

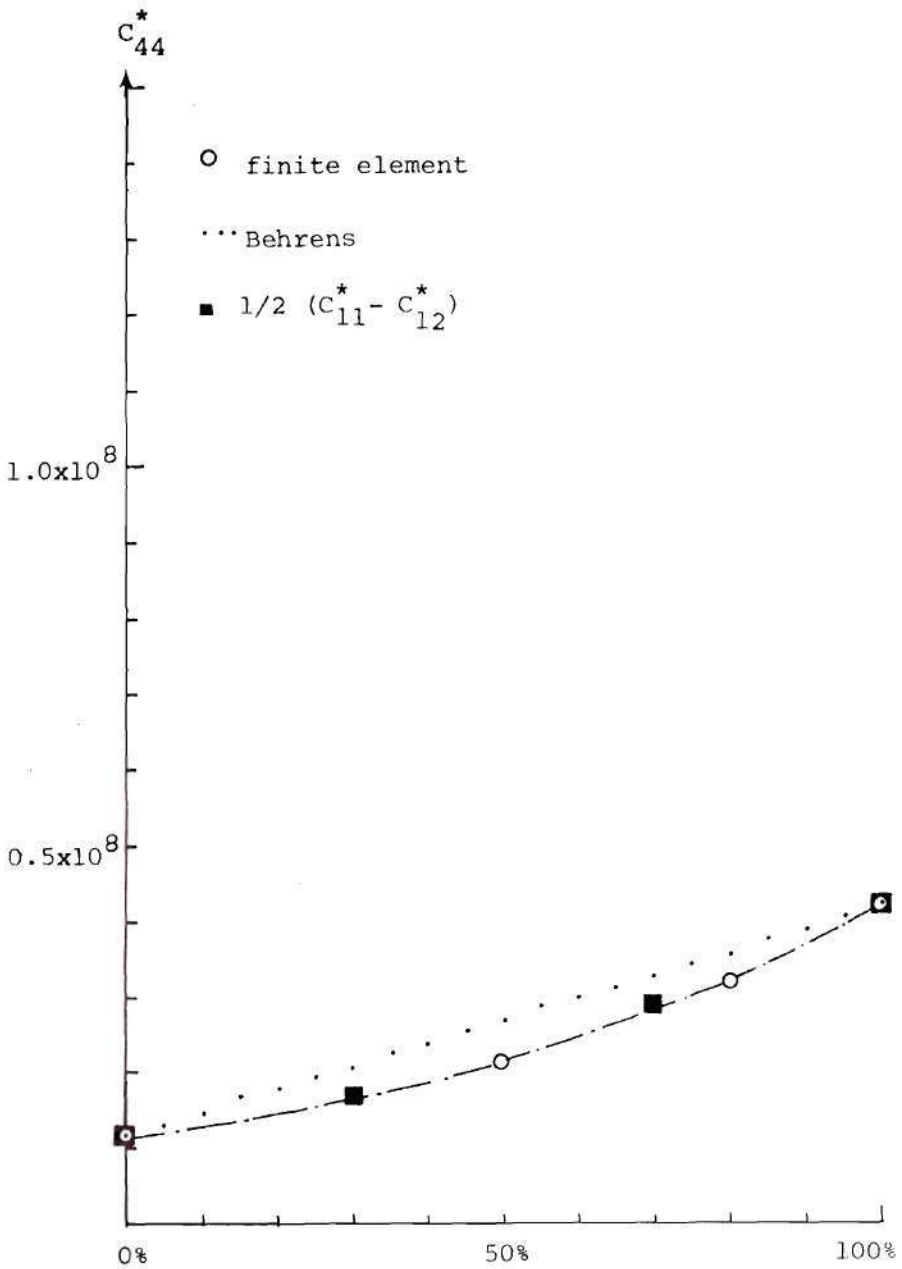

Figure 37. The Effective Modulus C^*_{44} of the Lamellar Composites

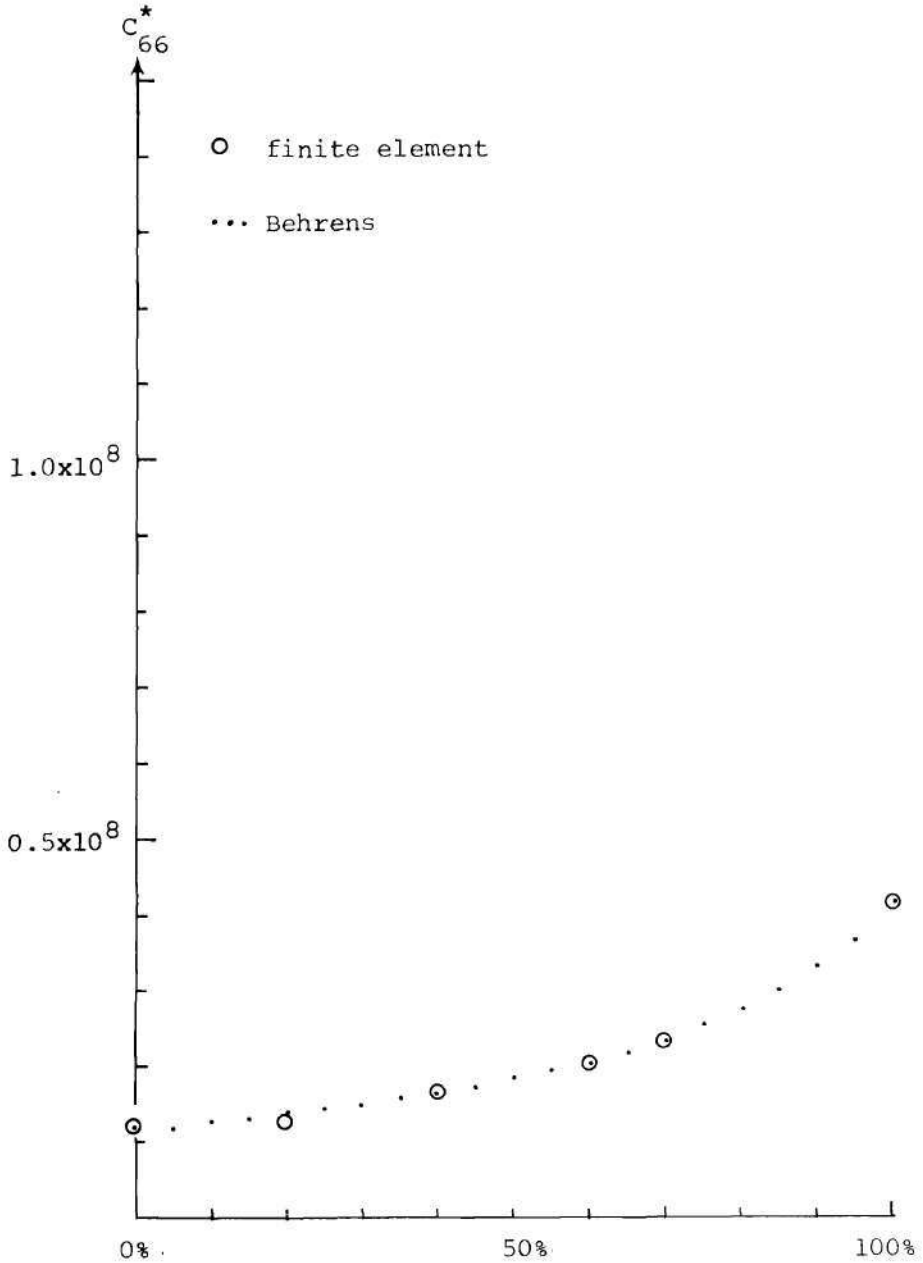

Figure 38. The Effective Modulus C^*_{66} of the Lamellar Composites

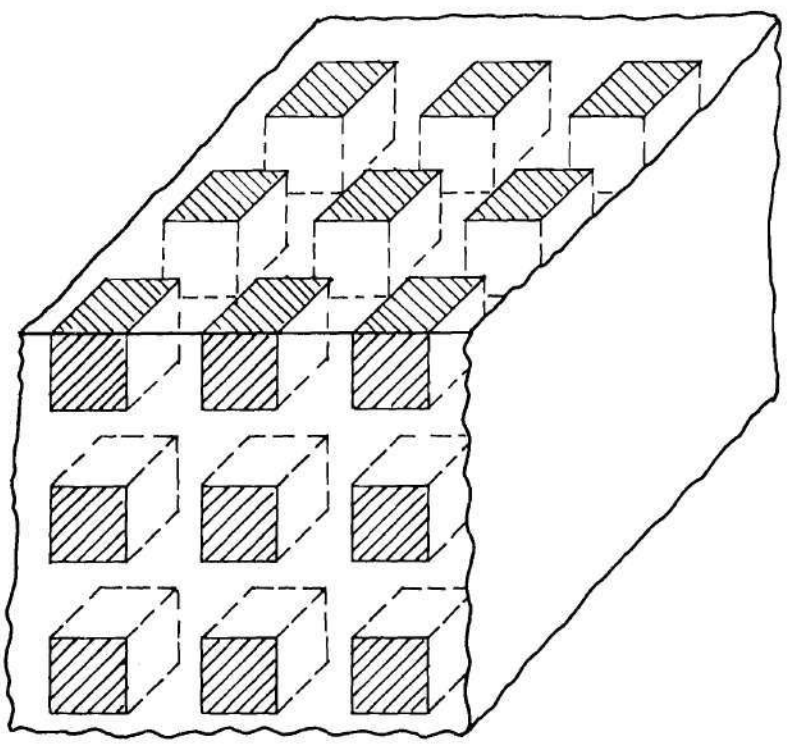

Figure 39. A Short Fiber Composite

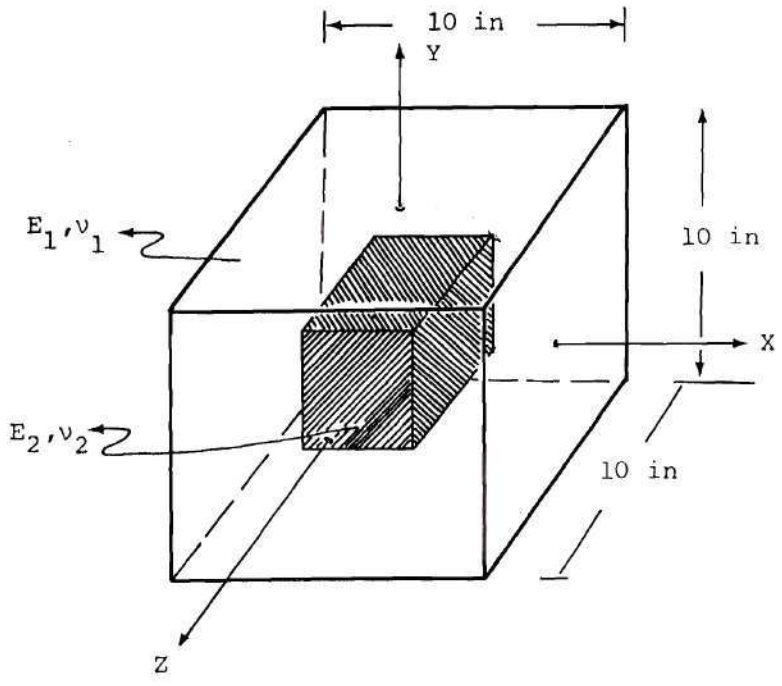

Figure 40. Basic Cell of the Short Fiber Composite

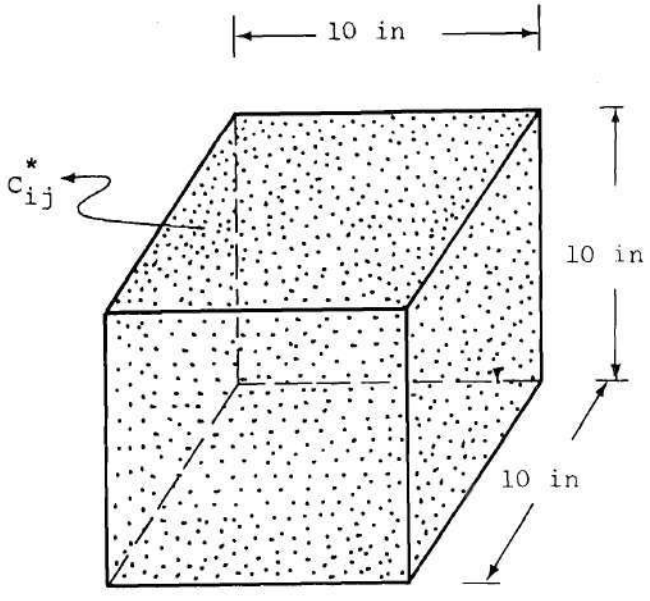

Figure 41. Equivalent Material

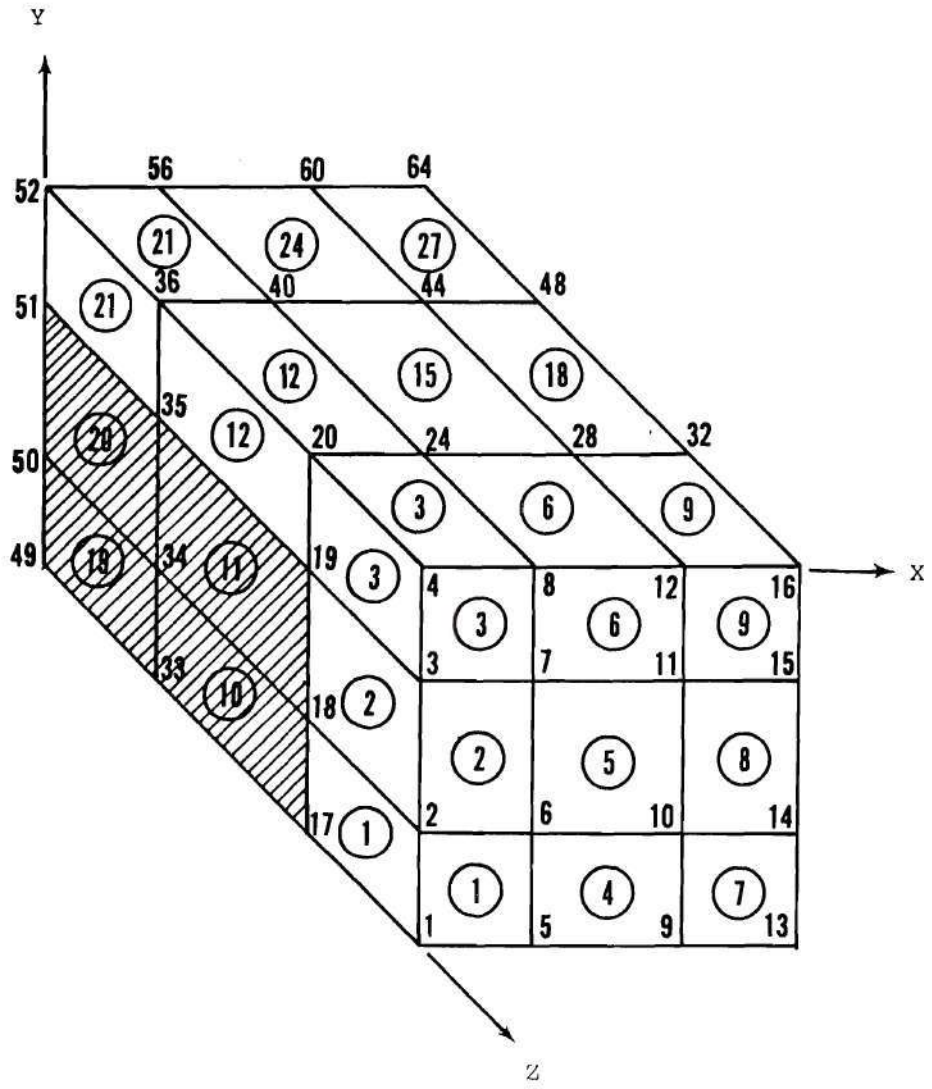

Figure 42. Discretization of One Octant of a Short Fiber Composite

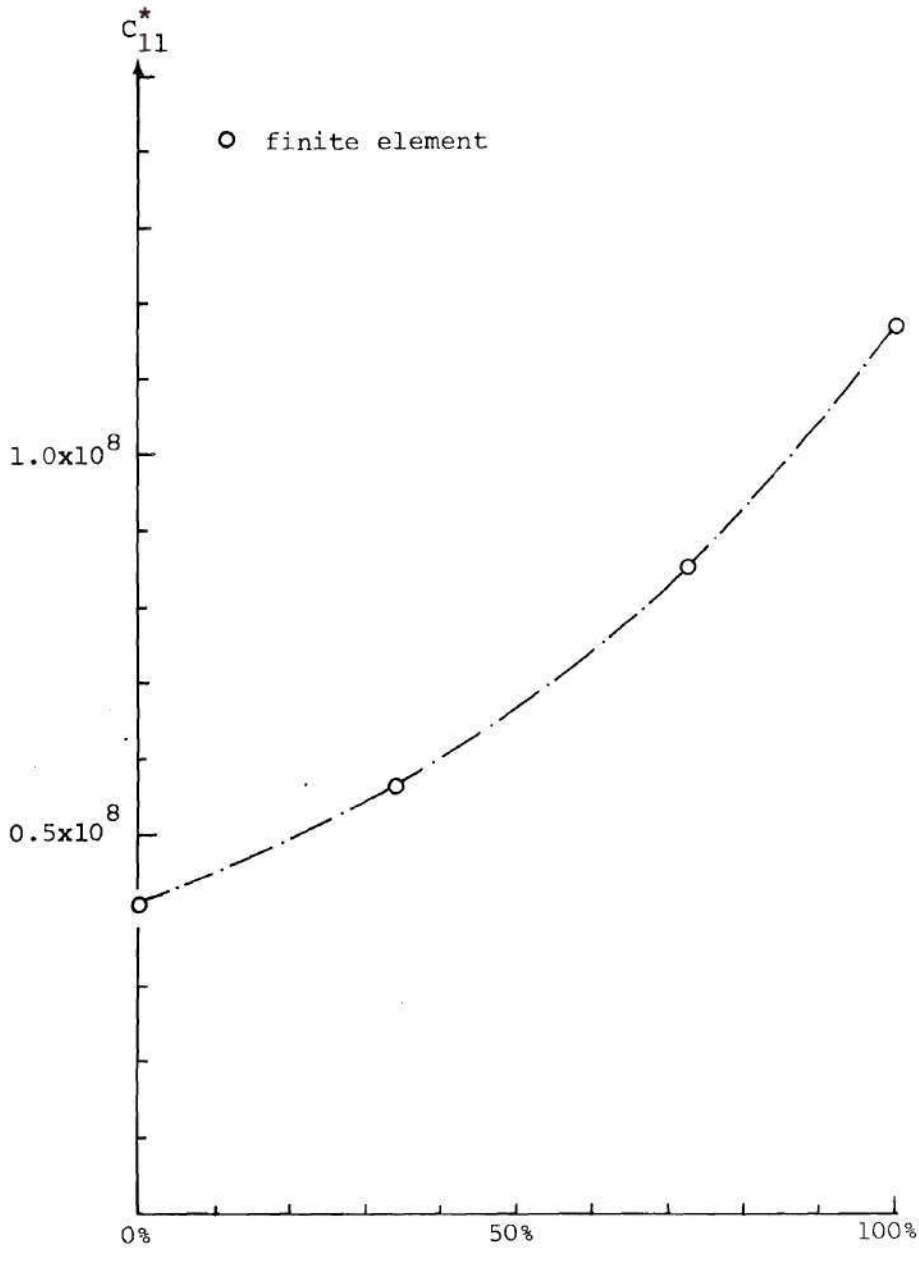

Figure 43. The Effective Modulus C_{11}^* of the Short Fiber Composites

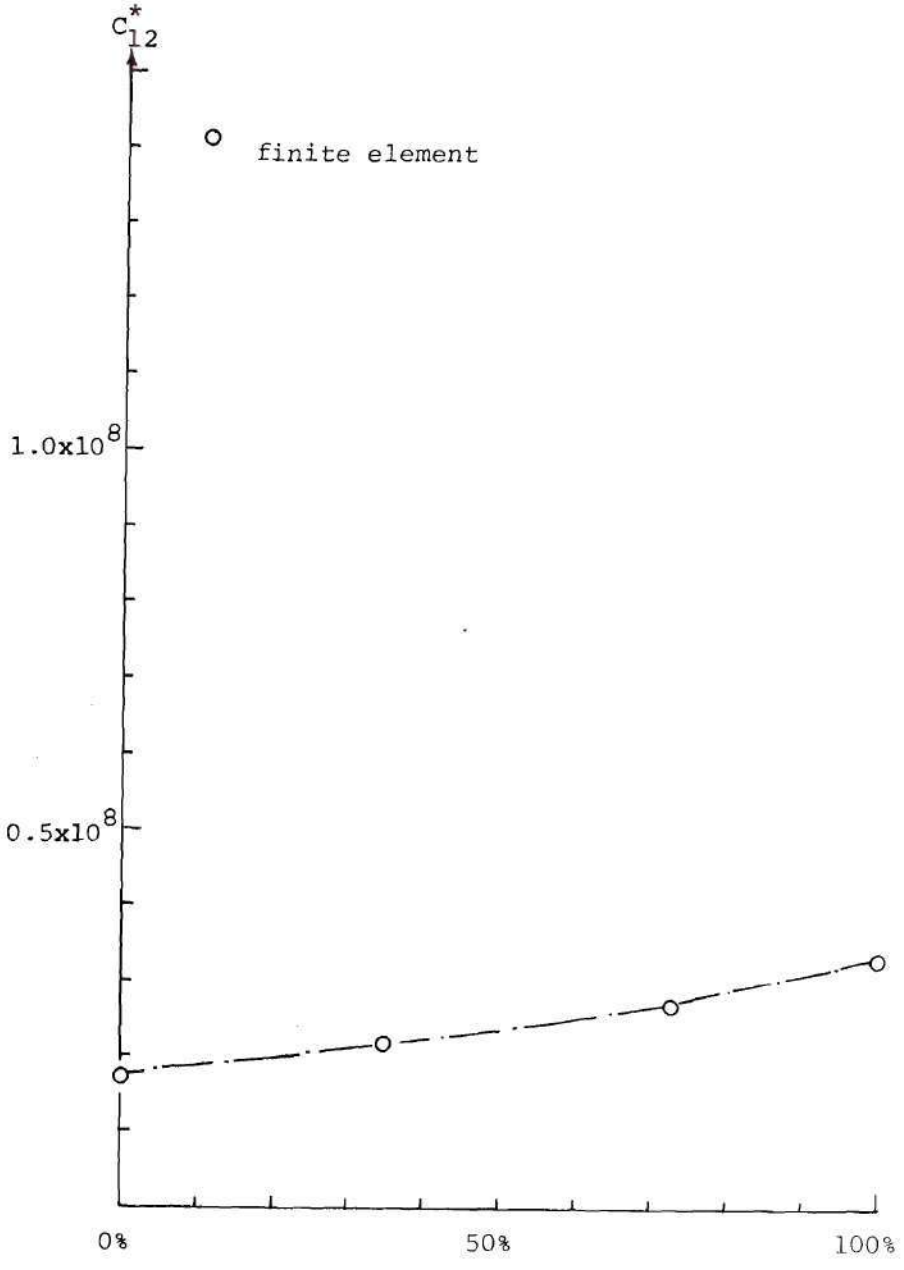

Figure 44. The Effective Modulus C_{12}^* of the Short Fiber Composites

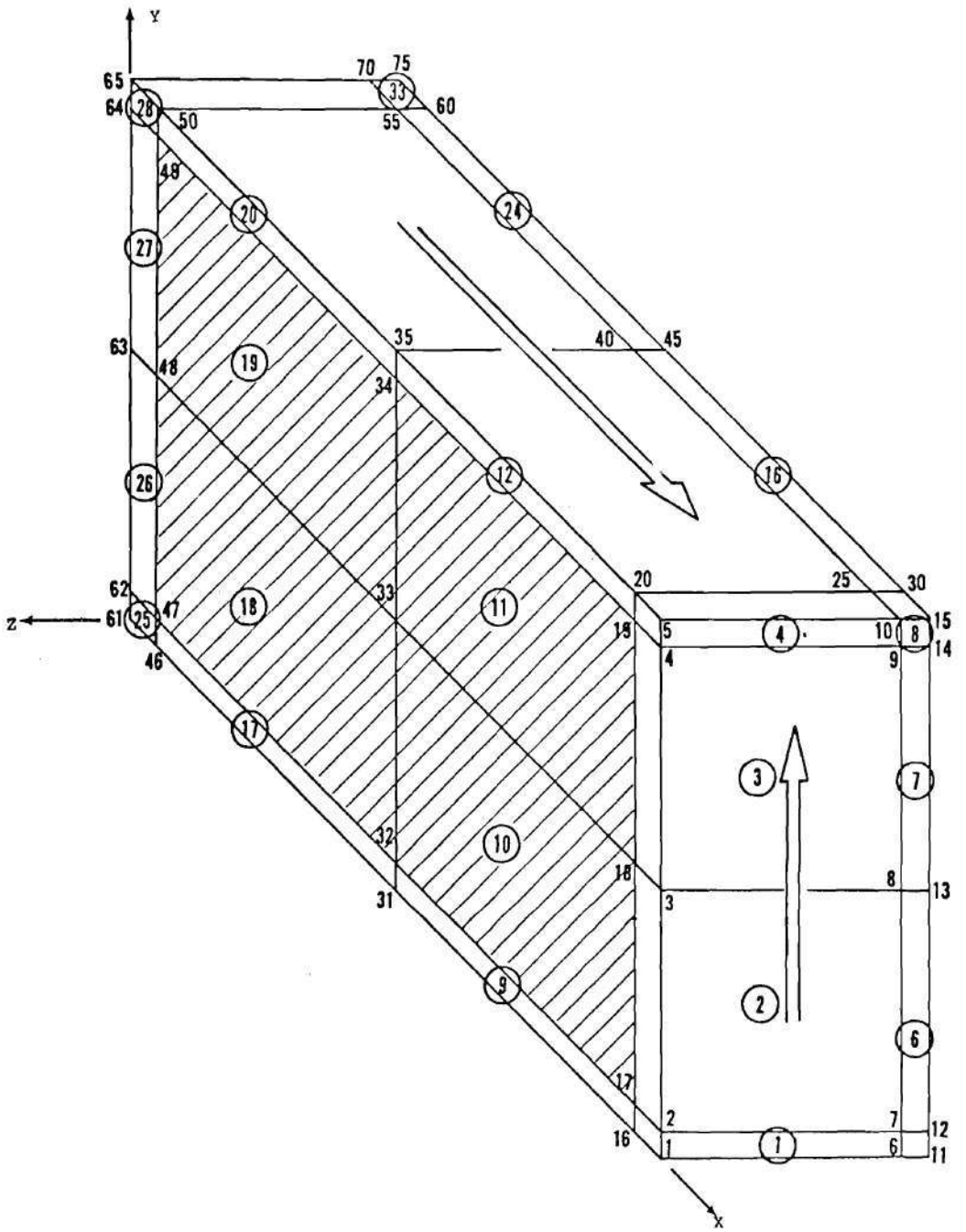

Figure 45. Discretization of One Half of a Basic Cell of a Short Fiber Composite for the Shear Test Loaded by T_{xy}

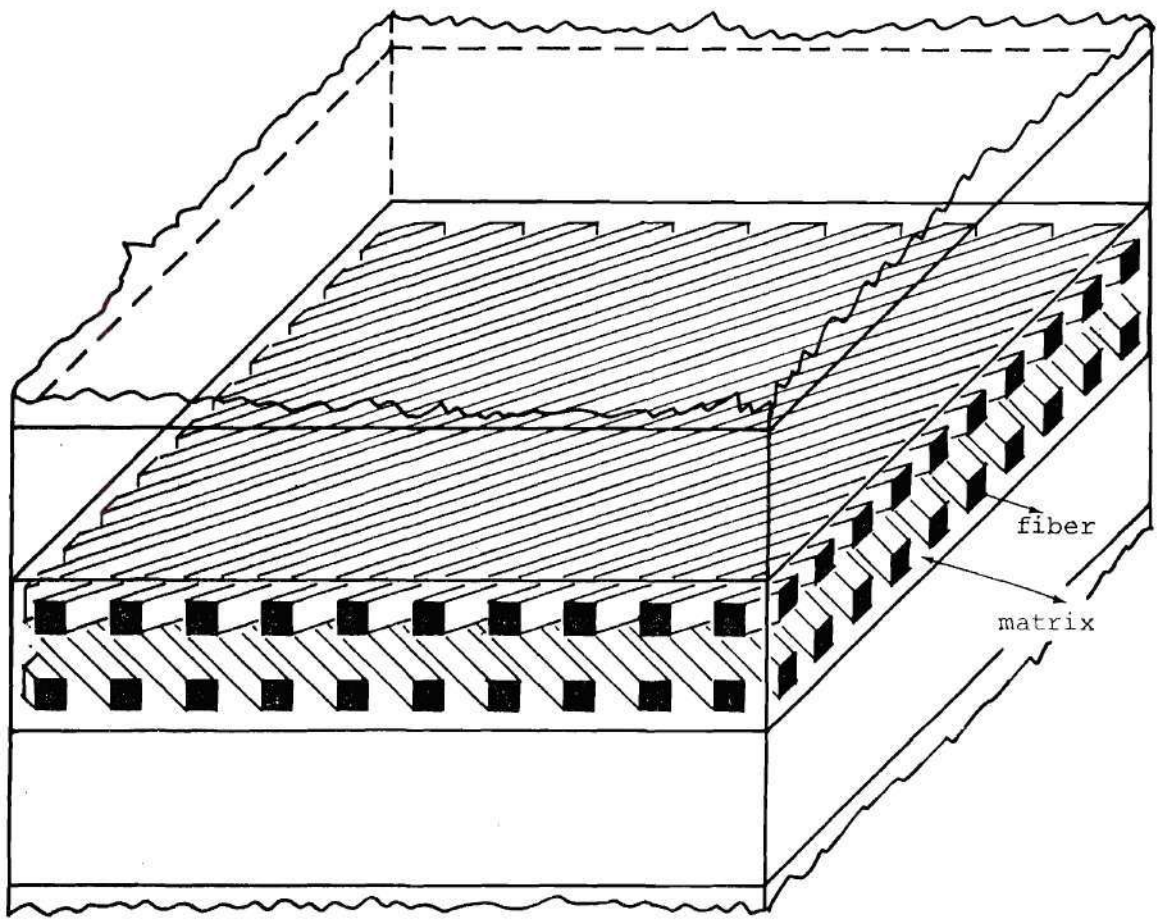

Figure 46. Laminated Composite

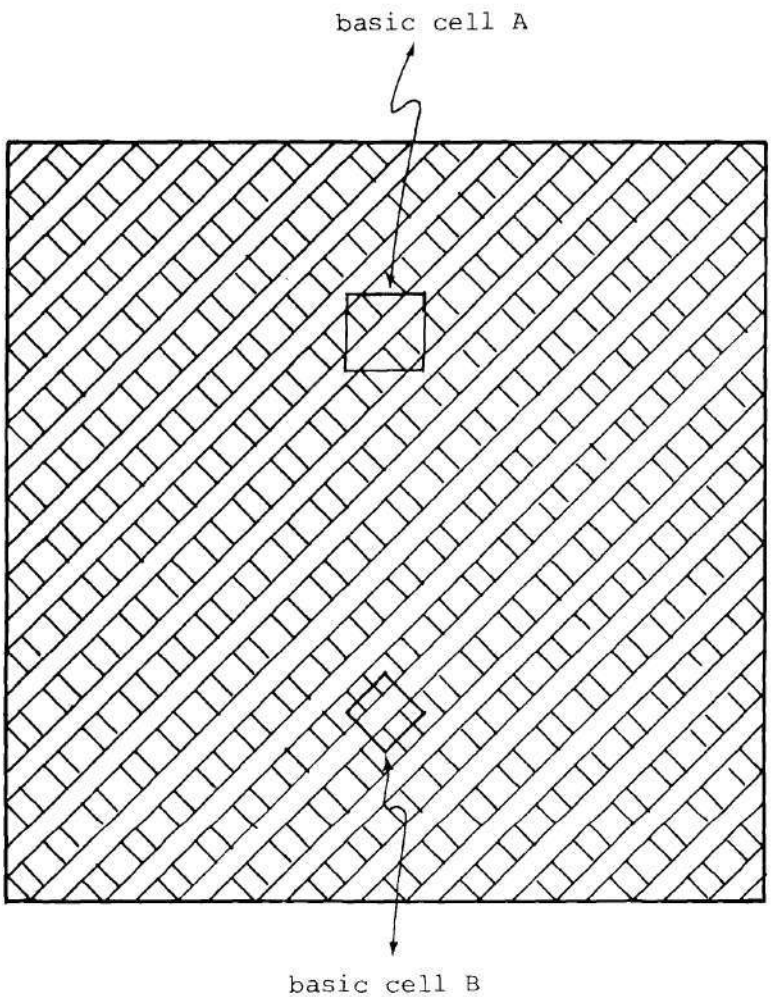

Figure 47. Possible Basic Cells for the Laminated Composite

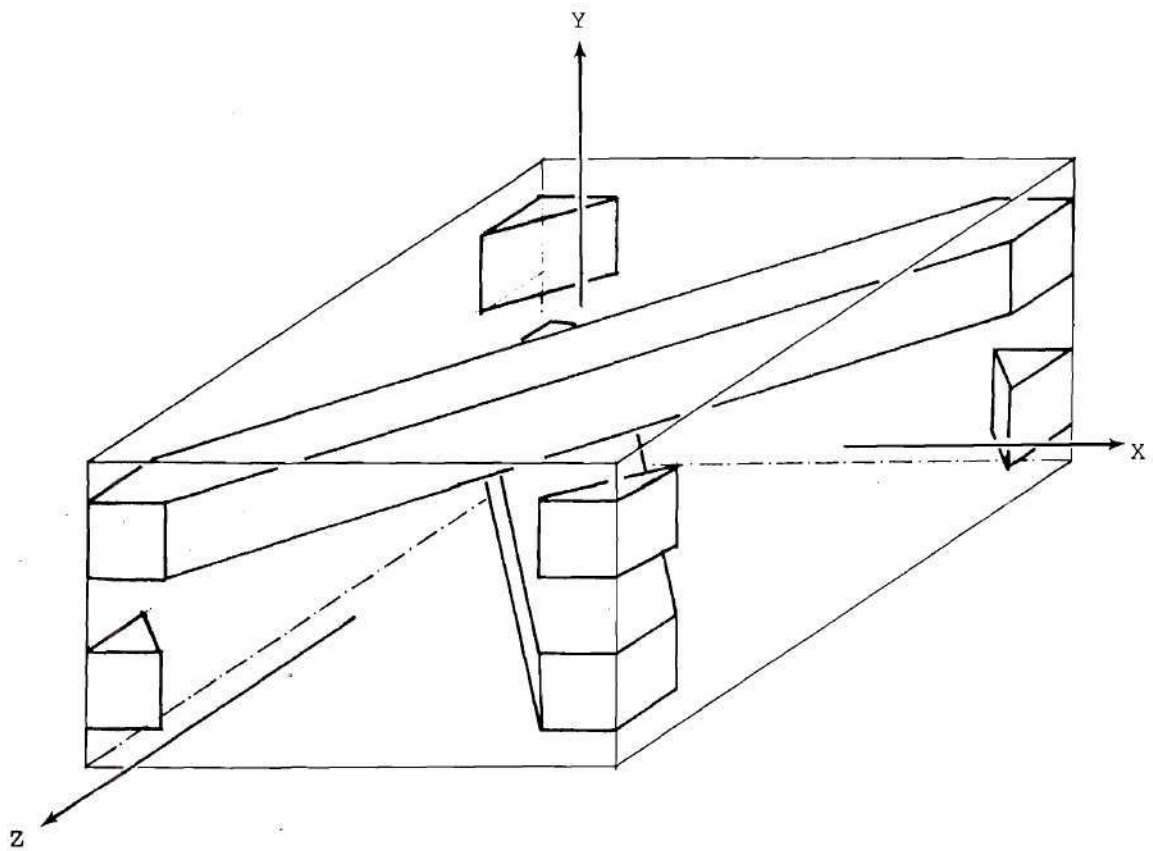

Figure 48. The Basic Cell of the Laminated Composite

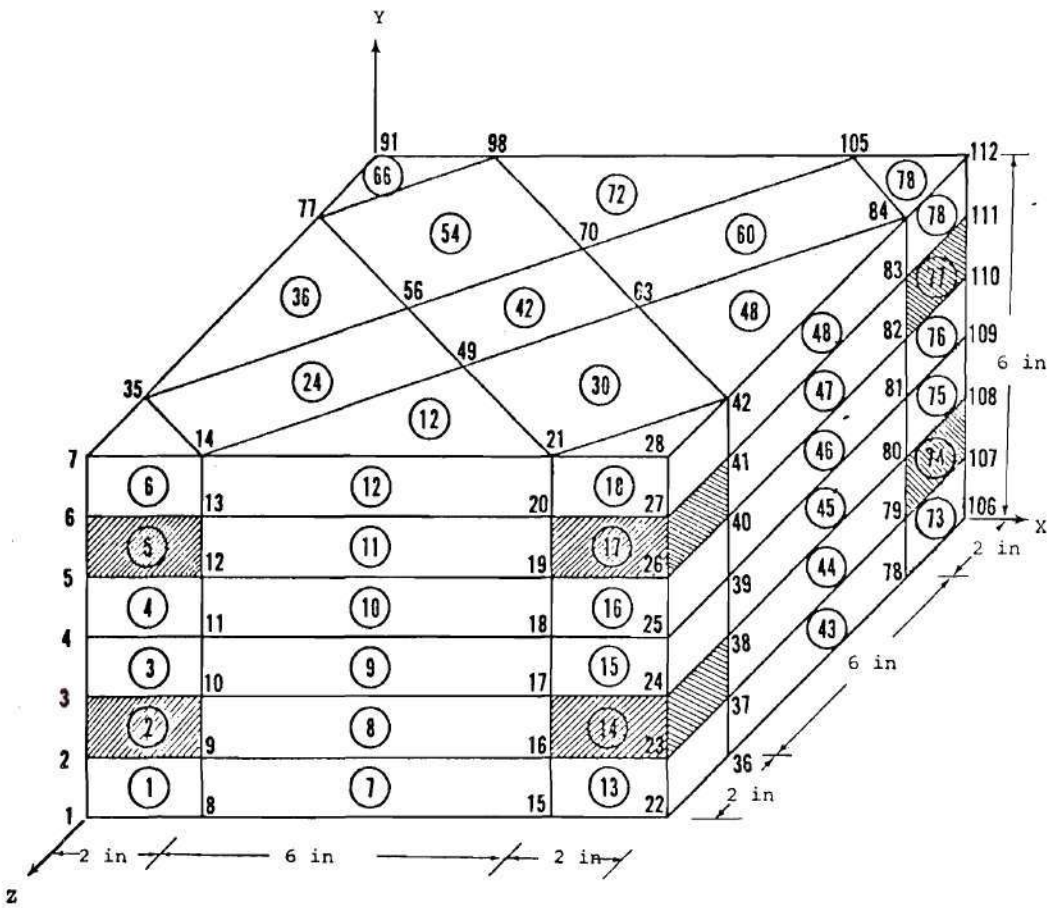

Figure 49. Discretization of the Basic Cell for the Laminated Composite

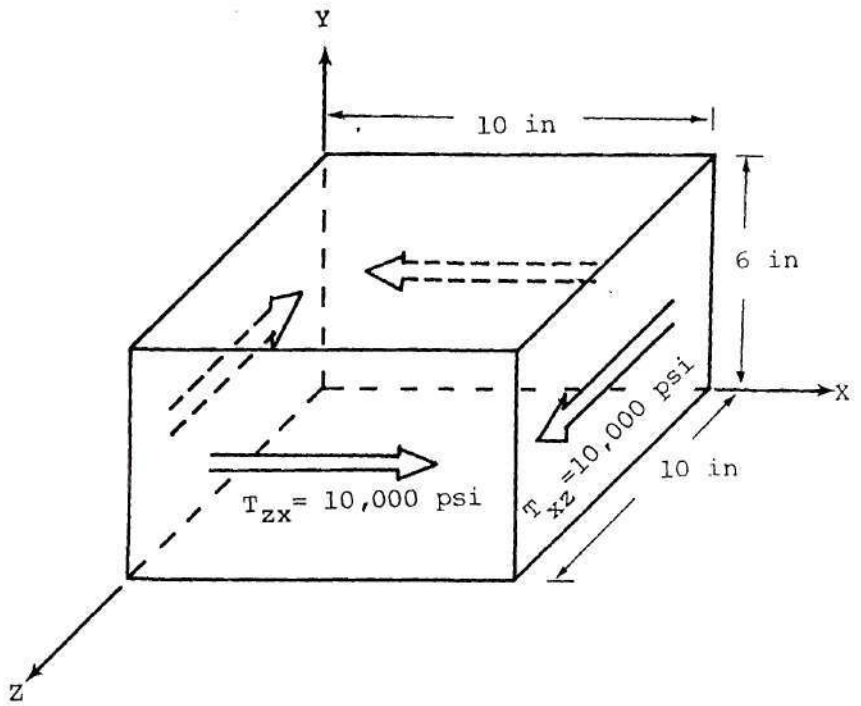

Figure 50. Shear Test Loaded by T_{zx}

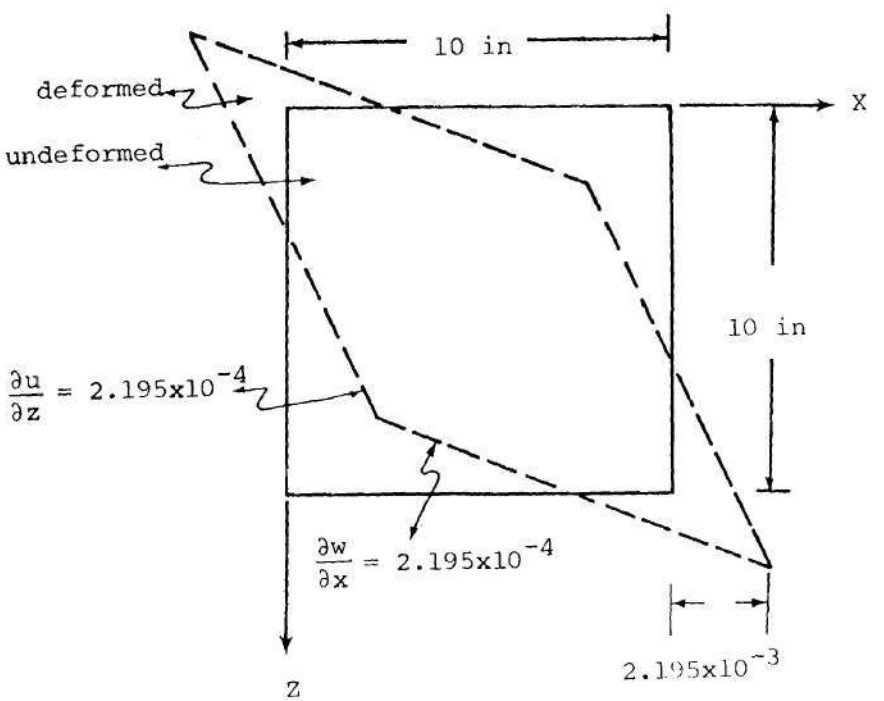

Figure 51. Deformed and Undeformed Shapes

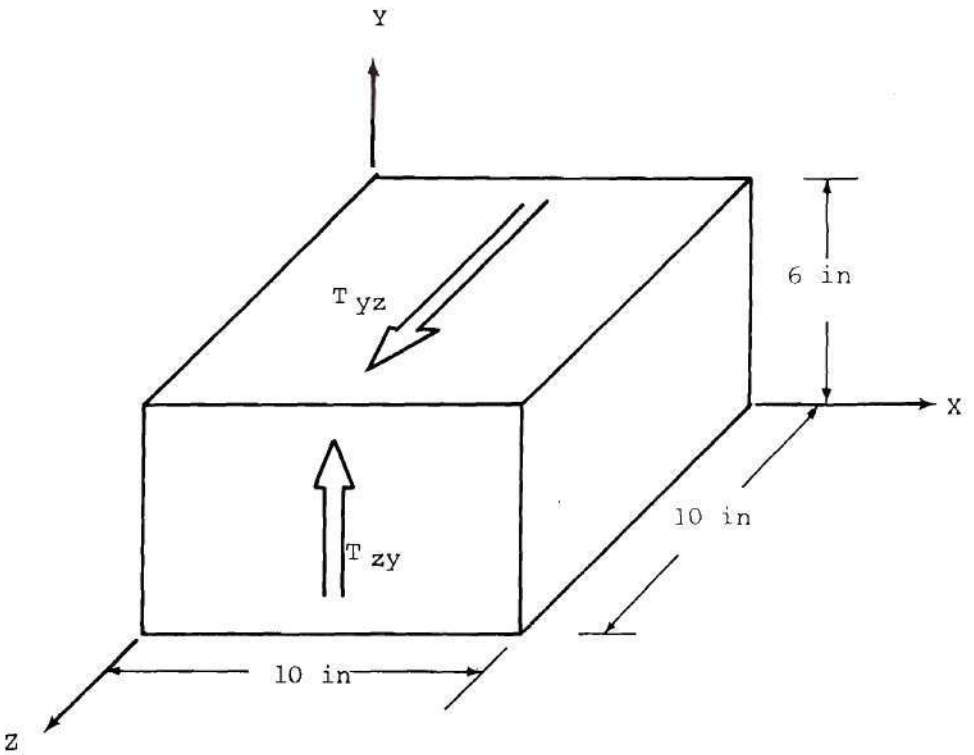

Figure 52. Shear Test Loaded by T_{yz}

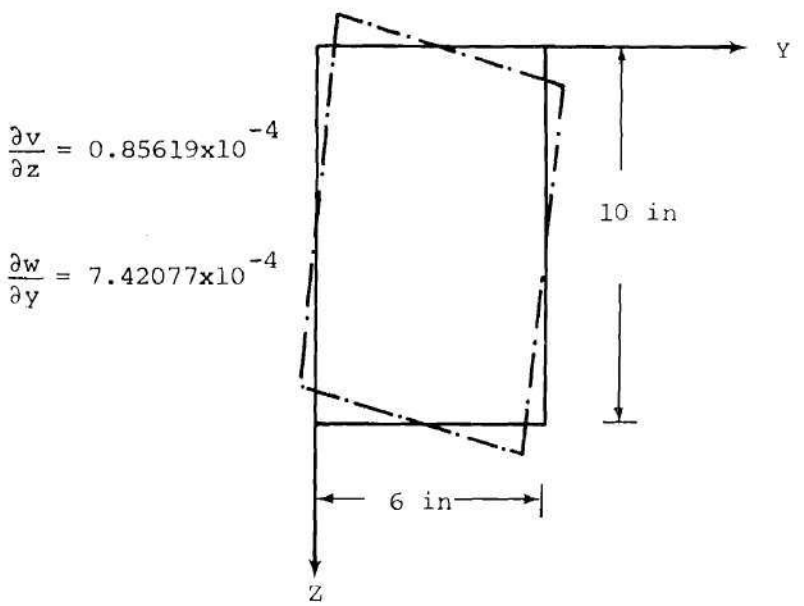

Figure 53. Average Shearing Strain

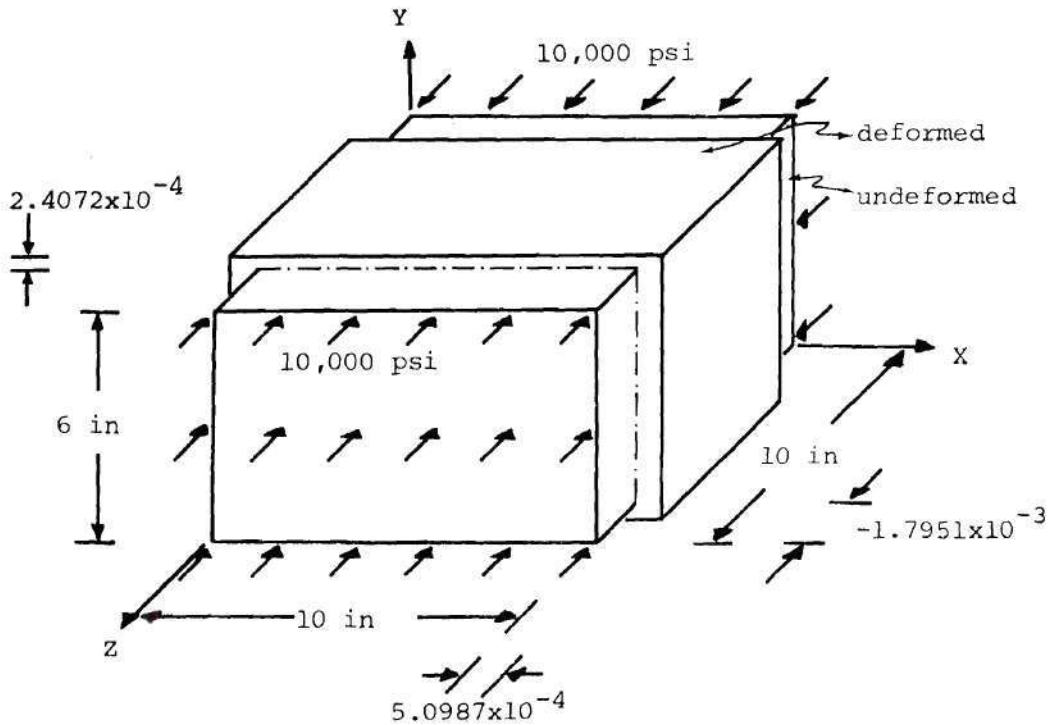

Figure 54. Compression Test Loaded along z-Direction

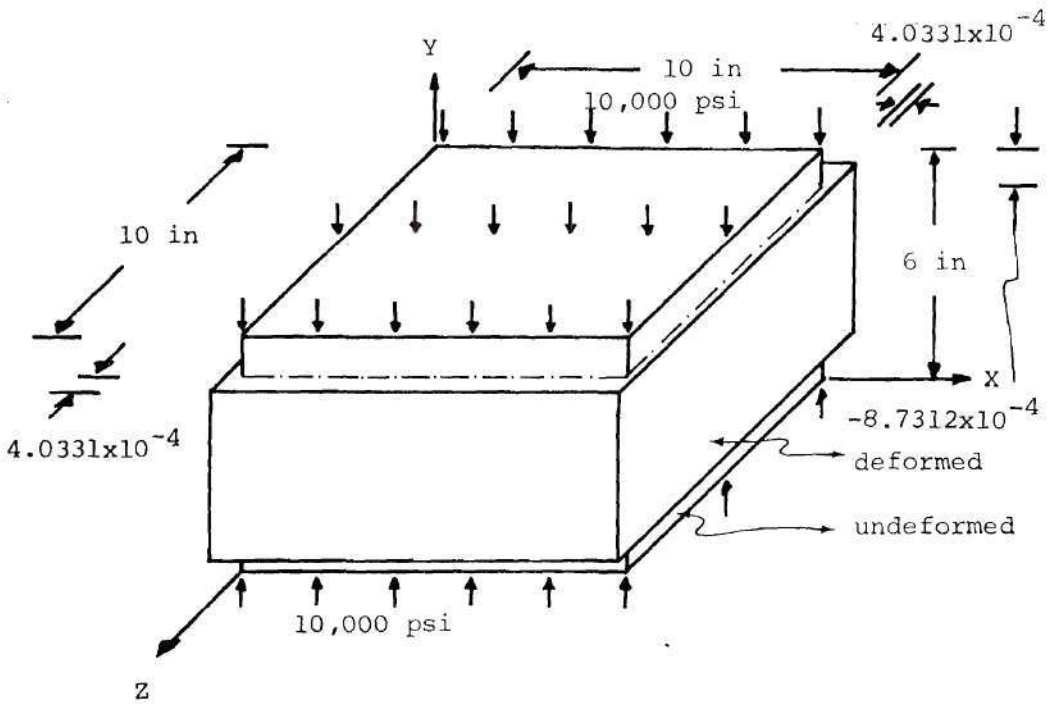

Figure 55. Compression Test Loaded along y-Direction

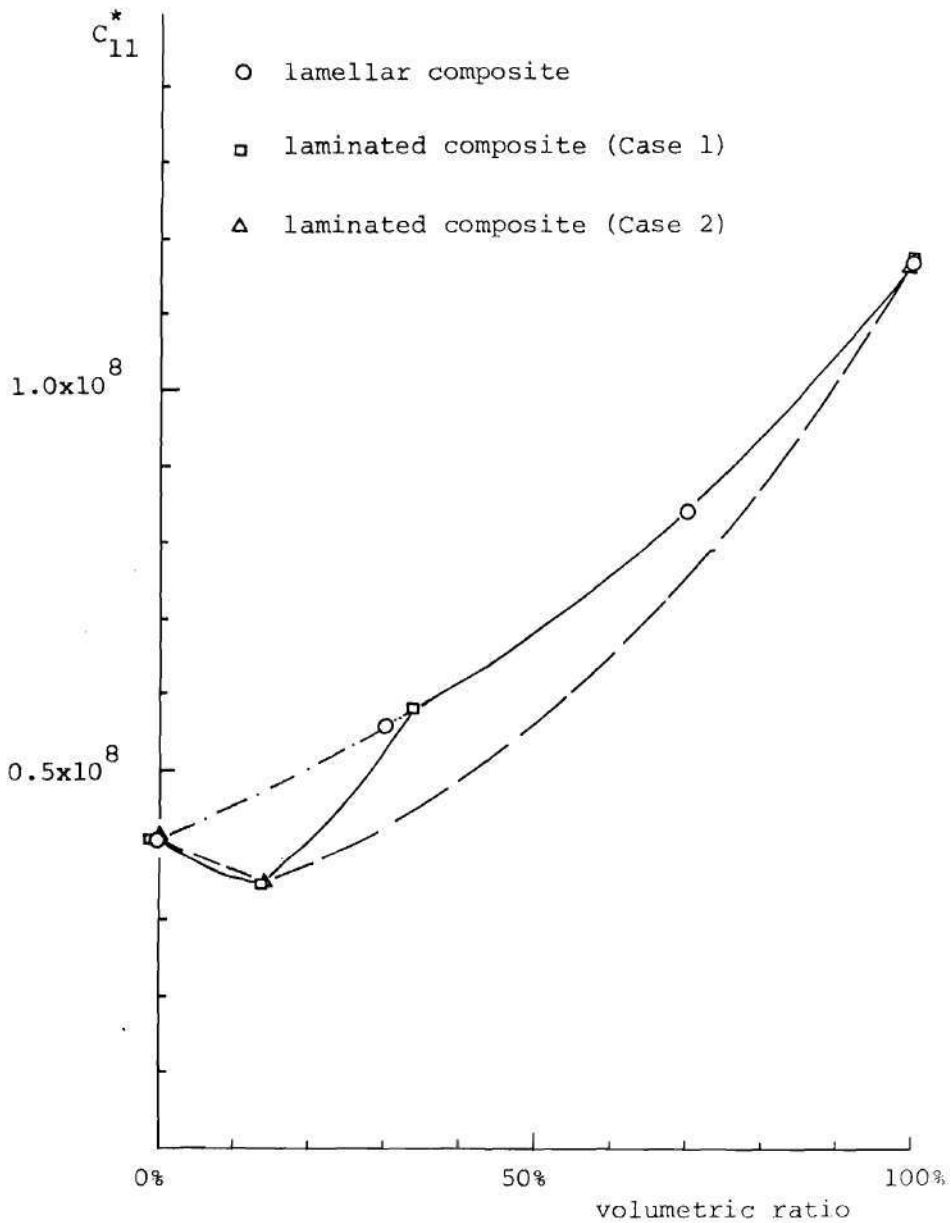

Figure 56. The Effective Modulus C_{11}^* of the Laminated Composites

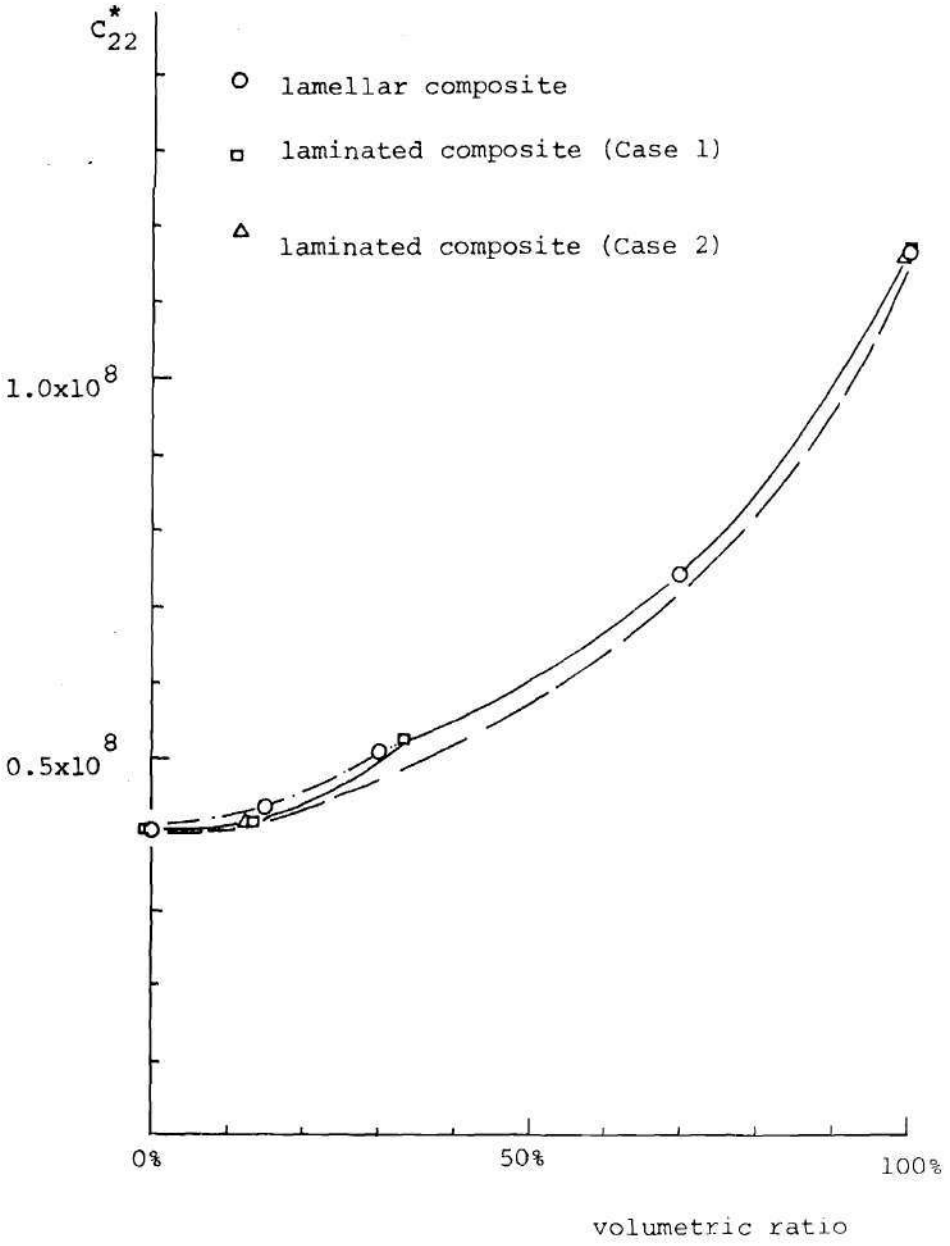

Figure 57. The Effective Modulus C_{22}^* of the Laminated Composites

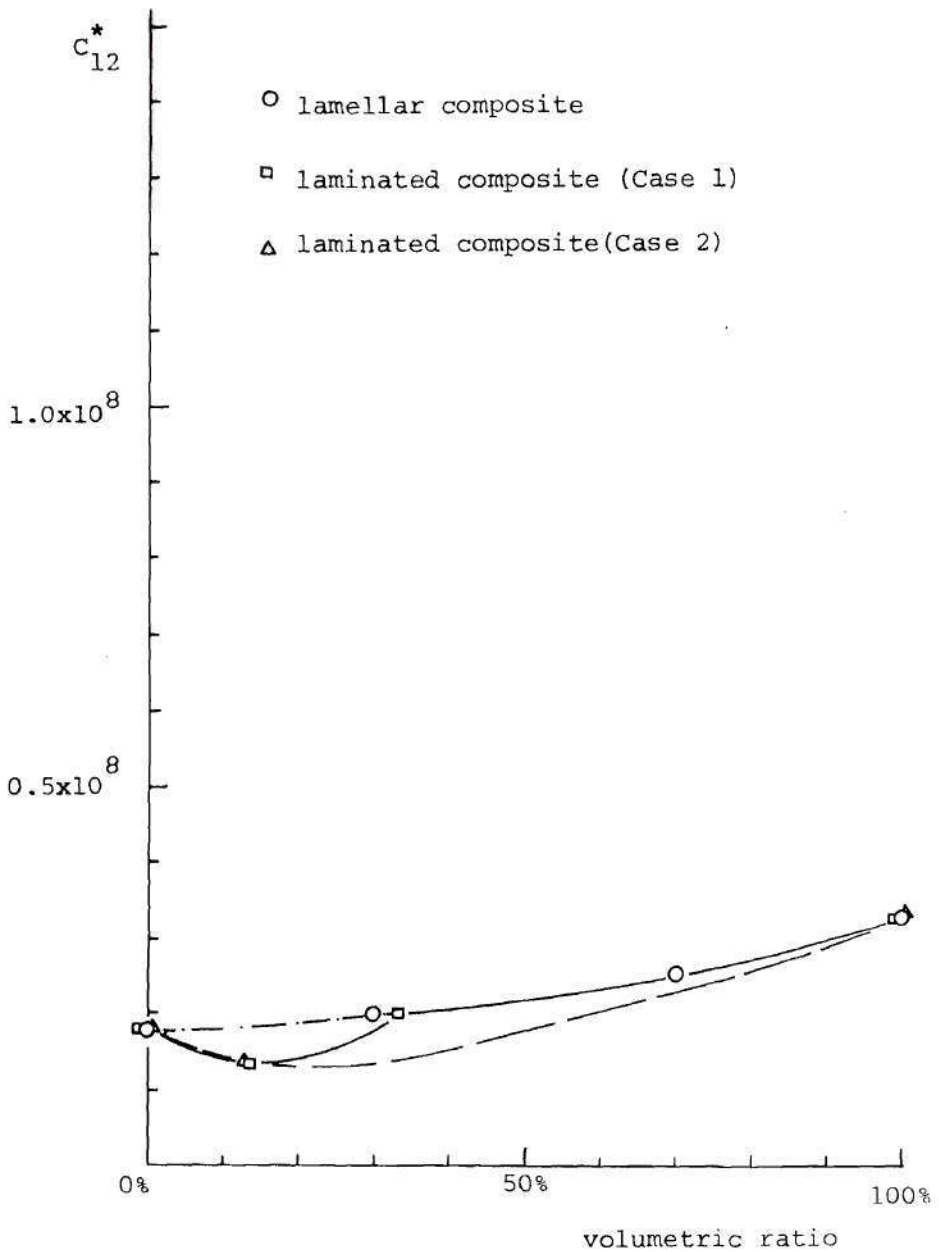

Figure 58. The Effective Modulus C_{12}^* of the Laminated Composites

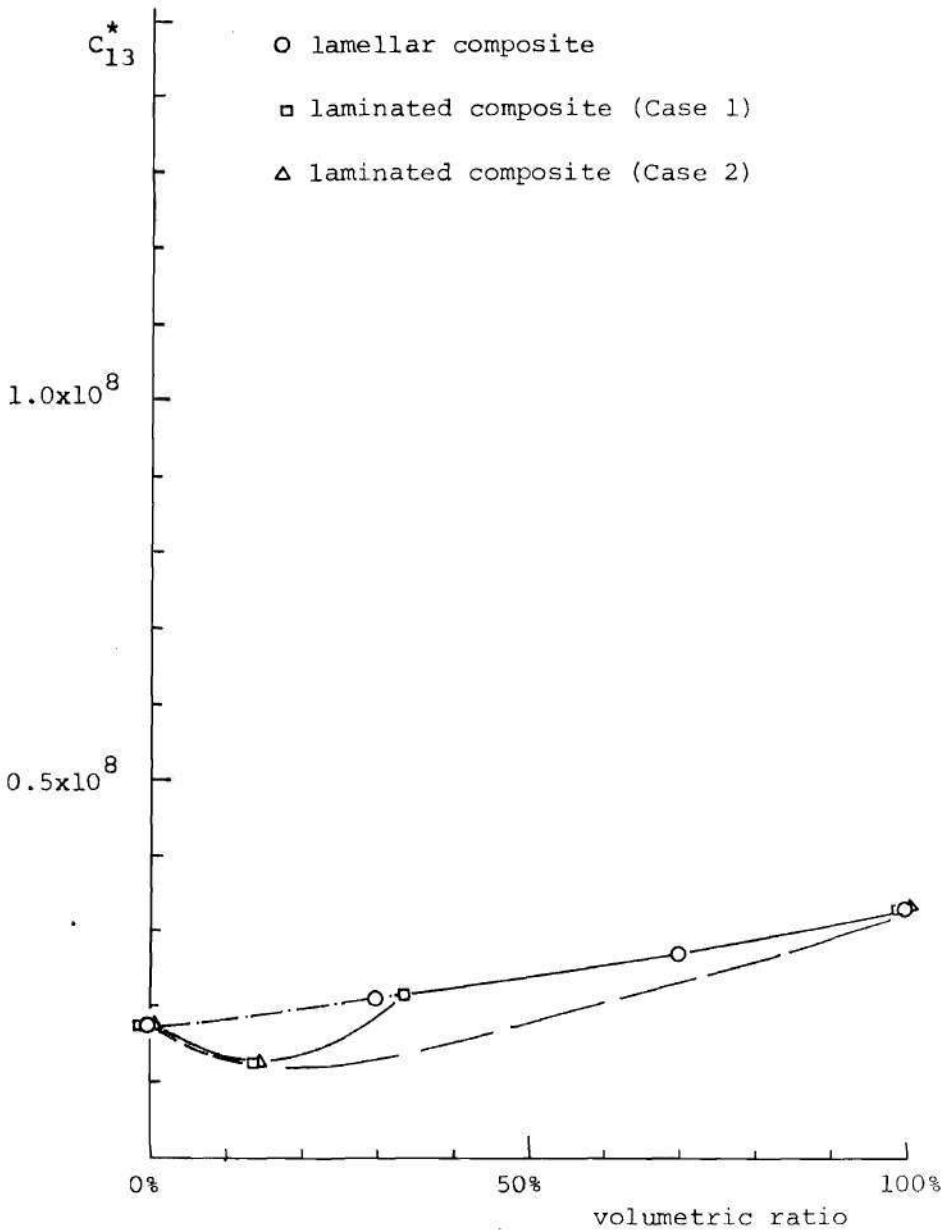

Figure 59. The Effective Modulus C^*_{13} of the Laminated Composites

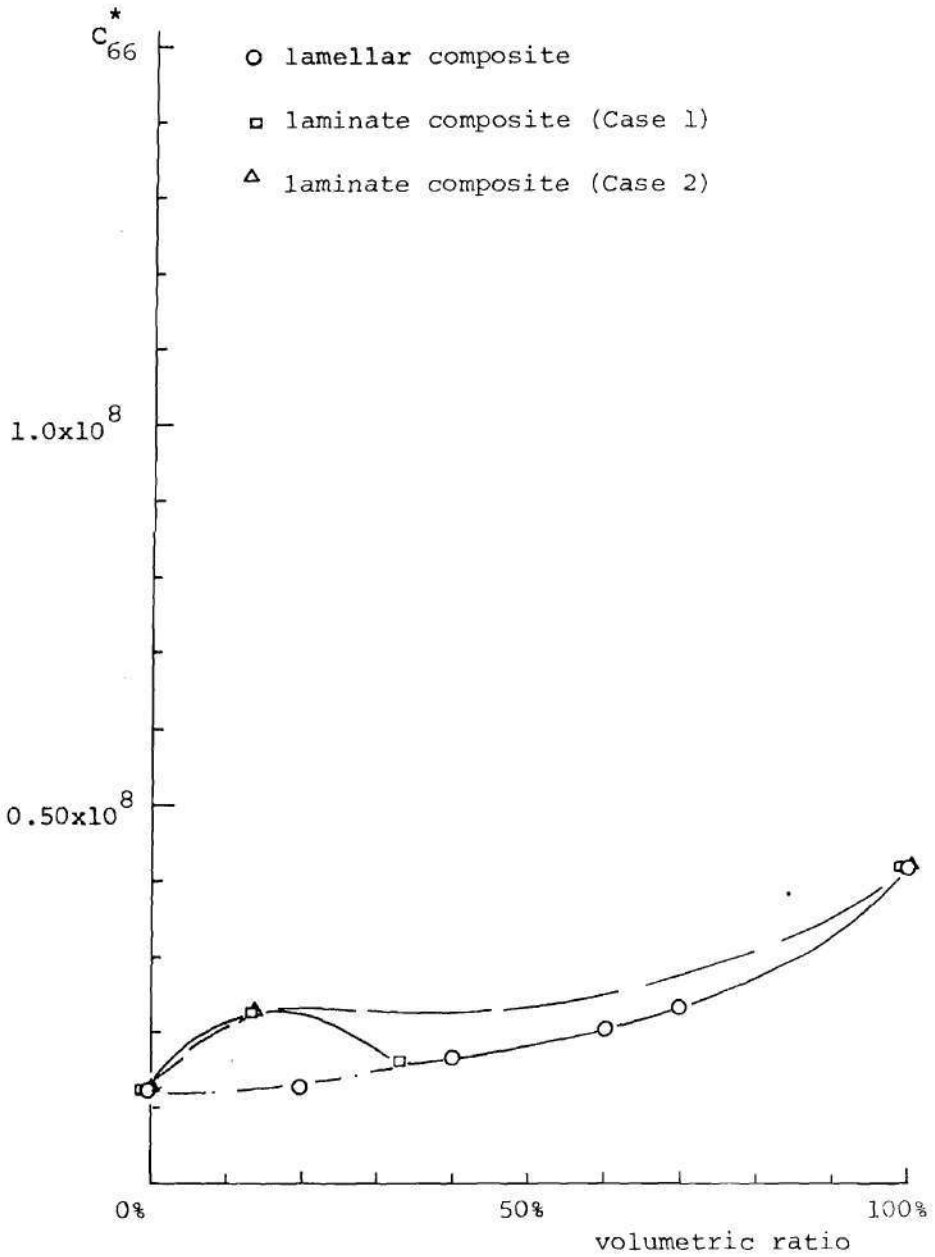

Figure 60. The Effective Modulus C^*_{66} of the Laminated Composite

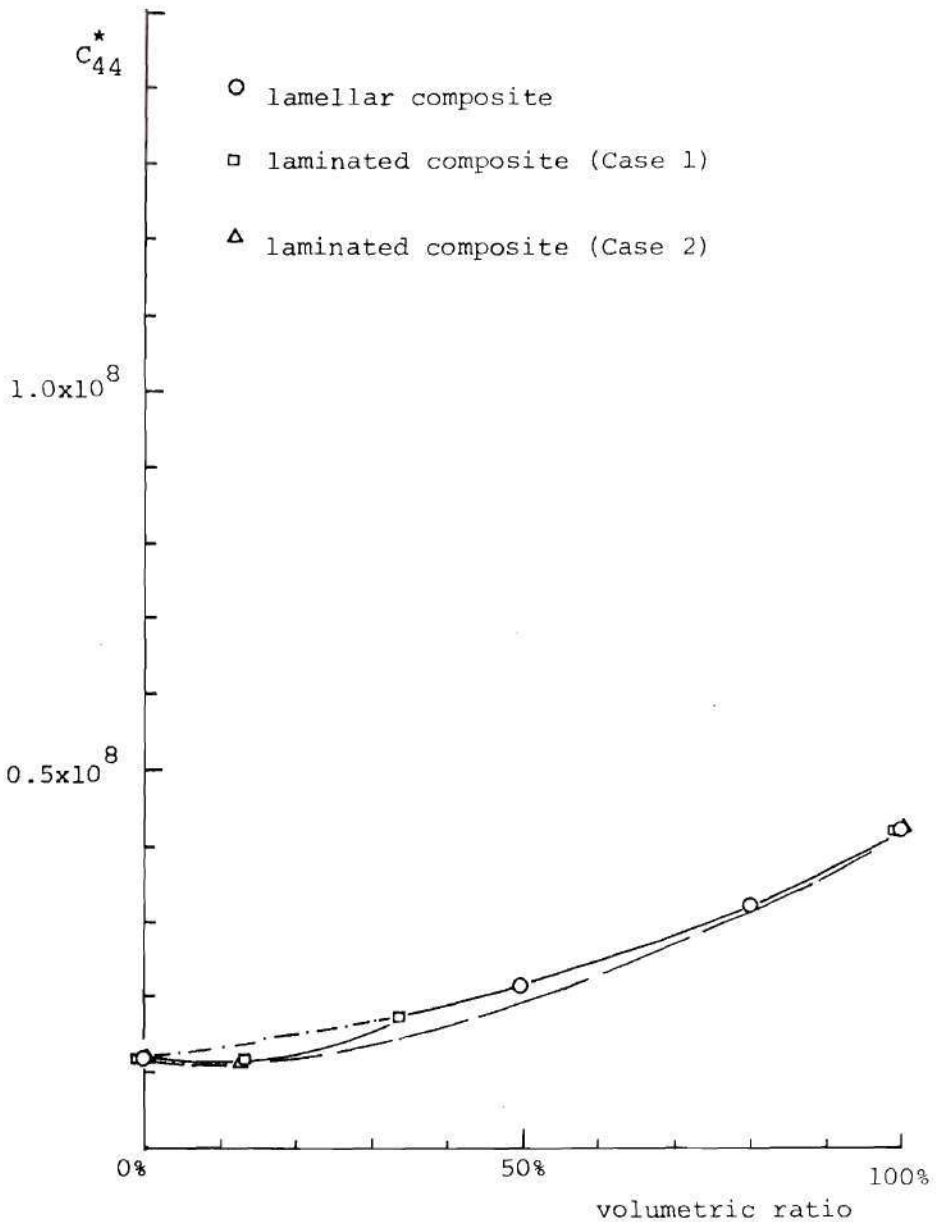

Figure 61. The Effective Modulus C_{44}^{*} of the Laminated Composites

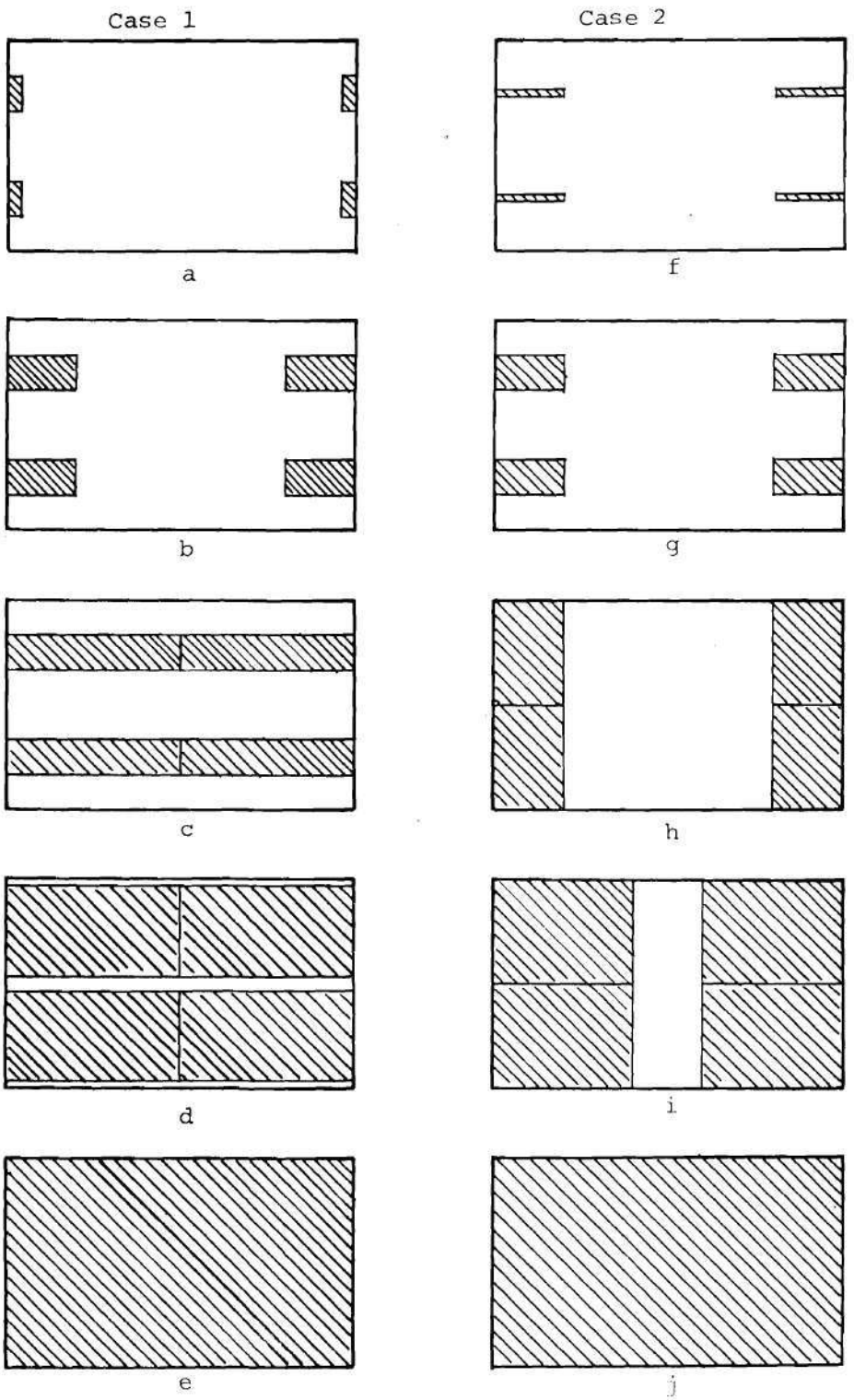

Figure 62. Two Illustration of Changing the Volumetric Ratios of Laminated Composites

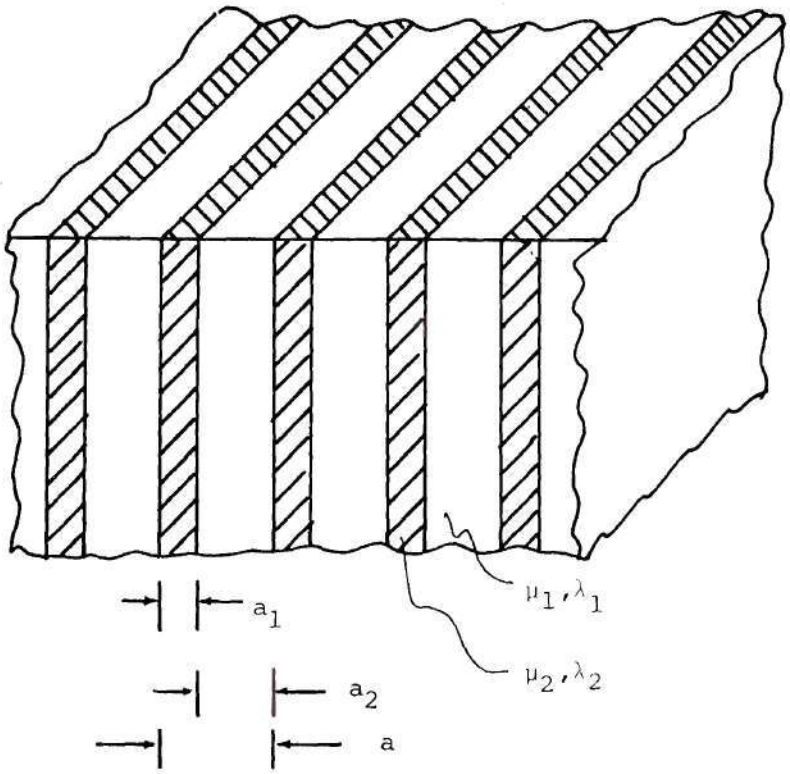

Figure 63. Lamellar Composite

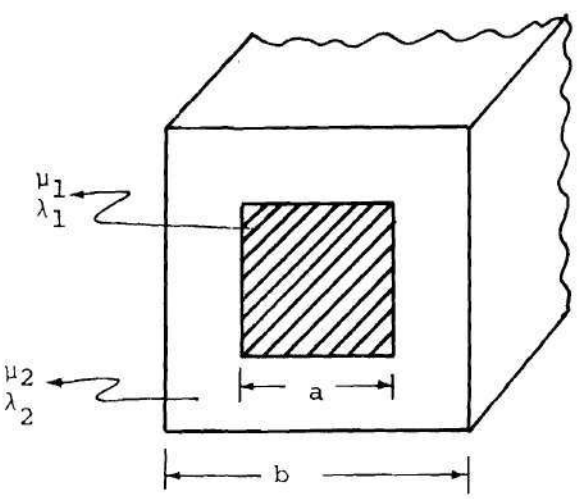

Figure 64. Unidirectional Fiber Composite

APPENDIX A

REDUCTION OF ELASTIC MODULI DUE TO SYMMETRIES

Consider the basic cells of the unidirectional fiber composite, the lamellar composite, the short fiber composite, and the laminated composite as shown in Figures 11, 29, 40, and 48 respectively. All these composites have 180° rotation symmetries about x-, y-, and z-axis. In other words, the composites maintain the same properties in the rotated coordinate systems, say, x', y', z' coordinate system. In matrix notation, the three sets of the direction cosines for such rotations are:

$$[\alpha]_{\substack{\text{x-rot.}\\ \theta=180^{\circ}}} = \begin{bmatrix} 1 & 0 & 0 \\ 0 & -1 & 0 \\ 0 & 0 & -1 \end{bmatrix} \tag{A-1}$$

$$[\beta]_{\substack{\text{y-rot.}\\ \theta=180^{\circ}}} = \begin{bmatrix} -1 & 0 & 0 \\ 0 & 1 & 0 \\ 0 & 0 & -1 \end{bmatrix} \tag{A-2}$$

$$[\gamma]_{\substack{\text{z-rot.}\\ \theta=180^{\circ}}} = \begin{bmatrix} -1 & 0 & 0 \\ 0 & -1 & 0 \\ 0 & 0 & 1 \end{bmatrix} \tag{A-3}$$

for 180° rotation about x-, y-, and z-axis respectively.

The transformation relationships of the stresses and strains between the primed and unprimed coordinate systems become

$$\sigma'_{ij} = \alpha_{im}\,\alpha_{jn}\,\alpha_{mn} \tag{A-4}$$

$$\varepsilon'_{ij} = \alpha_{im}\,\alpha_{jn}\,\varepsilon_{mn} \tag{A-5}$$

where i, j, m, n = 1,2,3 or i, j, m, n = x,y,z

and they are reduced to the following expressions for 180^0 rotation about x-axis.

$$\begin{aligned}
\sigma'_{xx} &= \sigma_{xx} \\
\sigma'_{xy} &= -\sigma_{xy} \\
\sigma'_{xz} &= -\sigma_{xz} \\
\sigma'_{yy} &= \sigma_{yy} \\
\sigma'_{yz} &= \sigma_{yz} \\
\sigma'_{zz} &= \sigma_{zz}
\end{aligned} \tag{A-6}$$

Similarly, for the strains, one obtains the following relationships:

$$\begin{aligned}
\varepsilon'_{xx} &= \varepsilon_{xx} \\
\varepsilon'_{xy} &= -\varepsilon_{xy} \\
\varepsilon'_{xz} &= -\varepsilon_{xz} \\
\varepsilon'_{yy} &= \varepsilon_{yy} \\
\varepsilon'_{yz} &= \varepsilon_{yz} \\
\varepsilon'_{zz} &= \varepsilon_{zz}
\end{aligned} \tag{A-7}$$

The material properties should not change whether they are referred in the primed or unprimed coordinate systems since they are symmetric in these systems. Hence the Hooke's laws in the two coordinate systems are

$$\begin{Bmatrix} \sigma_{xx} \\ \sigma_{yy} \\ \sigma_{zz} \\ \sigma_{xy} \\ \sigma_{yz} \\ \sigma_{zx} \end{Bmatrix} = \begin{bmatrix} C_{11} & C_{12} & C_{13} & C_{14} & C_{15} & C_{16} \\ C_{12} & C_{22} & C_{23} & C_{24} & C_{25} & C_{26} \\ C_{13} & C_{23} & C_{33} & C_{34} & C_{35} & C_{36} \\ C_{14} & C_{24} & C_{43} & C_{44} & C_{45} & C_{46} \\ C_{15} & C_{25} & C_{35} & C_{54} & C_{55} & C_{56} \\ C_{16} & C_{26} & C_{36} & C_{64} & C_{65} & C_{66} \end{bmatrix} \begin{Bmatrix} \varepsilon_{xx} \\ \varepsilon_{yy} \\ \varepsilon_{zz} \\ 2\varepsilon_{xy} \\ 2\varepsilon_{yz} \\ 2\varepsilon_{zx} \end{Bmatrix} \tag{A-8}$$

$$\begin{Bmatrix} \sigma'_{xx} \\ \sigma'_{yy} \\ \sigma'_{zz} \\ \sigma'_{xy} \\ \sigma'_{zx} \\ \sigma_{zx} \end{Bmatrix} = \begin{bmatrix} C'_{11} & C'_{12} & C'_{13} & C'_{14} & C'_{15} & C'_{16} \\ C'_{12} & C'_{22} & C'_{23} & C'_{24} & C'_{25} & C'_{26} \\ C'_{13} & C'_{23} & C'_{33} & C'_{34} & C'_{35} & C'_{36} \\ C'_{14} & C'_{24} & C'_{34} & C'_{44} & C'_{45} & C'_{46} \\ C'_{15} & C'_{25} & C'_{35} & C'_{45} & C'_{55} & C'_{56} \\ C'_{16} & C'_{26} & C'_{36} & C'_{46} & C'_{56} & C'_{66} \end{bmatrix} \begin{Bmatrix} \varepsilon'_{xx} \\ \varepsilon'_{yy} \\ 2\varepsilon'_{zz} \\ 2\varepsilon'_{xy} \\ 2\varepsilon'_{yz} \\ 2\varepsilon'_{zx} \end{Bmatrix} \tag{A-9}$$

where $C_{ij} = C_{ji}$. With use of Equations (A-6) through (A-9), one obtains

$$C_{14} = C_{24} = C_{34} = C_{54} = 0$$
$$C_{16} = C_{26} = C_{36} = C_{56} = 0 \tag{A-10}$$

Similarly, 180° rotation about y- and z-axis respectively give

$$C_{14} = C_{24} = C_{34} = C_{64} = 0$$
$$C_{15} = C_{25} = C_{35} = C_{64} = 0 \tag{A-11}$$

$$C_{16} = C_{26} = C_{36} = C_{46} = 0$$
$$C_{15} = C_{25} = C_{35} = C_{45} = 0 \tag{A-12}$$

Comparing Equation (A-10) through (A-12), Hooke's law becomes

$$\begin{Bmatrix} \sigma_{xx} \\ \sigma_{yy} \\ \sigma_{zz} \\ \sigma_{xy} \\ \sigma_{yz} \\ \sigma_{zx} \end{Bmatrix} = \begin{bmatrix} C_{11} & C_{12} & C_{13} & 0 & 0 & 0 \\ C_{12} & C_{22} & C_{23} & 0 & 0 & 0 \\ C_{13} & C_{23} & C_{33} & 0 & 0 & 0 \\ 0 & 0 & 0 & C_{44} & 0 & 0 \\ 0 & 0 & 0 & 0 & C_{55} & 0 \\ 0 & 0 & 0 & 0 & 0 & C_{66} \end{bmatrix} \begin{Bmatrix} \varepsilon_{xx} \\ \varepsilon_{yy} \\ \varepsilon_{zz} \\ 2\varepsilon_{xy} \\ 2\varepsilon_{yz} \\ 2\varepsilon_{zx} \end{Bmatrix} \tag{A13}$$

Unidirectional Fiber, Lamellar, and Short Fiber Composites

The unidirectional fiber, the lamellar, and the short fiber composites have further symmetries about z-axis. Consider the 90° rotation about z-axis. With the similar procedure as shown above, one obtains

$$\begin{Bmatrix} \sigma_{xx} \\ \sigma_{yy} \\ \sigma_{zz} \\ \sigma_{xy} \\ \sigma_{yz} \\ \sigma_{zx} \end{Bmatrix} = \begin{bmatrix} C_{11} & C_{12} & C_{13} & 0 & 0 & 0 \\ C_{12} & C_{11} & C_{13} & 0 & 0 & 0 \\ C_{13} & C_{13} & C_{33} & 0 & 0 & 0 \\ 0 & 0 & 0 & C_{44} & 0 & 0 \\ 0 & 0 & 0 & 0 & C_{66} & 0 \\ 0 & 0 & 0 & 0 & 0 & C_{66} \end{bmatrix} \begin{Bmatrix} \varepsilon_{xx} \\ \varepsilon_{yy} \\ \varepsilon_{zz} \\ 2\varepsilon_{xy} \\ 2\varepsilon_{yz} \\ 2\varepsilon_{zx} \end{Bmatrix} \tag{A-14}$$

where $C_{44} = 1/2\ (C_{11}-C_{12})$. Although there are other symmetries for the unidirectional fiber and the lamellar composites, they do not furnish any new conditions. Also, by inspection, it is apparent that there in no further simplification of moduli. However, for the short fiber composite, Hooke's law becomes

$$\begin{Bmatrix} \sigma_{xx} \\ \sigma_{yy} \\ \sigma_{zz} \\ \sigma_{xy} \\ \sigma_{yz} \\ \sigma_{zx} \end{Bmatrix} = \begin{bmatrix} C_{11} & C_{12} & C_{12} & 0 & 0 & 0 \\ C_{12} & C_{11} & C_{12} & 0 & 0 & 0 \\ C_{12} & C_{12} & C_{11} & 0 & 0 & 0 \\ 0 & 0 & 0 & C_{44} & 0 & 0 \\ 0 & 0 & 0 & 0 & C_{44} & 0 \\ 0 & 0 & 0 & 0 & 0 & C_{44} \end{bmatrix} \begin{Bmatrix} \varepsilon_{xx} \\ \varepsilon_{yy} \\ \varepsilon_{zz} \\ 2\varepsilon_{xy} \\ 2\varepsilon_{yz} \\ 2\varepsilon_{zx} \end{Bmatrix} \tag{A-15}$$

where $C_{44} = 1/2\ (C_{11} - C_{12})$. The result in Equation (A-15) is obtained by 90° rotation about x- and y-axis or direct inspection of symmetries.

Laminated Composite

The basic cell shown in Figure 48 maintains the same geometry if the basic cell is reflected about y = 0 plane and then rotated 90° about y-axis. The direction cosines for each operations are

$$[\alpha]_{\substack{\text{refl.} \\ y=0 \text{ plane}}} = \begin{bmatrix} 1 & 0 & 0 \\ 0 & -1 & 0 \\ 0 & 0 & 1 \end{bmatrix} \tag{A-16}$$

$$[\beta]_{\substack{\text{y-rot.} \\ \theta=90°}} = \begin{bmatrix} 0 & 0 & 1 \\ 0 & 1 & 0 \\ -1 & 0 & 0 \end{bmatrix} \tag{A-17}$$

After two successive operation with the two sets of direction cosines Equations (A-16) and (A-17), Hooke's law becomes

$$\begin{Bmatrix} \sigma_{xx} \\ \sigma_{yy} \\ \sigma_{zz} \\ \sigma_{xy} \\ \sigma_{yz} \\ \sigma_{zx} \end{Bmatrix} = \begin{bmatrix} C_{11} & C_{12} & C_{13} & 0 & 0 & C_{16} \\ C_{12} & C_{22} & C_{12} & 0 & 0 & 0 \\ C_{13} & C_{12} & C_{11} & 0 & 0 & -C_{16} \\ 0 & 0 & 0 & C_{44} & 0 & 0 \\ 0 & 0 & 0 & 0 & C_{44} & 0 \\ C_{16} & 0 & -C_{16} & 0 & 0 & C_{66} \end{bmatrix} \begin{Bmatrix} \varepsilon_{xx} \\ \varepsilon_{yy} \\ \varepsilon_{zz} \\ 2\varepsilon_{xy} \\ 2\varepsilon_{yz} \\ 2\varepsilon_{zx} \end{Bmatrix} \quad \text{(A-18)}$$

Remembering the fact that this composite has 180^0 rotation symmetry about x-, y-, and z-axis, the final form of Hooke's law, combining Equations (A-13) and (A-18), becomes

$$\begin{Bmatrix} \sigma_{xx} \\ \sigma_{yy} \\ \sigma_{zz} \\ \sigma_{xy} \\ \sigma_{yz} \\ \sigma_{zx} \end{Bmatrix} = \begin{bmatrix} C_{11} & C_{12} & C_{13} & 0 & 0 & 0 \\ C_{12} & C_{22} & C_{12} & 0 & 0 & 0 \\ C_{13} & C_{12} & C_{11} & 0 & 0 & 0 \\ 0 & 0 & 0 & C_{44} & 0 & 0 \\ 0 & 0 & 0 & 0 & C_{44} & 0 \\ 0 & 0 & 0 & 0 & 0 & C_{66} \end{bmatrix} \begin{Bmatrix} \varepsilon_{xx} \\ \varepsilon_{yy} \\ \varepsilon_{zz} \\ 2\varepsilon_{xy} \\ 2\varepsilon_{yz} \\ 2\varepsilon_{zx} \end{Bmatrix} \quad \text{(A-19)}$$

APPENDIX B

BEHRENS' RESULTS

Lamellar Composites

In the Behrens' paper [19], the effective moduli of Lamellar composites are computed as

$$C_{33}^{B} = a\left[\frac{a_1}{2\mu_1+\lambda_1} + \frac{a_2}{2\mu_2+\lambda_2}\right] \tag{B-1}$$

$$C_{11}^{B} = C_{22}^{B} = C_{33}^{B}\left[1 + \frac{4a_1a_2}{a^2}\frac{(\mu_1-\mu_2)(\mu_1+\lambda_1-\mu_2-\lambda_2)}{(2\mu_1+\lambda_1)(2\mu_2+\lambda_2)}\right] \tag{B-2}$$

$$C_{44}^{B} = a[a_1/\mu_1 + a_2/\mu_2]^{-1} \tag{B-3}$$

$$C_{66}^{B} = (\mu_1 a_1 + \mu_2 a_2)/a \tag{B-4}$$

$$C_{12}^{B} = C_{11}^{B} - 2C_{66}^{B} \tag{B-5}$$

$$C_{13}^{B} = \left[\frac{\lambda_1 a_1}{2\mu_1+\lambda_1} + \frac{\lambda_2 a_2}{2\mu_2+\lambda_2}\right]\left[\frac{a_1}{2\mu_1+\lambda_1} + \frac{a_2}{2\mu_2+\lambda_2}\right]^{-1} \tag{B-6}$$

where μ_1, λ_1 and μ_2, λ_2 are Lame constants for the constituents shown in Figure 63. In Equations (B-1) through (B-6) are used to denote the effective moduli computed by Behrens who uses a different expression of generalized Hooke's law, i.e.,

$$\begin{Bmatrix} \sigma_{xx} \\ \sigma_{yy} \\ \sigma_{zz} \\ \sigma_{yz} \\ \sigma_{xz} \\ \sigma_{xy} \end{Bmatrix} = \begin{bmatrix} C_{11} & C_{12} & C_{13} & C_{14} & C_{15} & C_{16} \\ C_{12} & C_{22} & C_{23} & C_{24} & C_{25} & C_{26} \\ C_{13} & C_{23} & C_{33} & C_{34} & C_{35} & C_{36} \\ C_{14} & C_{24} & C_{34} & C_{44} & C_{45} & C_{46} \\ C_{15} & C_{25} & C_{35} & C_{45} & C_{55} & C_{56} \\ C_{16} & C_{26} & C_{36} & C_{46} & C_{56} & C_{66} \end{bmatrix} \begin{Bmatrix} \varepsilon_{xx} \\ \varepsilon_{yy} \\ \varepsilon_{zz} \\ 2\varepsilon_{yz} \\ 2\varepsilon_{xz} \\ 2\varepsilon_{xy} \end{Bmatrix} \qquad \text{(B-7)}$$

In the Figure 63 the coordinate system with respect to the composite and the definition of the dimensions of the constituent are shown.

Unidirectional Fiber Composites with Rectangular Cross-Section

In Behrens' paper [20], the effective moduli of unidirectional fiber composites with rectangular cross-section are computed. The results are as follow:

$$C_{11}^B = C_{22}^B = (2\mu_2+\lambda_2)\left[\frac{\mu_1+\lambda_1+\mu_2}{(\mu_1+\lambda_1+\mu_2)-(\mu_1+\lambda_1-\mu_2-\lambda_2)s} + \frac{(\mu_1-\mu_2)s}{(\mu_1+\mu_2+\lambda_2)-(\mu_1-\mu_2)s^q}\right] \qquad \text{(B-8)}$$

$$C_{33}^B = (2\mu_2+\lambda_2)+(2\mu_1+\lambda_1-2\mu_2-\lambda_2)s - \frac{(\lambda_1-\lambda_2)^2 s(1-s)}{(\mu_1+\lambda_1+\mu_2)-(\mu_1+\lambda_1-\mu_2-\lambda_2)s} \qquad \text{(B-9)}$$

$$C_{44}^B = C_{55}^B = \mu_2 \frac{(\mu_1+\mu_2)+(\mu_1-\mu_2)s}{(\mu_1+\mu_2)-(\mu_1-\mu_2)s} \qquad \text{(B-10)}$$

$$C_{66}^B = \mu_2\left[1 + \frac{(\mu_1-\mu_2)s}{\mu_1-(\mu_1-\mu_2)s^{1/q}}\right]$$

$$C_{12}^{B} = \lambda_2+(2\mu_2+\lambda_2)s\ \left[\frac{\mu_1+\lambda_1-\mu_2-\lambda_2}{(\mu_1+\lambda_1+\mu_2)-(\mu_1+\lambda_1-\mu_2-\lambda_2)s} - \frac{\mu_1-\mu_2}{(\mu_1+\mu_2+\lambda_2)-(\mu_1-\mu_2)s^q}\right] \tag{B-12}$$

$$C_{13}^{B} = C_{23}^{B} = \lambda_2 + \frac{(\lambda_1-\lambda_2)(2\mu_2+\lambda_2)s}{\mu_1+\lambda_1+\mu_2)-(\mu_1+\lambda_1-\mu_2-\lambda_2)} \tag{B-13}$$

where $q = (2\mu_2+\lambda_2)/\mu_2$ and $s = a/b$. The definitions of the dimensions of the constituents are shown in Figure 64. λ_1, μ_1 and λ_2, μ_2 are Lame constants for the constituents.

REFERENCES

1. Einstein, A., Investigation on the Theory of Brownian Motion, Dover Publication Inc., 1956

2. Jeffery, G. B., "The Motion of Elliptical Particles Immersed in a Viscous Fluid", Proc. Roy. Soc., London, (A)102, p. 161, 1923

3. Taylor, G. I., "The Viscosity of a Fluid containing Small Drops of Another Fluid", Proc. Roy. Soc., London, (A)138, p.41, 1932

4. Bruggeman, D. A., "Die Elastischen Konstanten der Qusiisotropen Mischkorpen aus Isotropen Substanten", Ann. Phys., Vol. 29, p.160, 1973

5. Dewey, J. M., "The Elastic Constants of Materials loaded with Non-rigid Fillers", J. Appl. Phys., Vol. 18, p. 1947

6. Mackenzie, J. K., "The Elastic Constants of a Solid containing Spherical Holes", Proc. Phys. Soc.(B), Vol. 63. p. 2, 1950

7. Eshelby, J. D., "The Determination of the Elastic Field of an Ellipsoidal Inclusion and Related Problems", Proc. Roy. Soc., London, (A)241, p. 376, 1957

8. Kerner, E. H., "The Elastic and Thermoelastic Properties of Composite Media", Proc. Phys. Soc.(B), Vol. 69, p. 808, 1956

9. Hashin, Z., "The Elastic Moduli of Heterogeneous Materials", J. Appl. Mech., 29E, p. 143, 1962

10. Krivoglaz, M. A. and Cherevko, A. A., "On the Elastic Moduli of a Two Phase Solid", Fis. Metal. Metalloved, 8P, p. 161, 1959

11. Hill, R., "Report on Theories of the Elastic Properties of Reinforced Solids", British Iron and Steel Research Association, Rep. P/19/62, 1962; Mech. Phys. Solids, Vol. 11, p. 357, 1963

12. Hashin, Z. and Rosen, B. W., "The Elastic Moduli of Fiber Reinforced Materials", J. Appl. Mech., Vol. 31, p. 223, 1964

13. Paul, B., "Prediction of Elastic Constants of Multiphase Materials", Trans. AIME, Vol. 218, p. 36, 1960

14. Hashin, Z. and Shtrikman, S., "On Some Variational Principles in Elasticity and their Application to the Theory of Two-phase

Materials", University of Pennsylvania, Contr. NONR 551, p. 42, TR no. 1, 1961

15. Hashin, Z. and Shtrikman, S., "A Variational Approach to the Theory of the Elastic Behavior of Multiphase Materials", J. Mech. Phys. Solid., Vol. 11, p. 127, 1963

16. Dong, S. B., Pister, K. S., and Taylor, R. L., "On the Theory of Laminated Anisotropic Shells and Plates", J. Aerospace Sci., Vol. 29, p. 969, 1962

17. Calcote, L. R., The Analysis of Laminated Composite Structures, Van Nostrand Reinhold Co., New York, 1969

18. Lekhnitski, S. G., "Anisotropic Plates, Contribution to the Metallugy of Steel No. 50", American Iron and Steel Institute, 1965

19. Behrens, E., "Sound Propagation in Lamellar Composite Materials and Average Elastic Constants", J. Acoustical Soc. of America, Vol. 42, No. 2, p. 378, 1967

20. Behrens, E., "Elastic Constants of Filamentary Composites with Rectangular Symmetry", J. Acoustical Soc. of America, Vol. 42, No. 2, p. 367, 1967

21. Zienkiewicz, O. C., The Finite Element Method in Engineering Science, McGraw-Hill, 1971

22. Wilson, E. L., SAP a Generalized Structural Analysis Program, University of California, 1970

23. Sched, F., Numerical Analysis (Schaum's Outline Series), McGraw-Hill, 1968

24. Iron, B. M., "Numerical Integration Applied to; inite Element Methods", Conf. Use of Digital Computers in Structural Engin., University of Newcastle, 1966

25.

25. Iron, B. M., "Engineering Application of Numerical Integration in Stiffness Method", J. AIAA, Vol. 14, 2035, 1966

26. Kopal, Z., Numerical Analysis, 2nd ed., Chapman & Hall, 1961

27. Iron, B. M., "Quadrature Rules for Brick based Finite Element", Int. J. Num. Meth. Eng., 3, 1971

28. Toy, A. and Dickerson, E. O., "Crossplied Filamentary Metal-Matrix Composites", D-6, Vol. 12, 12th National SAMPE Symposium, Society of Aerospace Material Process Engineers, 1967

VITA

Sei In Kang was born in Manchuria, China on March 26, 1939. He received his Bachelor of Science degree in Physics from Yonsei University, Seoul, Korea in March, 1964. From 1964 to 1965, he did graduate study in physics and concentrated studying accelerator theory and experiments for the construction of the 300 KV Cockcroft-Walton accelerator at Yonsei University.

He received his Master of Science degree in physics from the Mississippi State University in January, 1968.

From 1967 to 1970, he was employed with U. S. Army Engineer Waterways Experiment Station and studied engineering mechanics at the Mississippi State University.

He entered the Georgia Institute of Technology in March, 1970, studied engineering mechanics for the doctoral degree, and was NDEA Fellow and research assistant there. While he was a graduate student, he presented the paper "On the Determination of Physical Properties of Composite Materials by a 3-Dimensional Finite Element Method" at the Third Conference of Composite Materials, ASTM, Williamsburg, Virginia, March 21-22, 1973.

He married Ye-Wha Lee on August 9, 1967. They have one daughter, Suzan.